RECEIVED
LAWRENCE
RADIATION LABORATORY

NOV 19 1970

LIBRARY AND
DOCUMENTS SECTION

UCRL-19685

c.2

VAPORIZATION MECHANISM OF GALLIUM ARSENIDE SINGLE CRYSTALS

Catherine Yuen-Chien Lou
(Ph. D. Thesis)

September 1970

AEC Contract No. W-7405-eng-48

TWO-WEEK LOAN COPY

This is a Library Circulating Copy which may be borrowed for two weeks. For a personal retention copy, call Tech. Info. Division, Ext. 5545

UCRL-19685 c.2

LAWRENCE RADIATION LABORATORY
UNIVERSITY of CALIFORNIA BERKELEY

DISCLAIMER

This document was prepared as an account of work sponsored by the United States Government. While this document is believed to contain correct information, neither the United States Government nor any agency thereof, nor the Regents of the University of California, nor any of their employees, makes any warranty, express or implied, or assumes any legal responsibility for the accuracy, completeness, or usefulness of any information, apparatus, product, or process disclosed, or represents that its use would not infringe privately owned rights. Reference herein to any specific commercial product, process, or service by its trade name, trademark, manufacturer, or otherwise, does not necessarily constitute or imply its endorsement, recommendation, or favoring by the United States Government or any agency thereof, or the Regents of the University of California. The views and opinions of authors expressed herein do not necessarily state or reflect those of the United States Government or any agency thereof or the Regents of the University of California.

TABLE OF CONTENTS

ABSTRACT ---------- 1

I. INTRODUCTION ---------- 1

II. PRINCIPLES OF VAPORIZATION ---------- 4

III. EXPERIMENTAL APPARATUS AND PROCEDURES ---------- 9

IV. EXPERIMENTAL RESULTS ---------- 14

A. Studies on Surface Morphology ---------- 14

B. Microbalance Studies ---------- 15

C. Mass Spectrometric Results ---------- 20

V. DISCUSSION ---------- 27

VI. PROPOSED VAPORIZATION MECHANISM OF GALLIUM ARSENIDE SINGLE CRYSTALS ---------- 37

APPENDIX I. Corrections for Fragmentations of Arsenic Molecules ---- 39

APPENDIX II. A Method to Find the Ratio of the Ionization Cross Sections for As_2 and As_4 ---------- 47

ACKNOWLEDGEMENTS ---------- 50

REFERENCES ---------- 51

TABLES ---------- 53

FIGURE CAPTIONS ---------- 60

FIGURES ---------- 63

VAPORIZATION MECHANISM OF GALLIUM ARSENIDE SINGLE CRYSTALS

Catherine Yuen-Chien Lou

Inorganic Materials Research Division, Lawrence Radiation Laboratory
Department of Chemistry, University of California
Berkeley, California

ABSTRACT

The kinetics of vaporization of gallium arsenide single crystals into vacuum have been investigated using microbalance and mass spectrometric techniques in the temperature range 700°C-900°C. It was found that gallium arsenide vaporized incongruently to give liquid gallium and arsenic vapor molecules. The total evaporation rates and the activation energies were found to be the same for both (111) and ($\bar{1}\bar{1}\bar{1}$) faces. The initial vacuum vaporization rate of gallium arsenide single crystals is lower than the maximum rate calculated from equilibrium vapor pressures by about a factor of two but the activation energy is the same (90 kcal/mole) as the heat of sublimation (per mole of GaAs). When excess gallium liquid was placed on top of the vaporizing surface, the rate was found to be increased by a factor of two compared to the calculated maximum rate, while the activation energy remained unchanged. Both Te-doped and Zn-doped GaAs samples give lower evaporation rates. The activation energy for Te-doped samples is 90 kcal/mole, the same as that found for pure samples. However the activation energy of vaporization is lower for the Zn-doped samples (76 kcal/mole). When excess gallium liquid was placed on top of the surface of these samples, the vaporization rate was found again to have increased to the maximum rate, with the activation energies remaining the same as those without the excess liquid gallium on top. The vapor

and desorption behavior,[8] etching,[9] and crystal growth rates[10] under a variety of experimental conditions. The (111) face will be referred to as the gallium face and the $(\bar{1}\bar{1}\bar{1})$ face as the arsenic face.

The vaporization studies were carried out using both microbalance and mass spectrometer. Microbalance studies yield the absolute vacuum vaporization rate by monitoring the weightloss of the single crystal sample with known surface area as a function of time. Mass spectrometric studies allow us to determine the vapor composition over the vaporizing specimen. When these investigations are carried out as a function of temperature, the mass spectrometric measurements yield the activation energies for vaporization of each vapor species whereas the microbalance studies gives an average activation energy of all species.

Gallium arsenide vaporize incongruently (i.e. its vapor composition is different from the crystal composition) according to the dominant net reaction:

$$GaAs(s) \rightarrow Ga(\ell) + X/2\ As_2(g) + (1-X)\ 4\ As_4(g)$$

in the temperature range of 700°C-900°C. In order to establish the sublimation mechanism, in addition to measuring the vacuum vaporization rates and the vapor compositions of both the gallium and arsenic faces as a function of time and as a function of temperatures, the vacuum vaporization rates of these faces covered with excess liquid gallium were also monitored. Mass spectrometric measurements of the vapor compositions were performed. Samples doped with tellurium and zinc were used to correlate evaporation rates with the defect concentrations and electrical properties of the crystals. Again, vaporization rates with excess liquid gallium on top of these doped samples were determined. From these studies, a mechan-

ism for the vaporization of gallium arsenide single crystals is proposed. It is likely that this mechanism is applicable to most other IIIA-VA compound semiconductors as well.

Before presenting a discussion of the experimental procedures and results, a review of the basic principles of vaporization will be presented.

II. PRINCIPLES OF VAPORIZATION*

Vaporization of solids is a process which involves a complex series of reaction steps. Among all of these steps, the one which proceeds at the slowest rate is called the rate-limiting step and its potential energy barrier is the activation energy. In vaporization, the rate-limiting step may involve bulk-diffusion, charge transfer, bond-breaking, rearrangement, association, or dissociation of the vaporizing surface atoms. It may also involve the atomic transport of these atoms on the crystal surface. The purpose of a kinetic study on vaporization is to find out which of these steps can be rate-controlling in the complex mechanism of evaporation. It should be noted that as the conditions of vaporization change (e.g. change of surface composition, temperature, etc.) the rate-limiting step may also change, thus perhaps giving rise to a different vaporization rate.

Hertz, Langmuir, and Knudsen were among the first who have investigated the relationship between the kinetic theory of gases and the rate of evaporation. From the kinetic theory of gases, assuming a Maxwellian distribution of molecular velocities, it was shown that the flux J of moles of vapor molecules that strike a unit surface area per unit time is given by

$$J_c = P/\sqrt{2\pi MRT}$$

where P is the pressure, R is the gas constant, M is the molecular weight, and T is the absolute temperature. The maximum possible rate of evaporation from the surface, J_{max}, at a given temperature, is the rate which would be

---

*Extensive reviews on this topic are presented in other references.[11-13] We therefore do not attempt to give a comprehensive discussion on the subject.

attained if the solid were in dynamic equilibrium with the vapor, i.e., the rate of vaporization is equal to the rate of condensation. Thus we found that the maximum vaporization rate of a monatomic solid is given by the expression

$$J_{max} = J_C = P_{eq} / \sqrt{2\pi MRT}$$

where P_{eq} is the equilibrium vapor pressure. During vacuum vaporization the rate is often found to be orders of magnitude lower than this calculated maximum rate. A factor α is thus introduced.

$$J_V \text{ (moles/cm}^2 \text{ sec)} = \alpha P_{eq} / \sqrt{2\pi MRT}$$

where α, the evaporation coefficient is defined as

$$\alpha(T) \equiv J_V(T) \; / \; J_{max}(T)$$

α can have values less or equal to unity. When $\alpha = 1$, i.e., when vacuum vaporization rate is equal to the calculated maximum rate, one must have a surface in which all of the atoms that would occupy the geometrical surface area are available for desorption. Furthermore, these atoms must be bound by an energy which is equal to the energy of vaporization, ΔE_V. In other words, the surface atoms must have the same internal states as the vapor atoms and all surface sites are equivalent and need activation energies for vaporization which is equal to the heat or enthalpy for vaporization.

However, in vaporization studies of most diatomic solids, one finds that α is usually much less than unity. At the same time, α may also be temperature dependent. This is due to the fact that most surfaces are heterogeneous. They contain sites that have atoms possessing binding energies greater than the heat of vaporization. The concentration of suitable low binding energy sites from which vaporization proceeds may

also be much lower than the total surface area. In addition, due to the structural differences between the vaporizing unit in the crystal lattice and in the vapor phase, the internal partition function of the surface atoms may differ greatly from the vapor atoms when the solid undergoes rearrangement, association, or dissociation upon vaporization. Aside from these reasons, the concentrations and interactions of crystal defects, the carrier concentrations and mobilities are also among the multiple factors that can cause the lowering of α from unity.

Consider a vaporization reaction X(solid) $\rightarrow$ X(vapor). The flux of monatomic vapor species F_V may be expressed as

$$F_V \text{ (moles/sec)} = k_V (X)_S \, a$$

where k_V is the rate constant of the rate-controlling uni-molecular reaction, $(X)_S$ is the surface concentration of X atoms in the rate-limiting step and a is the surface area of the vaporizing crystal face. If the area remains constant during vaporization, i.e., the vaporization proceeds at a steady state rate, we then have

$$J_V \text{ (moles/cm}^2\text{-sec)} = k_V (X)_S \qquad \text{II.1}$$

From Arrhenius equation for the rate constant, assuming that the activation energy is independent of temperature, we have

$$k_V = A \exp(-E_a/RT)$$

where E_a is the experimental activation energy required for the rate-controlling step and A is the pre-exponential factor.

From transition-state theory, we can arrive at the expression for the rate constant k_V as

$$k_V = \frac{kT}{h} \quad e^{\Delta S^{\ddagger}/R} \quad e^{-\Delta H^{\ddagger}/RT} \qquad \text{II.2}$$

where k is the Boltzman's constant, T is the temperature, h is the Planck's constant, $\Delta S^{\ddagger}$ and $\Delta H^{\ddagger}$ are the entropy and heat of activation of the activated complex, respectively. The $\Delta H^{\ddagger}$ is related to the experimental energy of activation E_a in the Arrhenius expression by $\Delta H^{\ddagger} = \Delta E^{\ddagger} + \Delta(PV^{\ddagger})$. In liquid and solid systems, the $\Delta(PV^{\ddagger})$ term is negligible at ordinary pressures. Thus we have

$$\frac{d \ \ell n \ k_V}{dT} = \frac{E_a}{RT^2} = \frac{\Delta H^{\ddagger} + RT}{RT^2}$$

$$\therefore \quad E_a = \Delta H^{\ddagger} + RT$$

For ideal gases, we have

$$\frac{d \ \ell n \ k_V}{dT} = \frac{E_a}{RT^2} = \frac{\Delta H^{\ddagger} - (n^{\ddagger} - 1) RT}{RT^2}$$

$$\therefore \quad E_a = \Delta H^{\ddagger} - (\Delta n^{\ddagger} - 1)RT \qquad \text{II.3}$$

The term $\Delta n^{\ddagger}$ is the number of moles of complex, which is equal to one minus the number of moles of reactants. Therefore, if one could determine the experimental k_V and E_a and utilizing Eqs. II.2 and II.3, one can then calculate for the entropy of activation, which in turn will provide us with one of the best indications to the nature of the transition state.

In our studies of the vaporization of GaAs we measure experimentally lower rates than the maximum rates calculated from equilibrium vapor pressures. However, at the same time, we obtain an activation energy which is equal to the heat of vaporization ($\Delta H^{\ddagger} = \Delta H_V$), i.e., we find that α is temperature

independent. Substituting the expression for k_V in Eq. II.2 into Eq. II.1 we obtain

$$J_V \text{ (moles/cm}^2 \text{ sec)} = \frac{kT}{h} e^{\Delta S^{\ddagger}/R} (X)_S e^{-\Delta H^{\ddagger}/RT}$$

This suggests that the preexponential term, $e^{\Delta S^{\ddagger}/R}(X)_S$, is rate-controlling in the process of evaporation. It is usually very difficult to distinguish the entropy factor from the surface concentration factor in this term. We may calculate the value of $\Delta S^{\ddagger}$ using a suitable model and compare it with the equilibrium entropy of vaporization ΔS_V, to determine whether the entropy factor is rate-limiting. We could also accomplish this by measuring the vapor compositions over the vaporizing solid under both vacuum and equilibrium conditions. A different vapor composition in vacuum evaporation than that found in equilibrium implies that the activated complex has a different atomic arrangement than the products of vaporization in equilibrium. Such a difference will likely lead to $\Delta S^{\ddagger}$ values that greatly differ from ΔS_V. If the concentration factor $(X)_S$ is rate-limiting, we would then be likely to obtain the same vapor composition in vacuum vaporization as that determined in equilibrium.

III. EXPERIMENTAL APPARATUS AND PROCEDURES

Gallium arsenide has zinc-blende structure and a melting point of 1238°C. High purity gallium arsenide single crystals, purchased from Cominco American Inc., Spokane, Washington, were used in the experiments. These crystals were n-type, had room temperature resistivities of 0.1-0.2 ohm-cm and mobilities of about 5×10^3 cm^2/volt-sec. Single crystals were also obtained from Bell and Howell Corp. in Pasendena, Ca. along with samples doped with zinc and tellurium in various concentrations. The pure single crystals were again n-type but with room temperature resistivities of 0.027 ohm-cm and mobilities of 5,000 cm^2/volt-sec. Zinc-doped crystals (p-type) had room temperature resistivities of 0.0045 ohm-cm and mobilities of 71 cm^2/volts-sec. Tellurium doped samples (n-type) had room temperature resistivities equal to 8.4×10^{-4} ohm-cm and mobilities equal to 2410 cm^2/volt-sec. These values are summarized in Table I. Electronic grade gallium metal was obtained from Eagle-Picher Co. with a minimum purity of seven 9's.

These crystals were X-ray oriented, cut into 3x3x6 mm pieces, polished, and etched with 5% Br_2-methanol solution for three minutes. Triangular etch pits for the gallium face and mirror finish for the arsenic face were obtained (Fig. 2). These differences in the etching behaviors could then be used as identification for the two crystal faces.[21] The samples were then rinsed in methanol solution and wrapped in W foil to expose only the gallium or the arsenic face.* The crystals were now ready for vaporization.

---

*There were a few times when the crystal was not wrapped tight enough and vaporization from the sides of the sample also occurred. However, this did not take place to any great extent and could only give rise to an estimated error of not more than 5%.

The microbalance used for weight loss measurements was made after a design by Honig and Czandera.[14,15] The balance was used as a null device. The restoring force for a change in sample weight was produced by the coupling of a magnet and a solenoid. The magnet was suspended from the balance inside the vacuum while the solenoid was outside the vacuum. Both magnet and sample were supported by quartz fibers with hooked ends, (Fig. 3). With a weight of 500 mg, the sensitivity of the balance is about 1μ gram. Due to error in hysteresis of the solenoid and thus in locating the true null point, the accuracy of any reading is of course less, usually not better than 10μ gm. Thermocouple monitoring sample temperatures was placed outside the quartz tube and was calibrated in reference to another thermocouple placed inside the quartz tube in the position where the sample should be. The calibration set up and results are shown in Fig. 4.

A typical vacuum vaporization experiment using the microbalance system proceeded as follows. As was described before, the sample was etched, rinsed, and wrapped in W foil to expose only the vaporizing surface. It was then mounted on the sample supporting fiber with the evaporation surface facing downward. Experiments were carried out to determine the effect of the direction of vaporization (i.e., vaporizing surface facing either upward or downward) and no observable differences were found in the evaporation rate. The system was then evacuated. Pressure during the runs was usually in the range of 10^{-7} torr so that the recondensation rates were orders of magnitude lower than the vaporization rates. The furnace, with a well known temperature profile (Fig. 5) was heated to the desired temperature, monitored by a thermocouple, and the temperature was then stabilized to within 1+. Once steady state temperature was reached,

the sample was lowered into the furnace and hooked over the balance pivot wire. Weight loss measurements were then taken at this temperature as a function of time. After the evaporation rate was determined, the sample was removed from the hot zone and the furnace was heated to another temperature. Again the sample was lowered and weight loss measurements were taken. After the entire temperature range was finished, the furnace was cooled and the system was then filled up to atmospheric pressure with dry nitrogen. The sample was removed from the vacuum system, etched, rinsed in methanol solution, wrapped to expose the opposite face, and then replaced onto the supporting fibre. The experiments were then repeated over the temperature range. Again the sample was removed from the vacuum system, etched, rinsed and wrapped to expose the vaporizing face that was the same as the first evaporation runs and the experiments were repeated. Measurements were also made both while increasing and while decreasing the temperatures. When the slight masking effect of the holder due to the receding of the crystal into the foil is taken into account,[16] these measurements always approach the same steady state at a given temperature. In addition experiments were run using a separate sample for each temperature and vaporize over a long period of time. Optical micrographs were taken of all sample surfaces before and after each vaporization run.

For vaporization experiments with excess liquid metal (~0.04 gm) on top of the evaporating surface, the exposed face of the sample was placed in the vaporization chamber facing upward. Excess liquid metal was then put on to cover the entire surface area and the vacuum vaporization experiment was carried out. Exhaustive vaporization was also performed where the entire sample was evaporated.

Studies of the vapor composition over the vaporizing GaAs surfaces were carried out in a separate vacuum system using a quadrupole mass spectrometer (Electronic Associates, Inc. (EAI) Model No. 200). This system is shown in Fig. 6. The sample was etched, rinsed, wrapped, in W foil to expose only the vaporizing surface, as was done in microbalance experiments. This was then placed in a high density graphite sample holder with the vaporizing surface facing upward. In the case of the mass spectrometer system, the thermocouple junction was placed in contact with the wrapping foil of the sample. The system was then evacuated first with sorption pumps, then with a Vac Ion pump down to a pressure of $\leq 4\times10^{-7}$ torr. The system was then baked out for eight hours with the furnace set at 300°C. After bake out, the ambient pressure was in the range of about 10^{-9} torr. The mean free paths of the vaporizing molecules were such that no collisions occurred between the molecules before they hit the detector or the chamber walls. The furnace was then turned on to heat the sample to the desired vaporization temperature. Simultaneously, the chamber was chilled with liquid nitrogen to decrease the diffuse scattering of arsenic molecules from the walls.* After the temperature was stabilized (about 30 min.) the intensities of the ion fluxes were measured for each of the ions of interest (As^+, As_2^+, As_3^+, As_4^+) with the slit moving in line and out of alignment with the ion source and the ionizer

---

*Both the dimer and the tetramer arsenic molecules are known to have low condensation coefficients[17] and can undergo multiple scattering. In addition, the association of dimers to form tetramers on the chamber walls has been the probable reason for the discrepancy of the reported vapor composition over GaAs in different effusion cell studies. Our system was designed in such a way so that only molecules which come directly from the vaporizing surface can contribute to the detector signal after a correction to the background intensity is made. The background intensity which is due by cooling the chamber walls to liquid nitrogen temperature.

so as to account for the background contributions.** These measurements were repeated at different temperatures. During a typical experiment, measurements were made both while increasing and while decreasing the temperatures between intensity measurements, as was done in the microbalance experiments. Results for these investigations are discussed in the next section.

**The mass spectrometer was operated using the following ionization parameters: electron energy = 50 eV, emission = 0.2 ma, electron trap voltage = 30 eV, ion energy = 6 eV, and focus voltage = -23 eV.

IV. EXPERIMENTAL RESULTS

We have divided this section into three parts: (A) Optical microscopy studies on surface morphology, (B) Microbalance studies on absolute vaporization rates, and (C) Mass spectrometric studies on vapor compositions.

A. Studies on Surface Morphology

Optical micrographs were taken of the crystal faces after vaporization at different temperatures. We found two types of distinctly different surfaces for the two opposing faces. These are shown in Fig. 7-17.

For gallium face, for temperatures below 800°C, various triangular thermal pits were observed, with gallium droplets covering part of the vaporizing surface. These triangular pits intersect each other and in general form terraced macroscopic ledges, giving rise to an appearance of a very rough surface. For temperatures above 850°C, vaporization rates were extremely rapid. Consequently, bigger gallium droplets were formed, (Figs. 7-9).

For arsenic face, we have found an entirely different situation. Big liquid gallium droplets were observed even at the lowest temperature (750°C) of our studies(Fig.10). As we increase the temperature no noticeable differences were found. When these liquid gallium droplets were being physically removed from the surface, flat regions were found underneath, (Fig. 11).

Excess gallium was placed on top of crystal surface before vaporization and the vacuum rates were monitored. The crystal face was covered with liquid gallium as shown in Fig. 12.

An unetched crystal was used in order to observe the relationship between the formation of thermal etch pits and vaporization rates. For gallium face, we can see a progressive development of the characteristic triangular pits. Mechanical damages on surface and edges of the sample seem to serve as nucleation sites for vaporization, (Fig. 13-15). When the gallium droplets in Fig. 15 were removed, again, we observe a flat surface region underneath (Fig. 16). For arsenic face, the surface regions not covered by gallium were flat and showed no pitting similiar to that of the gallium face. (Fig. 17).

B. Microbalance Studies

The weight loss of the sample was measured as a function of time at a given temperature. From these data and the geometric surface area, the evaporation rate (mg/cm^2-sec) was calculated. During the vaporization, the surface was of course not flat, as has been discussed previously, so that the geometric surface area is the lower limit of the total vaporizing area. However, Melville[18] has shown that the evaporation rate may not be appreciably larger from a rough surface than from a crystal with a smooth geometrical surface area. Thus the error involved in the estimation of surface area would certainly be within the experimental accuracy (±5%).

As a check on the calibration of our system, sodium chloride single crystals with high dislocation densities ($\sim 6\times10^6/cm^2$) were vaporized and the rates were found to be the same as that reported by Lester and Somorjai.[6]

Since gallium liquid droplets were readily discernible on both crystal faces after vaporization, it was concluded that gallium arsenide vaporizes incongruently into gallium liquid and arsenic molecules. Because liquid

gallium was being continuously accumulated on top of the vaporizing surface and as we can show later, the increase in coverage of liquid gallium on the surface accelerates the vaporization rates, the question was then raised whether we could get a steady state evaporation rate at a given temperature under these conditions. An exhaustive vaporization was performed in which a small crystal was completely evaporated at a given temperature and the vacuum vaporization rates were continuously monitored. The results are shown in Fig. 18.

Without any physical disturbance to the surface, e.g. shaking the crystal face to spread the liquid gallium so as to change the area covered by the metal, the vaporization rates remain constant for more than five hours at T = 849°C. A simple calculation assuming semi-spherical shape, i.e. with maximum surface tension, and applying the physical properties of these liquid gallium droplets shows that indeed this is a possibility, i.e. the liquid gallium coverage of the evaporation surface remains relatively constant during the initial period (approx. 5 hrs) of vaporization. In other words, the surface area covered by gallium liquid remains virtually constant. When the accumulated liquid gallium was then spread over the entire surface by violently shaking the sample a few times, the evaporation rates suddenly increase to that value which is equal to the evaporation rate where excess gallium was added. As the crystal continues to vaporize over an extended period of time, finally we come to the state where a decrease in rate was observed, probably corresponding to a depletion in the vaporizing material from the crystal holder. Thus, from this experiment, we can conclude that an initial "virtual steady state" vaporization rate of gallium arsenide can be obtained even though gallium arsenide single crystals vaporize incongruently.

To the limit of sensitivity of our apparatus (±1μ gm), a reproducible initial steady state vaporization rate was found at any temperature in the range of our study. However, there is a short induction period of transient evaporation before the steady state vaporization is obtained. The length of this transient period depends strongly on the history of the sample, e.g. preparation, etching, heat treatment. Unetched crystals usually have longer transient periods. Furthermore, the initial transient period during which the rates are changing is longer for arsenic face than for gallium face. (Fig. 19).

The steady state vacuum vaporization rates were measured for both crystal faces of gallium arsenide as a function of temperature. This is shown in Fig. 20.* Within our experimental accuracy the rates are the same for both gallium and arsenic faces. Previous treatments (e.g. annealing of a face while the opposite face was being vaporized) of the sample appeared to have no effect on the vaporization rates. The activation energy was measured at 90±3 kcal/mole of activated complex. Crystals (undoped) with slightly different electron carrier concentrations were found to have the same vaporization rates and the same activation energies (Fig. 21). When excess liquid gallium was put on top of the vaporizing face so as to cover the entire surface, evaporation rates were found to be increased by a factor of two (Fig. 20). Both crystal faces gave the same evaporation rates and the activation energy was found to be 86±5 kcal/mole of activated complex. Different crystals were vaporized at different temperatures over periods of 12 to 36 hours, depending on the particular temperature of the experiment. The results are shown in Fig.34.

*At least three sets of data were obtained for each experimental condition and they were found to be in good agreement with each other. In the figures, we shall only attempt to show one set of data and the slope represents the average activation energy of <u>all</u> the data obtained under the specified conditions.

In order to investigate the effect of impurities in the GaAs crystal in high concentrations on the kinetics of vaporization, the vacuum vaporization rates of crystals heavily doped with tellurium and zinc were measured concentration $\simeq 10^8/cm^3$. The rates of the Te-doped samples were found to be about half of the pure samples. Within our experimental accuracy, the activation energy remains the same, i.e., 90±3 kcal/mole of activated complex as that for pure GaAs. When we vaporize the same crystal face again for the second time, we found a slight increase in the rates. Conductivity measurements were made before and after vaporization and no conductivity change was detected. Diffusion rate of Te in gallium arsenide was also estimated and it was found to be low enough* so that the out-diffusion of tellurium from GaAs during vaporization is improbable. The small increase in the evaporation rates can be due to the incomplete removal of liquid gallium

---

*Diffusion can customarily be described by the equation

$$D = D_0 \exp(-E/kt)$$

In reference 19, Goldstein has reported values for diffusion of sulfur in GaAs as

$$D_0 = 4\times10^3 \text{ cm}^2/\text{sec}$$
$$E = 4.04 \text{ eV}$$

and for diffusion of selenium in GaAs as

$$D_0 = 3\times10^3 \text{ cm}^2/\text{sec}$$
$$E = 4.16 \text{ eV}$$

Thus the values for diffusion of tellurium in GaAs can be estimated as

$$D_0 = 2\times10^3 \text{ cm}^2/\text{sec}$$
$$E = 4.3 \text{ eV}$$

and we found

$$D_{800°C} = 2\times10^{-17} \text{ cm}^2/\text{sec}$$

and the time required to traverse the length of the sample (6 mm) from random walk agruments is

$$t = 7.5\times10^{13} \text{ min.}$$

deposited on the surface from previous vaporization runs. Excess gallium was put on top on these Te-doped crystals and the vaporization rates were found to be the same as that of the pure crystals with gallium liquid on top. The activation energy was found to be 87±3 kcal/mole of activated complex. (Fig. 22).

Crystals doped with zinc were also used in this kinetic study. They are p-type samples and the vacuum rates were found to be the lowest of all. In addition, the activation energy also decreases to 76±3 kcal/mole of activated complex (Fig. 23a,b). As we continued to vaporize the sample by alternating the crystal faces, we found a progressive increase in the vaporization rates. Conductivity and diffusion data indicate zinc is remaining in the crystal rather than vaporizing.* From Fig. 23a it suggests that these rates are gradually moving upward toward the vaporization rates of zinc-doped crystals with excess gallium on top of the vaporizing surface. Maybe indeed we did leave a thin film of liquid gallium on the surface even though we etched the crystal after each evaporation. When excess gallium was put on top of this p-type crystals, rates comparable to the one on top of pure samples were measured. But a very interesting fact was found. The activation energy of the vaporization rate of gallium on top of zinc-doped samples remains to be the same as that without the gallium, i.e. 76±3 kcal/mole of activated complex. This then gives us a clue as to the nature of the catalytic function of liquid gallium in the complex mechanism of vaporization.

---

*From reference 19 we obtained values for diffusion of Zn in GaAs

$$D_0 = 15 \text{ cm}^2/\text{sec}$$
$$E = 2.49 \text{ eV}$$

and we found

$$D_{800°C} = 3.98\times10^{-11} \text{ cm}^2/\text{sec}$$
$$t = 3.8\times10^{7} \text{ min.}$$

Due to the interesting findings that liquid gallium catalyses the vaporization of GaAs, an attempt was made to see if all liquid metals behave the same way. Unfortunately, tin is the only other material we could find that is a liquid and has a low vapor pressure ($< 10^{-8}$ torr) at the temperatures of our studies (700°C-900°C). The results are shown in Fig. 24. We found the absolute vaporization rate to be lower than that with excess Ga on top and an activation energy equal to 76±3 kcal/mole of activated complex. Since the Sn-GaAs system has not been studied extensively (e.g. solubility of GaAs in Sn, the activities of arsenic molecules in Sn as compared to that in Ga), the exact interpretation of these vaporization rates is rather difficult. Futhermore, during the vaporization of gallium arsenide crystals, liquid gallium is being formed continuously. The gallium thus produced then mixes with tin, giving a solution with constantly changing compositions. This further adds to the problem in elucidating an exact meaning from the Sn data.

C. Mass Spectrometric Results

A typical residual gas mass spectrum after bakeout was shown in Fig. 25. The ions which were readily detected in the mass spectra during the vaporization of gallium arsenide are As^+, As_2^+, As_3^+ and As_4^+. The dimer and tetramer ion peaks had the largest intensities and they were of comparable magnitude in the temperature range of our study.

Our experimental geometry has the advantage of allowing us to sample directly the vapor composition which emanates from the vaporizing gallium arsenide surface. Thus, any association reaction which may take place on the heater or chamber walls would only change the background intensity distribution, which can be measured independently and then subtracted from the signal. Direct reactions of the arsenic molecules with the hot thorium

coated tungsten ionizer filament (most likely to be dissociative reactions) can also change the vapor composition. However, we have found no observable change in the ion intensity ratios upon changing the emission current, thereby changing the temperature, of the ionizer filament. Xenon isotope spectra were run in order to calibrate the transmission of our mass spectrometer. It was found that we have a decrease in sensitivity of about 1.5% per increase of one mass unit (Table II). Due to the lack of accurate ionization cross section data and the experimental uncertainties in calibration of the system, we shall not attempt to compute the absolute vaporization rates of the different vapor species but rather use their relative intensity change as a function of temperature to monitor changes in intensity ratios and calculate their activation energies.

Appearance potential curves for all the ions were determined, as shown in Fig. 26. These are comparable with the literature values shown in Table III. As it can be seen, all the ions appear at electron energies below 15 eV. The practical lower limit for electron energy in our mass spectrometer is about 20 eV. Thus it would be experimentally very difficult to work at electron energies low enough to eliminate the fragmentation problem. Therefore, in order to determine the fragmentation pattern of the arsenic molecules, we then vaporized pure arsenic crystals at 500°K where the vapor was shown to consist mainly of tetramer molecules.[4,20] Table IV gives the equilibrium vapor pressures of arsenic molecules from the vaporization of arsenic crystals. In the vaporization of GaAs single crystals, both the As and As_3 molecules can be identified as fragmentation products of electron impact ionization of As_2 and As_4 molecules according to the following reactions:

$$As_4 + e^- \rightarrow As_4^+ + 2e^-$$
$$As_4^+ \rightarrow As_3^+ + As$$
$$As_4^+ \rightarrow As_3 + As^+$$
$$As_2 + e^- \rightarrow As_2^+ + 2e^-$$
$$As_2^+ \rightarrow As^+ + As$$

Corrections for fragmentations from As_4 to As_2 molecules were also made in the intensities detected for As_2 and As_4.

$$As_4 + e^- \rightarrow As_4^+ + 2e^-$$
$$As_4^+ \rightarrow As_2^+ + As_2$$

The method for these corrections are discussed in greater detail in Appendix I. Since As_4 is a monoisotopic molecule, we do not have any way of distinguishing the contribution of As_4^{++} to the intensities detected for As_2^+. However, comparing the ionization potentials and the dissociation energies for the reactions*

$$As_4^+ \rightarrow As_4^{++} + e^- \quad > 8.84 \text{ eV}$$
$$As_4^+ \rightarrow As_2^+ + As_2 \quad 4.00 \text{ eV}$$

we can safely assumed that the contribution of As_4^{++} to As_2^+ intensities will be small as compared to that from fragmentation of higher molecules and the ionization of neutral dimer molecules ($As_2 \rightarrow As_2^+ + e^-$). This same argument also applies to As_2^{++} and As^+.

---

*From Table III, we have

Fragmentation of As_4^+

As_2	$\rightarrow$	$As^+ + As$	3.94 eV
As_3^+	$\rightarrow$	$As_2^+ + As$	5.35 eV
As_4^+	$\rightarrow$	$As_3^+ + As$	2.59 eV
As_4^+	$\rightarrow$	$As_2^+ + As_2$	4.00 eV

Ist ionization potential of As_4 $\quad As_4 \rightarrow As_4^+ + e^-$ 8.84 eV

2nd ionization potential of As_4 $\quad As_4^+ \rightarrow As_4^{++} + e^- > 8.84$ eV

No gallium peek was detected as coming from the vaporizing gallium arsenide crystals in the temperature range of our study (700°C-900°C). Inspection of the high density graphite sample holder and the stainless steel vaporization chamber did not reveal the occurrence of any possible solid state reaction with gallium. Presumably except for a small undetectable fraction that corresponds to the low vapor pressure of gallium on the GaAs surface all of the gallium has remained in the liquid state on top of the vaporizing surface. Thus we have been unable to monitor the vaporization of gallium as a function of temperature and to calculate its activation energy of vaporization.

The intensities corrected for fragmentation of As_2^+ and As_4^+ peaks from vaporization of GaAs single crystals for both gallium (111) and arsenic ($\bar{1}\bar{1}\bar{1}$) faces are plotted as a function of temperature. For the vaporization of the gallium face, after correction for fragmentation, only the tetramers were found, with an average activation energy of 92±5 kcal/mole of activated complex (Figs. 27 and 28) according to the net reaction

$$GaAs(s) \rightarrow Ga(\ell) + 1/4\ As_4(g) \quad \Delta H^{\ddagger} = 92\pm5 \text{ kcal/mole}$$

However, for arsenic face, we found both the dimers and the tetramers with activation energies of 88±5 kcal/mole of activated complex and 98±5 kcal/mole of activated complex (Figs. 29, 30, 31) respectively, according to the reactions:

$$GaAs(s) \rightarrow Ga(\ell) + 1/2\ As_2(g) \quad \Delta H^{\ddagger} = 88\pm5 \text{ kcal/mole}$$

$$GaAs(s) \rightarrow Ga(\ell) + 1/4\ As_4(g) \quad \Delta H^{\ddagger} = 98\pm5 \text{ kcal/mole}$$

The net reaction for vaporization from arsenic face of GaAs single crystals will be

$$GaAs(s) \rightarrow Ga(\ell) + X/2\ As_2(g) + (1-X)4\ As_4(g)$$

When excess liquid gallium was placed on top of the vaporizing surface, again, we found different vapor compositions for the two opposing faces. For gallium face, we found only the tetramers (As_4), just as for the vaporization of Ga-face without liquid gallium on top (Fig. 32). For the arsenic face, both the dimers (As_2) and the tetramers (As_4) were found (Fig. 33); however, the ratio As_2/As_4 seems to be slightly higher in this case than for the pure crystals without gallium liquid on top. These intensities are plotted as a function of temperature and the activation energies calculated. Within experimental accuracy, it was found that the activation energies are the same as in vaporization without excess liquid metal on top, i.e., for gallium face ΔH^* for As_4 is 92 ± 5 kcal/mole of activated complex and for arsenic face ΔH^* for As_2 is 88 ± 5 kcal/mole of activated complex. The ratios of P_{As_2}/P_{As_4} for some of the representative mass spectrometric runs are shown in Table V.

In concluding this section, we would like to summarize the results we have thus found:

(1) We have observed triangular thermal etch pits with small gallium droplets partially covering the vaporizing surface on gallium face and just liquid gallium droplets on arsenic face. Thus it appears that gallium face is rougher than arsenic face after vaporization.

(2) Vaporization seems to take place preferentially on regions damaged mechanically (source of macroscopic ledges).

(3) Vacuum vaporization rates of pure and doped GaAs crystal samples were found to be much lower than the calculated maximum rate. Within our experimental accuracy, there were no observable differences in the evaporation rates for Ga and As faces of each of the different samples. See the following page for table.

(4) Only the tetramers (As_4) were found to vaporize from the gallium face whereas both the dimers (As_2) and the tetramers (As_4) were found to vaporize from the arsenic face. Excess liquid gallium on top of the vaporizing surface does not change the vapor composition significantly. The activation energies (in kcal/mole of activated complex) for each species with and without liquid gallium on top of the sample were as follows:

	As_4	As_2
Ga face	92±5	--
As face	98±5	88±5

Supplier of samples	Doping	Liquid gallium on top?	Initial α* (T=1124°K)	ΔH* Kcal / mole of activated complex
Cominco			0.46	90
		yes	1	87
		excess tin on top	0.49	76
Bell and Howell			0.46	90
	Te		0.29	90
	Te	yes	1	87
	Zn		0.15	76
	Zn	yes	1	76

* Considerable disagreement was found in literature concerning the exact equilibrium vapor composition of gallium arsenide. Arthur[22] has studied the equilibrium vapor pressures of GaAs using a mass spectrometer and has reported the equilibrium vapor to consist mainly of As_2 molecules. He has also found the heat of dissociation of $As_4(g) \rightarrow 2\ As_2(g)$ to be 62.5 kcal. De Maria et al.[23] has studied the equilibrium vapor pressures with mass spectrometer also. However, he has found comparable intensities for As_2 and As_4 in the vapor phase and a heat of dissociation equal to 73.5 kcal. Recently Hudson,[24] using electron impact ionization, has reported the heat of dissociation of $As_4 \rightarrow 2\ As_2$ to be 68.5 kcal. After corrections for the entropy factor in the data reported by De Maria, we found similar values for the heat of dissociation as that reported by Hudson. Based on these facts, we will then use the equilibrium vapor pressures reported by De Maria in our calculations of α. Table IV gives the equilibrium vapor pressures of GaAs and the corresponding maximum evaporation rates. These are shown in Figs. 35 and 36, respectively. We should like to point out that the absolute vaporization rates and the ratio of As_2/As_4 we found for vaporization of GaAs with excess $Ga(\ell)$ on top of the surface are similar to the maximum rates calculable from the equilibrium data reported by De Maria.

V. DISCUSSION

Liquid gallium droplets were discernible on top of the surface after evaporation of every gallium arsenide surface that was studied. Mass spectrometric studies of the vapor composition over the vaporizing samples revealed the presence of As_2 and As_4 molecules but no gallium was ever detected in the vapor phase in the temperature range of our vaporization studies. Therefore, we have concluded that gallium arsenide single crystals vaporize incongruently according to the equation:

$$GaAs(s) \rightarrow Ga(\ell) + X/2\ As_2(g) + (1-X)/4\ As_4(g)$$

From exhaustive vaporization experiments, we have found that even though evaporation rates increase slowly with increasing coverage of gallium liquid on the crystal face, virtual steady state rates can be obtained for more than five hours at temperature T = 850°C, a time span that is much longer than needed to complete a rate measurement. This indicates that the liquid gallium coverage can be assumed to stay constant for the usual experimental time of 0.5 - 2.5 hours. Thus the initial vaporization rates are reproducible and we could obtain an activation energy of vaporization. From our microbalance studies, we obtained the average activation energy of vaporization, $\Delta H^* = 90 \pm 3$ kcal/mole. The average activation energies of vaporization were identical for both (111) and $(\bar{1}\bar{1}\bar{1})$ crystal faces.

The vapor compositions of emanating from the vaporizing Ga face and As face are found to be different. For the vaporization from Ga face, we found predominantly As_4 molecules whereas the vaporization of As face yields both As_2 and As_4 molecules in comparable quantities. Liquid gallium does not seem to affect the vapor compositions significantly, i.e., we still

observe only the As_4 molecules for Ga face and both As_2 and As_4 molecules for As face. Thus the vapor compositions emanating from the two crystal faces do not change with increasing concentrations of liquid gallium on the surfaces even though that excess liquid gallium increases the evaporation rate by a factor of two.

In spite of the different vapor compositions found for the two crystal faces, the fact that the initial rates and the activation energies of vaporization are the same for both Ga and As faces, with and without the excess liquid gallium on top of the vaporizing surface, indicates that the rate-limiting step for evaporation is the same for both faces. This rate-limiting step then must be followed by another more rapid reaction step that establishes the vapor compositions of the two opposing faces. The latter step is different for the two faces and thus depends on the different surface structures of the (111) and $(\bar{1}\bar{1}\bar{1})$ crystal faces. Thus we can distinguish at least two steps in the sequence of reactions leading to vaporization.

In order to verify the rate-limiting step let us review those experimental parameters that influence this slowest step in the process of evaporation and thereby change the absolute vaporization rates and/or the activation energy.

First of all, we observe that gallium liquid increases the vaporization rates <u>without</u> changing the activation energy. This catalytic effect of liquid metals or evaporation has been observed before (Tl on As[20] and Ga and In on GaN).[2] Catalysis by liquid metals is also well documented in the reverse process, i.e., in condensation or crystal growth.[25] This catalytic effect may be attributed to one of the following reasons: (1) liquid metal provides electrons at the surface that faciliatate charge

transfer during vaporization or condensation, (2)liquid metal dissolves the vaporizing or the condensing species and thus provides an alternate route for evaporation or crystal growth, (3) liquid metal changes the defect concentrations at the surface that might play an important role in vaporization or condensation. Since liquid metal increases the absolute evaporation rates of gallium arsenide and arsenic crystals, the concentrations of these surface defect sites must be increased by liquid metal if the latter effect is the cause of this catalytic behavior.

Secondly, we observed that both Zn or Te when present in the GaAs crystal lattice decreased the vaporization rates. Furthermore, the activation energy of Zn-doped samples are lowered in comparison to that of pure samples. ΔH^* (Zn-doped) = 76±5 kcal/mole and ΔH^*(pure) = 90±3 kcal/mole. Due to the relatively low concentrations of these impurities in the crystal ($\approx$ 0.1 atom %) it is very unlikely that the lowering of the vaporization rates is caused by the blocking of the GaAs surfaces by foreign atoms. Both Zn and Te could also form compounds in GaAs lattice, e.g. Zn_3As_2 and Ga_3Te_2. However these compounds have higher vapor pressures[26] and consequently are expected to have higher vaporization rates than GaAs. In addition, in the temperature range of our study, the bulk diffusion rates of both Zn and Te (Fig. 37)[27] are much lower than the evaporation rates so that the impurity concentrations throughout the crystal would remain virtually constant, as indicated by the conductivity measurements before and after each experiment (Section IV, Experimental Results).

Te impurities in GaAs produce donor states (ionization energy = 0.02 eV)while Zn impurities introduce acceptor states (ionization energy = 0.08 eV). Doping the samples with these elements will change the free carrier concentrations and the type of majority free carriers (electrons or holes).

In addition, these impurities also change the vacancy concentrations of GaAs crystals. Both Te and Zn are known to enter into the crystal lattice substitutionally,[27] i.e.,

$$V_{As} + Te_{(surface)} \rightarrow Te_{As}$$

$$V_{Ga} + Zn_{(surface)} \rightarrow Zn_{Ga}$$

where the subscripts denote the sites being occupied by the atoms and V_{As} and V_{Ga} are the unionized arsenic and gallium vacancies, respectively. In effect, doping the GaAs crystals with impurities will decrease the concentrations of one of the two types of vacancies. Since these impurities are introduced during crystal growth at high temperatures, equilibria among defects can easily be established. We can then apply Schottky defect equilibrium condition:

$$N.O. \rightarrow V_{Ga} + y\, V_{As}$$

where N.O. is the density of normally occupied atom sites. (V_{Ga}) and (V_{As}) will always be orders of magnitude smaller than the concentration of N.O., thus the normally occupied site density could be assumed to remain constant when the vacancy concentrations change. We then have

$$(V_{Ga})^x\ (V_{As})^y = K_s$$

where K_s is the Schottky disorder constant.

Charge transfer has been found to be the rate - limiting step in the evaporation of pure CdS single crystals.[7] The activation energy for vaporization (50 kcal) was found to be similar to the band gap energy (2.41 eV). However, if this were also the rate - limiting step in evaporation of GaAs, we would expect an activation energy similar or equal to the band gap energy (1.4 eV or 32 kcal). The observed activation energy

(90 kcal) is much greater than the band gap energy. It seems unlikely that the rate-limiting step for vaporization would be related to the electronic properties of pure GaAs. Furthermore, the difference in activation energies of vaporization (~15 kcal or 0.6 eV) between Te-doped and Zn-doped GaAs samples is much too great to be attributed to the difference in the position of the donor and the acceptor levels within the band gap or any other electrical properties of these impurities in the GaAs crystal lattice. At the temperatures of our studies (700°C-900°C) all of the impurities are expected to be ionized because of the shallow ness of these levels. In addition, crystals with different charge carrier concentrations have been found to have the same vaporization rates. Therefore, we conclude that Ga(ℓ), Te, and Zn in GaAs crystal lattice do not influence the vaporization rates by changing its electronic properties.

The vapor compositions over the vaporizing gallium and arsenic crystal faces remained unchanged when liquid gallium was placed on top of the surface. Also liquid gallium has not changed the activation energies of vaporization of the different Zn and Te-doped crystal samples. Thus, it appears that liquid gallium does not change the reaction path, i.e. does not provide alternate route for the vaporization reaction. Therefore we conclude that Ga(ℓ), Te and Zn in the GaAs crystal lattice influence the evaporation rate by <u>changing the defect concentrations at the surface</u>. While the arsenic atoms associate and are subsequently removed into the vapor phase the gallium atoms precipitate out in the form of liquid at the surface due to their low vapor pressure. We propose that the rate of vaporization is limited by the rate of formation of divacancies (V_{Ga} V_{As}) at the vaporizing surface. That is the observed

activation energy of vaporization is that energy necessary to remove simultaneously on arsenic <u>and</u> a gallium atom from the crystal lattice.

$$Ga_{Ga} + As_{As} \rightarrow [V_{Ga}\ V_{As}] + Ga_{(surface)} + As_{(surface)}$$

The solubilities of either gallium or arsenic in GaAs are very limited.[28] Therefore, every time an arsenic atom (gallium atom) leaves the lattice, a gallium atom (arsenic atom) would leave the lattice as well. We may separate this reaction into two steps:

(1) The formation of single vacancies

$$Ga_{Ga} \rightarrow V_{Ga} + Ga_{(surface)}$$

$$As_{As} \rightarrow V_{As} + As_{(surface)}$$

(2) The association of the single vacancies to form the divacancies

$$V_{Ga} + V_{As} \rightarrow [V_{Ga}\ V_{As}]$$

In our vaporization studies, we have found lower vaporization rates for crystals doped with Te or Zn. Te in GaAs lattice reduces the V_{As} concentration and Zn in GaAs lattice reduces V_{Ga} concentration. A decrease in either V_{Ga} (Zn-doped samples) or V_{As} (Te-doped samples) will result in a decrease in $[V_{Ga}\ V_{As}]$, giving rise to a lower rate. In the case of vaporization of pure samples where we seem to have optimum concentrations of V_{Ga} and V_{As} for pairing, we find high vaporization rates. It is likely that in an undoped gallium arsenide single crystal, we have predominantly V_{Ga}.[33] In other words, we would be limited by the concentration of arsenic vacancies in the vaporization of pure gallium arsenide crystals. The formation of divacancies would be independent of small variations in charge carrier concentrations in the pure crystals. Thus, as

expected, we found identical rates in vaporization of samples obtained from two different companies (with different carrier concentrations).

Koster and Thoma have made extensive studies on the phase diagram of the gallium-arsenic system.[29] It was found that GaAs does not dissolve significantly in liquid gallium. The diffusion of Ga into the crystal lattice is extremely slow,[27] consequently, during the time that is required to measure vaporization rates, little or no gallium is expected to be incorporated into the lattice. In our experiments, we have observed that excess liquid gallium on top of the vaporizing surface increases the rates with the activation energies remaining the same as those without the excess gallium on. This effect could be explained by the fact that even though GaAs does not dissolve in liquid gallium to any great extent, the small but finite solubility (ppm) of the molecular GaAs in Ga(ℓ) increases the surface concentration of divacancies ($[V_{Ga}V_{As}]$), thereby increasing the rates of evaporation. Thus the observed transient vaporization before the onset of steady state vaporization is probably due to the accumulation of liquid gallium which slowly changes the concentration of associated vacancies on the crystal surface. The virtual steady state rates then correspond to an approximately constant coverage of the surface area by gallium droplets.

We have found differences in the activation energies of vaporization of Zn-doped crystals and pure or Te-doped crystals. There is a great deal of evidence that Zn in the GaAs crystal lattice associates with divacancies.[34] Thus it is not surprising that the energy of formation

of a divacancy in the presence of Zn in the crystal lattice is different than that for the pure samples. Te impurity does not seem to associate with divacancies or change their formation energy.

Kendall et al.[35] have studied the self-diffusion in InSb. He has proposed that the In:Sb divacancy is the defect primarily responsible for self-diffusion of both components in InSb. The enthalpy of formation for the divacancy is estimated to be about 3.2 eV and that of the single vacancies is 1.76 eV. The energy for atomization of InSb has been reported as 5.52 eV. Thus the formation energy for divacancies is about 58% of the energy for atomization. The energy for atomization of GaAs is reported to be 156 kcal/mole.[22] Therefore the activation energy (90 kcal/mole) we found would be too high as the energy of formation for single vacancies. In addition, there is good agreement in the ratio we found for divacancy formation and atomization energy in both InSb and GaAs (approx. 58%).

The diffusion rates of Sn in GaAs have been studied and were found to be similar to that of Zn (Fig. 37).[27] The activation energies for diffusion of Sn or Zn in GaAs are very similar ($E_D \approx 2.5$ eV). Thus it is not surprising that we find the same activation energies of vaporization of GaAs in the presence of excess liquid tin on the vaporizing surface as those found for the vaporization of Zn-doped GaAs crystals ($\approx$ 76 kcal/mole). It appears that Sn atoms, when entering the GaAs crystal lattice at the vaporizing surface, affects the vacancy concentrations of the host lattice the same way as Zn atoms.

Since the (111) and ($\bar{1}\bar{1}\bar{1}$) faces of III A-VA compounds are known to behave differently under a variety of experimental conditions, e.g.

chemical dissolution,[9] adsorption and desorption of molecules,[8] LEED studies,[30] one might suspect that the surface structural differences will also play an important role in their mechanisms of vaporization. The fact that we obtained the same evaporation rates for both the gallium face and the arsenic face implies that the surface configurations do not influence the rate-limiting step. However, we obtained different compositions for the two opposing faces. This suggests that the surface structures do influence the formation of vapor molecules even though this step is not rate-limiting. In the case of evaporation from Ga face (Fig. 38) we can see that all the As atoms that would form the tetrahedral unit are available for vaporization (i.e., none of the As atoms are blocked by Ga atoms on top). When an As_4 molecule finally forms, it could desorb immediately. This is not the case for As face (Fig. 39). Three of the As atoms that would form the tetrahedral unit have Ga atoms directly on top of them. This will make the formation and subsequent removal of the As_4 molecules difficult. Consequently, some of the surface As atoms have opportunity to form As_2 units and vaporize. Thus, the effect of steric hinderance for the formation of As_4 molecules in the As face could then provide a clue in the observation of different vapor compositions from different faces.

It will be interesting to speculate how do the As_4 molecules form at the surface. In the vapor phase, the bond angle and bond distance for the tetrahedral As_4 molecules are 60° and 2.44Å, respectively.[31] In gallium arsenide crystals, the As_4 unit has bond angles and bond distances of 60° and 3.99Å, respectively.[32] Thus the bond distances of As_4 unit in the crystal lattice have to change drastically in vaporization to form gaseous As_4 molecules. This process may require a certain configuration of neigh-

boring vacancies, thereby breaking up the regular arrangement of bonds and making it much easier for the As atoms to vibrate into the tetrahedral configuration which is required for vaporization. Further studies would have to be carried out before any definite proposals on the structures of the complex can be made.

VI. PROPOSED VAPORIZATION MECHANISM OF GALLIUM ARSENIDE SINGLE CRYSTALS

Utilizing all of the experimental evidence, a model for the vaporization mechanism of gallium arsenide single crystals can now be proposed.

The formation of lattice vacancies during vaporization can be written as:

$$Ga_{Ga} \rightleftharpoons V_{Ga} + Ga_{(surface)} \qquad \text{VI.1}$$

$$As_{As} \rightleftharpoons V_{As} + As_{(surface)} \qquad \text{VI.2}$$

where the subscripts indicate the sites that are being occupied by the different species. The vacancy concentrations for a given crystal (doped or undoped) follow the Schottky defect equilibria:

$$(V_{Ga})^x(V_{As})^y = K_s$$

where K_s is the Schottky disorder constant.

The next step in the vaporization mechanism is the association of the two single vacancies V_{Ga} and V_{As} to form vacancy pairs (divacancies)

$$V_{Ga} + V_{As} \rightarrow [V_{Ga}V_{As}].$$

Experimentally we cannot detect these two steps separately. Consequently, we can only deduce a general step:

$$Ga_{Ga} + As_{As} \rightarrow Ga_{(surface)} + As_{(surface)} + [V_{Ga}V_{As}]$$

We have proposed this particular step to be the rate-limiting step in the vaporization of gallium arsenide single crystals and the activation energy we measured experimentally corresponds to the formation energy of a divacancy in the crystal. At the temperatures of our studies the divacancies could be significant concentrations. Divacancies may in the bulk or on the surface and they can interact by diffusion

$$[V_{Ga}V_{As}]_{bulk} \rightleftharpoons [V_{Ga}V_{As}]_{surface}$$

The surface atoms need a specific configuration (i.e. formation of an activated complex, e.g. $n([V_{Ga}V_{As}]_{surface}\ 4\ As_{surface})$ before it can desorb. Limited to the different surface structural arrangements of gallium and arsenic atoms on the two opposing faces, we can then obtain different vapor composition from evaporation.

For gallium face, we have

$$Ga_{(surface)} \rightleftharpoons Ga_{(liquid)}$$

$$n\ V_{Ga}V_{As} \bullet 4\ As \rightleftharpoons As_{4(surface)}$$

$$As_{4(surface)} \rightleftharpoons As_{4(vapor)}$$

For arsenic face, we have

$$Ga_{(surface)} \rightleftharpoons Ga_{(liquid)}$$

$$n'V_{Ga}V_{As} \bullet 2As \rightleftharpoons As_{2(surface)}$$

$$As_{2(surface)} \rightleftharpoons As_{2(vapor)}$$

$$n\ V_{Ga}V_{As} \bullet 4As \rightleftharpoons As_{4(surface)}$$

$$As_{4(surface)} \rightleftharpoons As_{4(vapor)}$$

APPENDIX I

Corrections for Fragmentations of Arsenic Molecules

Fragmentation of As_4 molecules from vaporization of pure arsenic crystals at 500°K and 1.5×10^{-7} torr.

As_2/As_4	As_3/As_4	As/As_4
0.50	0.11	0.21

*

For vaporization of gallium (111) face of gallium arsenide single crystals, we obtained the ratios

T(°C)	As_2/As_4	As_3/As_4	As/As_4
728	0.47	0.12	0.20
758	0.59	0.11	0.16
758	0.44	0.08	0.14
780	0.52	0.09	0.10
780	0.49	0.09	0.15
838	0.48	0.07	0.14
832	0.44	0.07	0.12
782	0.51	0.09	0.12
730	0.48	0.09	0.14

*The ratios are taken directly from intensity measurements.

T(°C)	As_2/As_4	As_3/As_4	As/As_4
726	0.54	-	-
781	0.50	0.11	0.27
781	0.49	0.09	0.29
781	0.45	0.13	0.23
783	0.48	0.15	0.22
832	0.49	0.12	0.23
843	0.50	0.13	0.22
808	0.50	0.12	0.18
808	0.46	0.10	0.16
808	0.51	0.11	0.20
808	0.52	0.12	0.21
775	0.61	0.11	0.25
723	0.47	0.14	0.22

and with excess liquid gallium placed on top of the vaporizing surface, we have

T(°C)	As_2/As_4	As_3/As_4	As/As_4
656	0.50	-	-
738	0.49	-	-
739	0.55	0.11	0.22
774	0.50	0.10	0.24
797	0.47	0.10	0.17
822	0.61	0.11	0.19
760	0.46	0.13	0.31
825	0.56	0.12	0.24

continued

T(°C)	As_2/As_4	As_3/As_4	As/As_4
815	0.50	0.10	0.16
817	0.50	0.12	0.19
786	0.49	0.16	0.26
756	0.51	0.16	0.24
721	0.40	0.17	0.23
679	0.42	-	0.25

Careful inspection of these ratios tells us that they are, within our experimental accuracy, identical to the ones we have obtained from vaporization of pure arsenic crystals. Thus we can conclude that the peaks we have detected for As, As_2 and As_3 on vaporization of gallium (111) face of gallium arsenide single crystals are products of fragmentations from As_4 molecules. In other words, we have only the tetramers from the vaporization of gallium face.

For vaporization of arsenic ($\bar{1}\bar{1}\bar{1}$) face of gallium arsenide single crystals, we obtained the ratios for the intensities measured:

T(°C)	As_2/As_4	As_3/As_4	As/As_2
746	3.56	-	-
806	0.93	0.10	0.27
807	0.83	0.09	0.26
809	0.74	0.09	0.27
809	0.71	0.10	0.29
809	0.73	0.11	0.26
842	0.71	0.09	0.30
798	0.78	0.11	0.26
746	0.81	-	0.25

T(°C)	As_2/As_4	As_3/As_4	As/As_2
698	1.12	-	-
727	1.28	0.06	0.28
765	1.07	0.06	0.16
821	0.81	0.08	0.25
824	0.94	0.10	0.23
803	0.79	0.07	0.17
803	0.86	0.09	0.20
803	0.81	0.09	0.24
763	0.73	0.05	0.20
731	1.10	0.13	0.16
706	0.98	0.10	0.16
702	0.80	0.13	0.22

T(°C)	As_2/As_4	As_3/As_4	As/As_2
685	1.40	-	-
713	1.46	-	0.27
751	1.38	0.11	0.24
784	1.06	0.08	0.20
785	1.06	0.10	0.20
817	1.03	0.09	0.21
842	0.99	0.13	0.32
820	1.12	0.12	0.27
820	0.99	0.10	0.27
820	1.14	0.12	0.31
733	1.11	0.13	0.25
730	1.35	0.14	0.20
726	1.37	0.11	0.17

After we placed excess liquid gallium on top of the vaporizing surface, we found

T(°C)	As_2/As_4	As_3/As_4	As/As_2
638	2.46	-	-
690	3.01	-	-
697	3.09	0.14	0.30
734	3.61	0.06	0.26
734	3.52	0.08	0.22
781	1.94	0.14	0.21
779	1.78	0.11	0.23
779	1.59	0.08	0.23
825	1.23	0.09	0.26
825	1.13	0.09	0.30
816	1.08	0.09	0.27
816	1.10	0.10	0.27
771	1.05	0.14	0.26
771	1.04	0.07	0.28
715	3.27	-	0.20

Part of the intensities we have measured for As peak came from the fragmentation of As_4 molecules. The ratio As (from As_4)/As_4 should remain constant throughout the entire temperature range. Part of the As_2 peaks were also fragments of As_4 molecules. The ratio As_2 (from As_4)/As_4 should also be constant

$$\frac{As\ (\text{from } As_4)}{As_4} \times \frac{As_2\ (\text{from } As_4)}{As_4} = \text{const.}$$

$$\frac{As\ (\text{from } As_4)}{As_4} \times \frac{As_4}{As_2\ (\text{from } As_4)} = \text{const.}'$$

$$\frac{As(\text{from } As_4)}{As_2\ (\text{from } As_4)} = \text{const.}'$$

If the remaining intensity of an As peak were completely due to fragmentation of As_2 molecules, then the ratio of As (from As_2)/As_2 (from vaporization) will be constant.

$$\frac{As\ (\text{from } As_2)}{As_2\ (\text{from vap.})} + \frac{As\ (\text{from } As_4)}{As_2\ (\text{from } As_4)} = \text{const.}$$

Since the part of As_2 that is fragmented from As_4 does not contribute to the fragmentations to As molecules, these two ratios will remain independent of each other. Thus we have:

If As/As_2 = const., the As peak can be entirely attributed to fragmentations of higher molecular weight species. To our experimental accuracy, this seems to be the case for vaporization of arsenic face of gallium arsenide single crystals, i.e. we do not have As molecules in our vapor.

Looking at the ratios obtained from vaporization of arsenic face of gallium arsenide single crystals, the values of As_2/As_4 are bigger than 0.5, which is the ratio we have found for the fragmentation of As_4 to As_2. Thus, we can safely conclude that the intensities we have detected for As_2 molecules, in addition to the contribution from fragmentation of As_4 molecules, also include the ionization of neutral As_2 molecules directly from vaporization.

The values for As_3/As_4 remain practically constant throughout the entire temperature range, suggesting that As_3 is a product of fragmentation.

To summarize the results so far: we have found that the vaporization of gallium (111) face yield only the tetramer (As_4) molecules whereas for arsenic ($\bar{1}\bar{1}\bar{1}$) face, both the dimers (As_2) and the tetramers (As_4) are found.

Based on the ratios we have found from vaporization of arsenic crystals, we can now correct for the contribution of fragmentations of As_4 to the intensities measured experimentally.

Using

$$\frac{As_2}{As_4} = 0.50$$

$$\frac{As_3}{As_4} = 0.10$$

$$\frac{As\ (\text{from } As_4)}{As_4} = 0.20$$

We have for the correction of As_4 intensities:

$$As_4 = As_4\ (\text{measured})\ [1 + 0.50 + 0.10 + 0.20]$$

$$= As_4\ (\text{measured}) \times 1.80$$

Knowing the ratios

$$\frac{As\ (\text{from } As_4)}{As_4}$$

and

$$\frac{As_2}{As_4}$$

and that the As intensities we found are all from fragmentations of As_2 and As_4, we can then find the ratio

$$\frac{As\ (\text{from vaporized } As_2)}{As_2\ (\text{vaporized})},$$

which is equal to 0.20. Now we can correct for the intensities of As_2 peaks:

$$As_2 = [As_{2(meas)} - As_{4(meas)} \times 0.50]\ (1 + 0.20)$$

$$= [As_{2(meas)} - As_{4(meas)} \times 0.50]\ (1.20)$$

It is also very interesting to note that, from Table III, we obtained

$$As_4^+ \rightarrow As_3 + As^+ \qquad 5.19 \text{ eV}$$
$$As_2^+ \rightarrow As + As^+ \qquad 3.89 \text{ eV}$$

Thus, As_2^+ makes a bigger contribution to the As peak than As_4^+, which is what we have found in our experiment.

APPENDIX II

A Method to Find the Ratio of the Ionization Cross Sections for As_2 and As_4

Definition of the symbols used:

P_i = pressure

subscript D = dimer

subscript T = tetramer

R = total vaporization rate

R_G = gas const.

T = temperature

M = average molecular weight in the vapor phase

I_i = intensities detected

α_i = conversion factor from intensity to pressure

σ_i = ionization cross section

γ_i = yield of the electron multiplier

f_i = transmission probability of the mass spectrometer

K = instrumental const. depending on the distance from sample to ionizer and the length of the electron beam crossed by the molecular beam.

$$P_{total} = P_D + P_T$$

$$R\left(\frac{mg}{cm^2\text{-sec}}\right) = \frac{P_{total}}{\left(\frac{2\pi R_G T}{M}\right)^{1/2}}$$

$$P_D = \alpha_D I_D T$$

$$P_T = \alpha_T I_T T$$

$$R\left(\frac{2\pi R_G T}{M}\right)^{1/2} = \alpha_D I_D T + \alpha_T I_T T$$

$$M = \frac{P_D}{P_D + P_T} M_D + \frac{P_T}{P_D + P_T} M_T$$

$$M = M_D \left[\frac{\alpha_D I_D T}{\alpha_D I_D T + \alpha_T I_T T} + \frac{2\alpha_T I_T T}{\alpha_D I_D T + \alpha_T I_T T}\right]$$

$$R(2\pi R_G T)^{1/2} M_D^{-1/2} = \left[\alpha_D I_D T + \alpha_T I_T T\right]^{1/2} \left[\alpha_D I_D T + 2\alpha_T I_T T\right]^{1/2}$$

$$R^2 \left(\frac{2\pi R_G T}{M_D}\right)\left(\frac{1}{I_T T}\right) = \left[\alpha_D \frac{I_D}{I_T} + \alpha_T\right]\left[\alpha_D \frac{I_D}{I_T} + 2\alpha_T\right]$$

Thus, knowing the total vaporization rates and the vapor compositions at different temperatures, we can then determine $\alpha_D + \alpha_T$

$$P_i = \alpha_i I_i T$$

$$= K \frac{I_i T}{\sigma_i \gamma_i f_i}$$

$$\alpha_i = \frac{K}{\sigma_i \gamma_i f_i}$$

Since the instrumental constant K does not change for different vapor species

$$\frac{\alpha_D}{\alpha_T} = \frac{\sigma_T \gamma_T f_T}{\sigma_D \gamma_D f_D}$$

Using xenon isotope spectrum, we can determine the ratio f_T/f_D. The yield of the electron multiplier γ_i can be individually calibrated for different vapor species. Thus knowing α_D/α_T, we can then determine σ_T/σ_D, the ratio of the ionization cross sections. As a check for the value of α_T calculated since only the tetramer molecules are detected for gallium face, we could obtain

$$R\left(\frac{mg}{cm^2\text{-sec}}\right) = \frac{P_{total}}{\left(\frac{2\pi R_G T}{M}\right)^{1/2}}$$

$$R_{measured} = \frac{P_T}{\left(\frac{2\pi R_G T}{M_T}\right)^{1/2}}$$

$$P_T = R_{measured}\left(\frac{2\pi R_G T}{M_T}\right)^{1/2}$$

$$\alpha_T I_T T = R_{measured}\left(\frac{2\pi R_G T}{M_T}\right)^{1/2}$$

$$\alpha_T = R_{measured}\left(\frac{1}{I_T T}\right)\left(\frac{2\pi R_G T}{M_T}\right)^{1/2}$$

Substituting in the proper numbers, this should give us the same value for α_T as that found before.

Given:

$$\frac{P_D}{P_T} = \frac{\alpha_D I_D T}{\alpha_T I_T T}$$

$$\frac{P_D}{P_T} = \frac{\sigma_T \gamma_T f_T}{\sigma_D \gamma_D f_D} \frac{I_D}{I_T}$$

It is usually assumed that $\gamma \propto M^{1/2}$, or $\gamma_T/\gamma_D = \sqrt{2}$. From our calibration, $f_I/f_D \approx 1/3$. The ratio of the ionization cross sections σ_T/σ_D is assumed to be 2.

Thus

$$\frac{\sigma_T}{\sigma_D} \frac{\gamma_T}{\gamma_D} \frac{f_T}{f_D} = 2(\sqrt{2})(1/3)$$

$$\simeq 1$$

$\therefore$ we assume in our calculation that

$$\frac{P_D}{P_T} \cong \frac{I_D^+}{I_T^+}$$

ACKNOWLEDGEMENTS

I wish to express my deepest and most sincere gratitude to my research adviser, Professor G. A. Somorjai, for his patient guidance and inspirational discussions during my graduate studies. I am also indebted to the members of my research group and out next door neighbor, Dr. Reggie Powell, for the many informative talks and their helpful suggestions. Particularly, I wish to acknowledge the many stimulating discussions with Dr. G. M. Rosenblatt, Dr. L. Brewer, and Dr. A. W. Searcy.

I am grateful to Emery Kozak for his technical assistance. Special thanks are due to Shirley Ashley, Jane Ball and Gloria Pelatowski for their help in the preparation of this dissertation. Last but not least, I would like to thank my family and my friends for their constant encouragement throughout my graduate work.

This work was performed under the auspices of the United States Atomic Energy Commission.

REFERENCES

1. Z. A. Munir and A. W. Searcy, J. Chem. Phys. 42, 4223 (1965).
2. R. C. Schoonmaker, A. Buhl, and J. Lemley, J. Phys. Chem. 69, 3455 (1965).
3. D. L. Hildenbrand and W. F. Hall, J. Phys. Chem. 67, 888 (1963).
4. G. M. Rosenblatt, P. K. Lee, and M. B. Dowell, J. Chem. Phys. 45, 3454 (1966).
5. G. M. Rosenblatt and P. K. Lee, J. Chem. Phys. 52, 1452 (1970).
6. J. E. Lester, Ph.D. Thesis, University of Calif., Berkeley, UCRL-17794 (1967).
7. G. A. Somorjai, J. E. Lester, J. Chem. Phys. 43, 1450 (1965).
   G. A. Somorjai, H. B. Lyon, J. Chem. Phys. 43, 1456 (1965).
8. J. R. Arthur, to be published.
9. H. C. Gatos and M. C. Lavine, J. Electrochem. Soc. 107, 427 (1960).
10. S. G. Ellis, J. Appl. Phys. 30, 947 (1959).
11. G. A. Somorjai and J. E. Lester in Progress in Solid State Chemistry (Pergamon Press, Oxford, England, 1967), Vol. IV.
12. O. Knacke, I. N. Stranski, Progr. Met. Phys. 6, 181 (1956).
13. R. J. Ackermann, R. J. Thorn and G. H. Winslow in The Characterization of High Temperature Vapors, edited by J. L. Margrave (John Wiley and Sons, Inc., N. Y., 1967). J. P. Hirth, same as above.
14. A. W. Czanderna, J. M. Honig, Anal. Chem. 29, 1206 (1957).
15. Vacuum Microbalance Techniques, Vol. I-IV (Plenum Press, N. Y. 1961).
16. R. D. Freeman and J. G. Edwards in Reference 13.
17. F. Metzger, Helv. Phys. Acta. 16, 323 (1943).
18. H. W. Melville , Trans. Faraday Soc. 32,(1936).

19. B. Goldstein in Compound Semiconductors, V. I. edited by R. K. Willardson and H. L. Goering (Reinhold Publ. Corp., N. Y., N. Y. 1962).

20. L. Brewer and J. S. Kane, J. Phys. Chem. 59, 105 (1955).

21. J. G. White and W. C. Roth, J. Appl. Phys. 30, 946 (1959).

22. J. R. Arthur, J. Phys. and Chem. Solids, Nov., 2257 (1967).

23. G. De Maria, L. Malaspina, and V. Piacente, J. Chem. Phys. 52, 1019 (1970).

24. J. E. Hudson, Ph. D. Thesis, The Pennsylvania State University, (1969).

25. J. R. Arthur, J. Appl. Phys. 39, 4032 (1968).

26. H. Rupprecht and G. Somorjai, IBM Research Note, T. J. Watson Research Center, Yorktown Heights, NC-233.

27. D. L. Kendall in Semiconductors and Semimetals, edited by R. K. Willardson and A. C. Beer (Academic Press, N. Y., N. Y., 1968) Vol. IV.

28. N. N. Sirota, same as in Ref. 27.

29. W. Koster and B. Thoma, Z. Metallk. 46, 293 (1955).

30. A. U. MacRae, Surf. Sci. 4, 247 (1966).
A. U. MacRae, J. Appl. Phys. 35, 1629 (1964).
Jona, IBM J. Res. Div. 9, 375 (1965).

31. L. R. Maxwell, S. B. Hendricks, and V. M. Mosley, J. Chem. Phys. 3, 699 (1935).

32. G. Giesecke in Semiconductors and Semimetals, edited by R. K. Willardson and A. C. Beer (Academic Press, N. Y., N. Y. 1968) Vol. II.

33. D. L. Kendall, private communication.

34. M. B. Parrish and H. C. Casey, Jr., J. Phys. Chem. Solids, 29, 1719 (1968).

35. D. L. Kendall and R. A. Huggins, J. Appl. Phys., 40, 2750 (1969).

TABLE I. Electronic Properties of the Samples Used in Our Studies

Crystal	Doping	Type	Room Temperature		
			ρ(ohm-cm)	μ $\frac{cm^2}{volt\text{-}sec}$	n (no./cm^3)*
Cominco		n	0.105	4.7×10^3	1.3×10^{16}
Bell and Howell		n	0.027	5.0×10^3	4.6×10^{16}
	Zn	p	0.0045	71	1.9×10^{19}
	Te	n	8.4×10^{-4}	2.4×10^3	2.6×10^{18}

*The intrinsic carrier conc. is estimated to be about $9\times10^6/cm^3$ at room temperature.

TABLE II. Xenon Transmission Probability Calibration

Mass No.	124	126	128	129	130	131	132	134	136
Xenon Isotope Ratio	0.096	0.090	1.92	26.44	4.08	21.18	26.89	10.44	8.87
Intensity Measured				8.00		6.80	8.20	2.95	2.92
Intensity Calculated from Isotope Ratio				8.00		6.42	8.15	3.15	3.37
Difference Between (2) and (3)						0.38	0.05	0.20	0.45
Percentage Difference						6%	0.6%	6%	13%
Percentage Difference Per Mass Unit						3%	0.2%	1.2%	1.9%

average value 1.5% decrease per mass unit

TABLE III. Ionization Potentials, Dissociation Energies, and Electronic Affinities of Arsenic Molecules[24]

Ionization Potentials	
As	9.88 eV
As_2	9.86 eV ± 0.16 eV
As_4	8.84 eV ± 0.16 eV
Dissociation Energies at 0°K	
As_2 - As_2	2.98 eV ± 0.18 eV
As - As	3.94 eV ± 0.12 eV
As_3 - As	4.22 eV ± 0.20 eV
As_2 - As	2.70 eV ± 0.20 eV
As_3^+ - As	2.59 eV ± 0.32 eV
As_2^+ - As	5.35 eV ± 0.32 eV
As^+ - As	3.89 eV ± 0.16 eV
Electron Affinities	
As	0.74
As_2	0.35±0.2
As_3	1.1± 0.2

TABLE IV Equilibrium Vapor Pressures of As, As_2, As_3 and As_4 From Vaporization of Arsenic Crystals[24]

T°K	P(As) atm	P(As_2) atm	P(As_3) atm	P(As_4) atm
298	2×10^{-46}	2×10^{-30}	9×10^{-36}	1.04×10^{-17}
400	7×10^{-33}	1×10^{-20}	3×10^{-24}	5.21×10^{-11}
500	5×10^{-25}	6×10^{-15}	2×10^{-17}	3.81×10^{-7}
600	8×10^{-20}	3×10^{-11}	6×10^{-13}	1.31×10^{-4}
700	4×10^{-16}	2×10^{-8}	8×10^{-10}	7.87×10^{-3}
800	3×10^{-13}	2×10^{-6}	2×10^{-7}	1.61×10^{-1}
900	4×10^{-11}	5×10^{-5}	1×10^{-5}	1.61
1000	2×10^{-9}	9×10^{-4}	3×10^{-4}	9.69
ΔH°_{298}	72.1	52.6	62.3	36.15 kcal/mole

TABLE V. Representative Ratios of $P(As_2)/P(As_4)$ From the Vaporization of Arsenic Face of GaAs Single Crystals

T°(C)	P_{As_2}/P_{As_4}*	
1019	2.04	Sample No. 20, Side No. 2 (First Time)
1082	0.15	
1115	0.14	
1071	0.18	
1019	0.20	
978	1.92	

T°(C)	P_{As_2}/P_{As_4}	
971	0.04	
1000	0.52	Sample No. 20, Side No. 2 (Second Time)
1038	0.38	
1097	0.29	
1076	0.20	
1036	0.15	
1004	0.40	
979	0.33	
975	0.19	

T(°K)	P_{As_2}/P_{As_4}	
958	0.61	
986	0.64	Sample No. 22, Side No. 2
1024	0.58	
1058	0.37	
1090	0.36	
1115	0.33	
1093	0.43	
1003	0.56	
999	0.57	

T(°K)	P_{As_a}/P_{As_4}	
911	1.31	
963	1.67	Sample No. 20, Side No. 2
970	1.72	Excess Ga on top (continued on following page)

TABLE V. Continued.

T(°K)	P_{As_a}/P_{As_4}	
1007	2.02	Sample No. 20, Side No. 2
1052	0.73	continued from previous page
1098	0.42	
1089	0.40	
1044	0.36	
986	0.12	
951	0.16	

*These ratios have been corrected for fragmentation. We have also assumed that $I_{As_2^+}/I_{As_4^+} = P_{As_2}/P_{As_4}$. See Appendix II.

TABLE VI. Equilibrium Vapor Pressures and the Corresponding Maximum Vaporization Rates of GaAs Single Crystals[23]

T(°K)	$10^4/T$ (°K)	$P_{As_2} \times 10^6$ (atm)	$P_{As_4} \times 10^6$ (atm)	$P_{total} \times 10^6$ (atm)	$J_{max} \times 10^2$ (mg/cm^2-sec)
1106	9.04	0.76	0.94	1.70	1.02
1119	8.94	0.01	1.04	1.05	0.55
1121	8.92	0.93	1.00	1.93	1.16
1122	8.91	1.05	1.07	2.12	1.29
1129	8.86	1.45	1.71	3.16	1.89
1131	8.84	1.45	1.65	3.10	1.86
1135	8.81	1.86	2.34	4.20	2.49
1151	8.69	3.76	5.46	9.22	5.36
1152	8.68	3.88	5.55	9.43	5.46
1162	8.61	4.43	5.65	10.1	5.92
1163	8.60	4.70	6.00	10.7	6.26
1163	8.60	4.72	6.05	10.8	6.32
1174	8.52	6.84	6.26	13.1	7.85
1186	8.43	7.32	6.68	14.0	8.33
1194	8.38	7.32	6.80	14.1	8.33
1195	8.37	7.34	6.86	14.2	8.42
1197	8.35	8.15	7.20	15.4	9.12

FIGURE CAPTIONS

1. Cubic zinc-blende structure of gallium arsenide single crystals.
2. Gallium and arsenic faces of gallium arsenide after etching in 5% Bi_2 methanol solution for three minutes.
3. Microbalance system.
4. Calibration of furnace temperatures vs. sample temperatures.
5. Temperature profile of the furnace.
6. Mass spectrometer system.
7. Ga face after vaporization at 750°C.
8. Ga face after vaporization at 800°C.
9. Ga face after vaporization at 750°C, then at 800°C and then back at 750°C.
10. As face after vaporization at 750°C.
11. Same crystal face as in Fig. 10 but with the liquid Ga removed.
12. Crystal face after vaporization with excess Ga placed on top of the surface.
13. Unetched Ga face after vaporization at 800°C for 1 hour.
14. Same crystal face as in Fig. 13 where we have a macroscopic ledge serving as sites for thermal pit formation.
15. Edge of the crystal shown in Fig. 13.
16. Same crystal face as in Fig. 15 with liquid Ga removed.
17. Unetched As face after vaporization at 800°C for 1 hour.
18. Exhaustive vaporization of a gallium arsenide single crystal at temperature T = 870°C.
19. Transient vaporization rates of gallium and arsenic faces at 849°C.

20. Total evaporation rates of pure samples from Cominco Corp.

21. Total evaporation rates of pure samples from Bell and Howell Corp.

22. Total evaporation rates of Te-doped samples.

23a. Total evaporation rates of Zn-doped samples.

23b. Vaporization rates from gallium face of Zn-doped samples. (First evaporation of the crystal face.)

24. Total evaporation rates of pure samples with excess Sn placed on top of the surface before vaporization.

25. Background spectrum at pressure 4.0×10^{-8} torr.

26. Appearance potenital curves of various vapor species from vaporization of gallium arsenide.

27. Vapor composition of gallium face over gallium arsenide single crystals from Cominco Corp. Sample No. 20.

28. Vapor composition of gallium face over gallium arsenide single crystals from Cominco Corp. Sample No. 22.

29. Vapor composition of arsenic face over gallium arsenide single crystals from Cominco Corp. (First vaporization of the crystal face) Sample No. 22.

30. Vapor composition of arsenic face over gallium arsenide single crystals from Cominco Corp. (Second vaporization of the crystal face) Sample No. 20.

31. Vapor composition of arsenic face over gallium arsenide single crystals from Cominco Corp. Sample No. 22.

32. Vapor composition of gallium face over gallium arsenide single crystals with excess gallium placed on top of the surface before evaporation. Sample 26.

33. Vapor composition of gallium face over gallium arsenide single crystals with excess gallium placed on top of the surface before evaporation. Sample No. 20.

34. Total vaporization rates of gallium arsenide single crystals using one sample for each temperature and over an extended period of time.

35. Equilibrium vapor pressures of gallium arsenide.

36. Calculated maximum evaporation rates from equilibrium vapor pressures of gallium arsenide.

37. Diffusion coefficients of various impurities in gallium arsenide at low concentration limit.

38. Ga(111) face of gallium arsenide showing the As_4 unit.

39. As($\bar{1}\bar{1}\bar{1}$) face of gallium arsenide showing both the As_2 and the As_4 units.

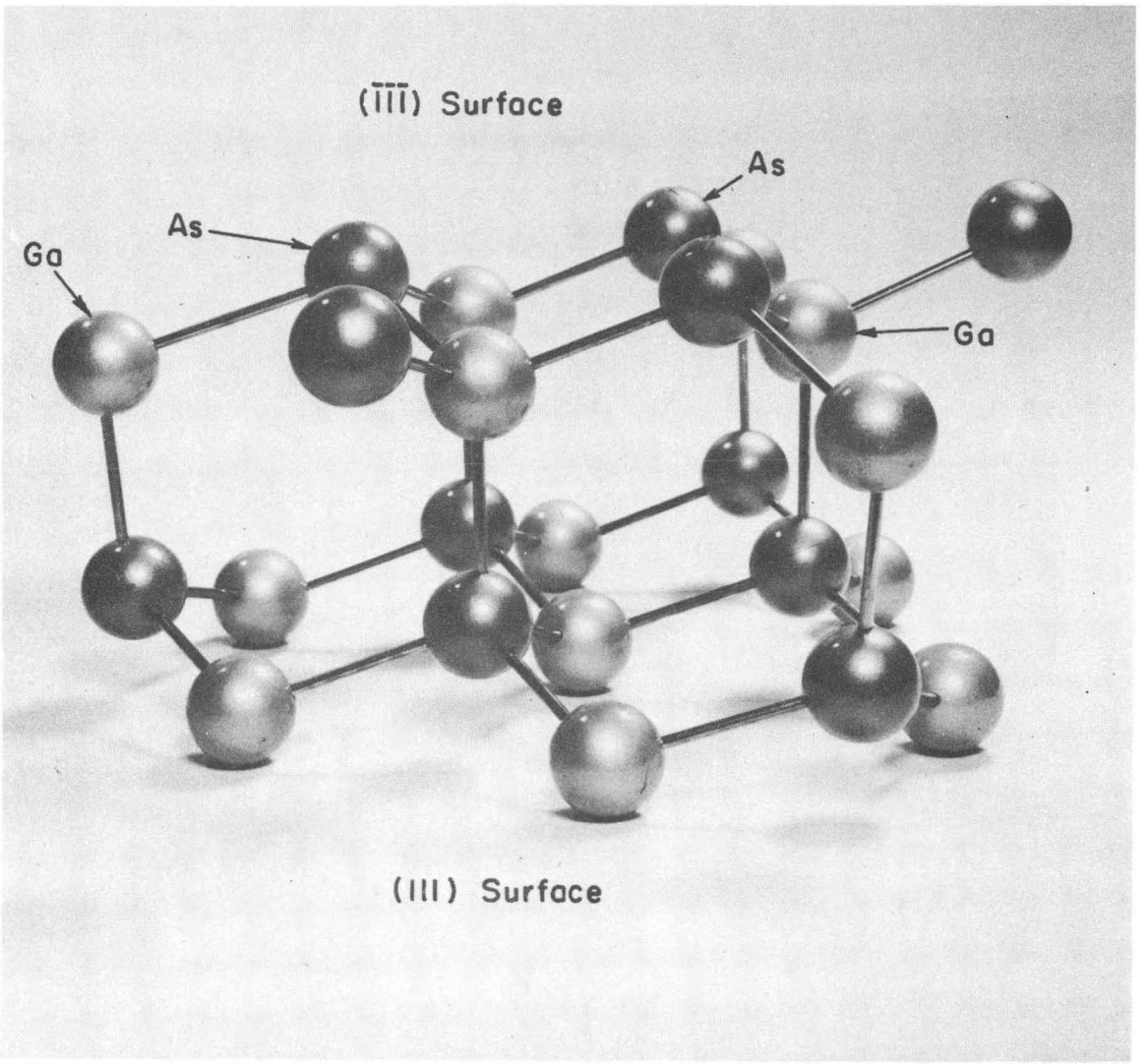

XBB708-3837

Fig. 1.

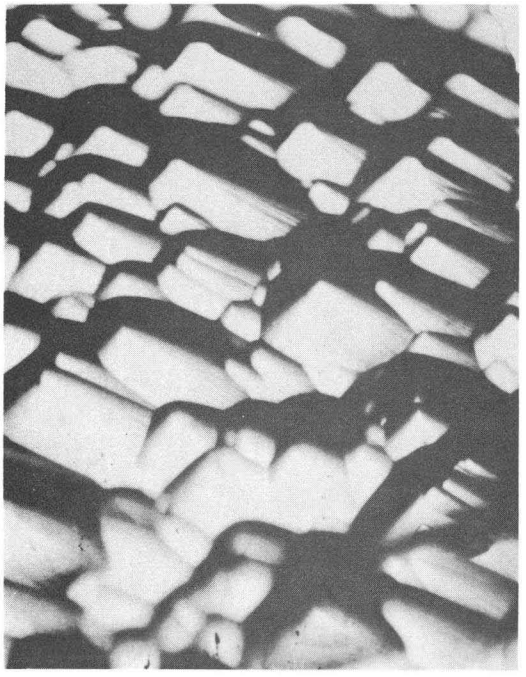

Ga Face

As Face

XBB709-4106

Fig. 2.

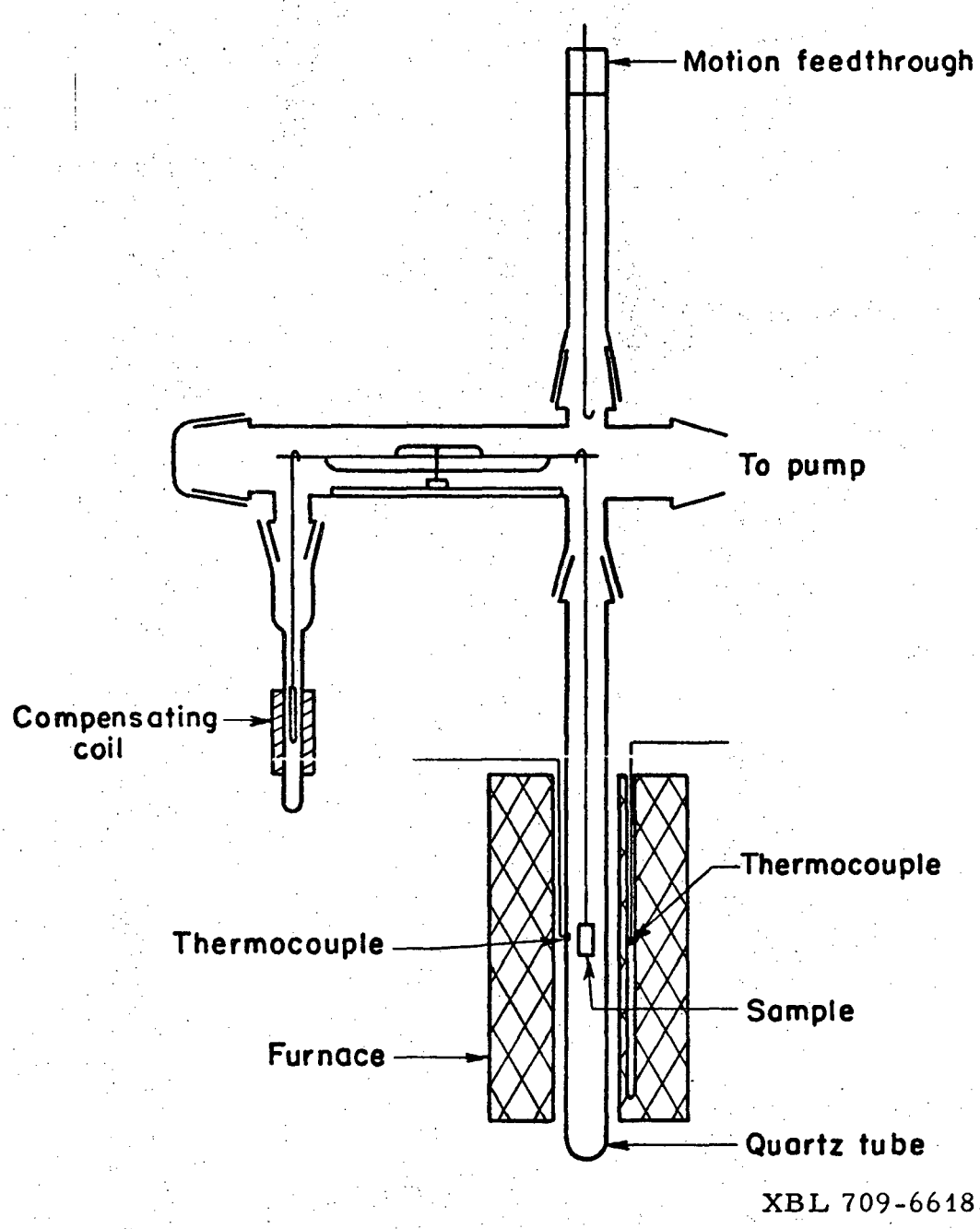
Motion feedthrough
To pump
Compensating coil
Thermocouple
Thermocouple
Sample
Furnace
Quartz tube
XBL 709-6618

Fig. 3.

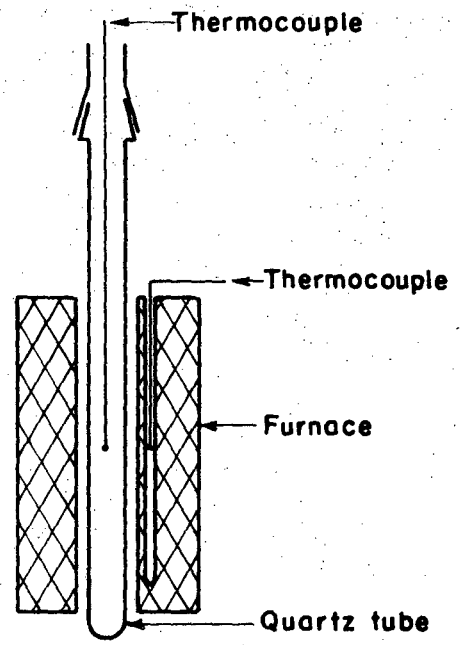

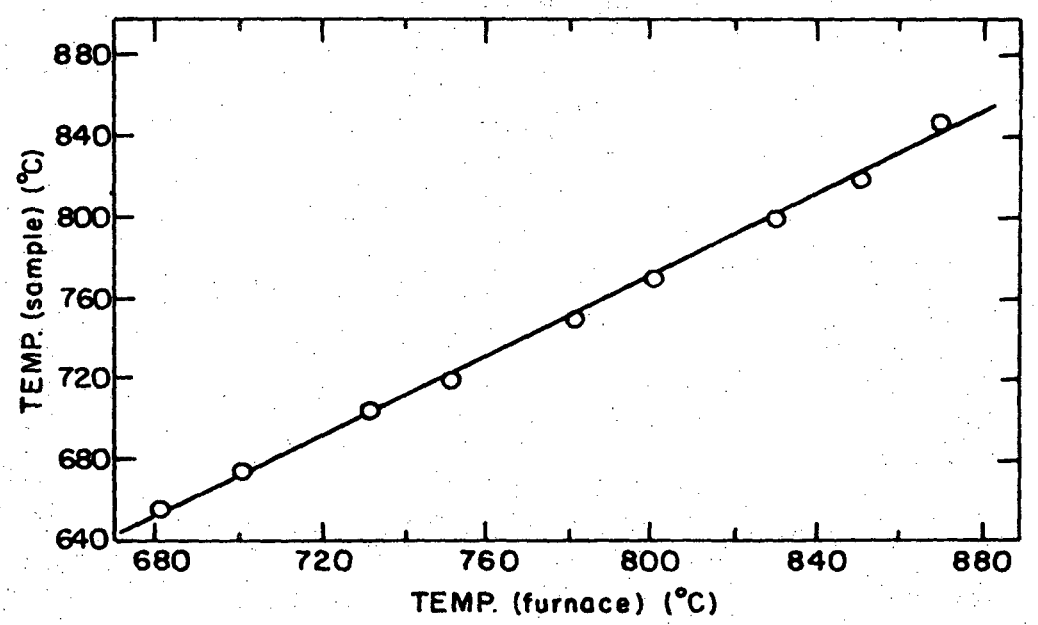

XBL 709-6615

Fig. 4.

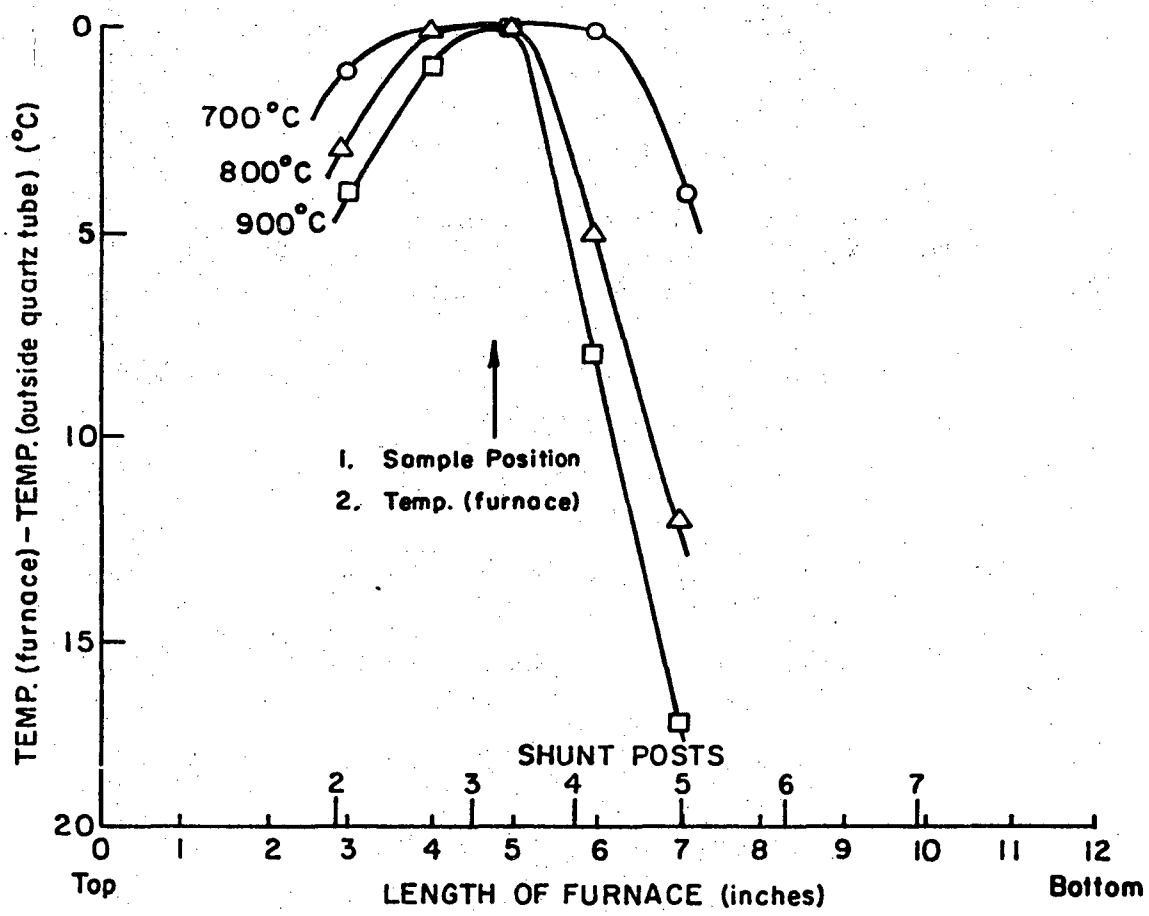

XBL 709-6616

Fig. 5.

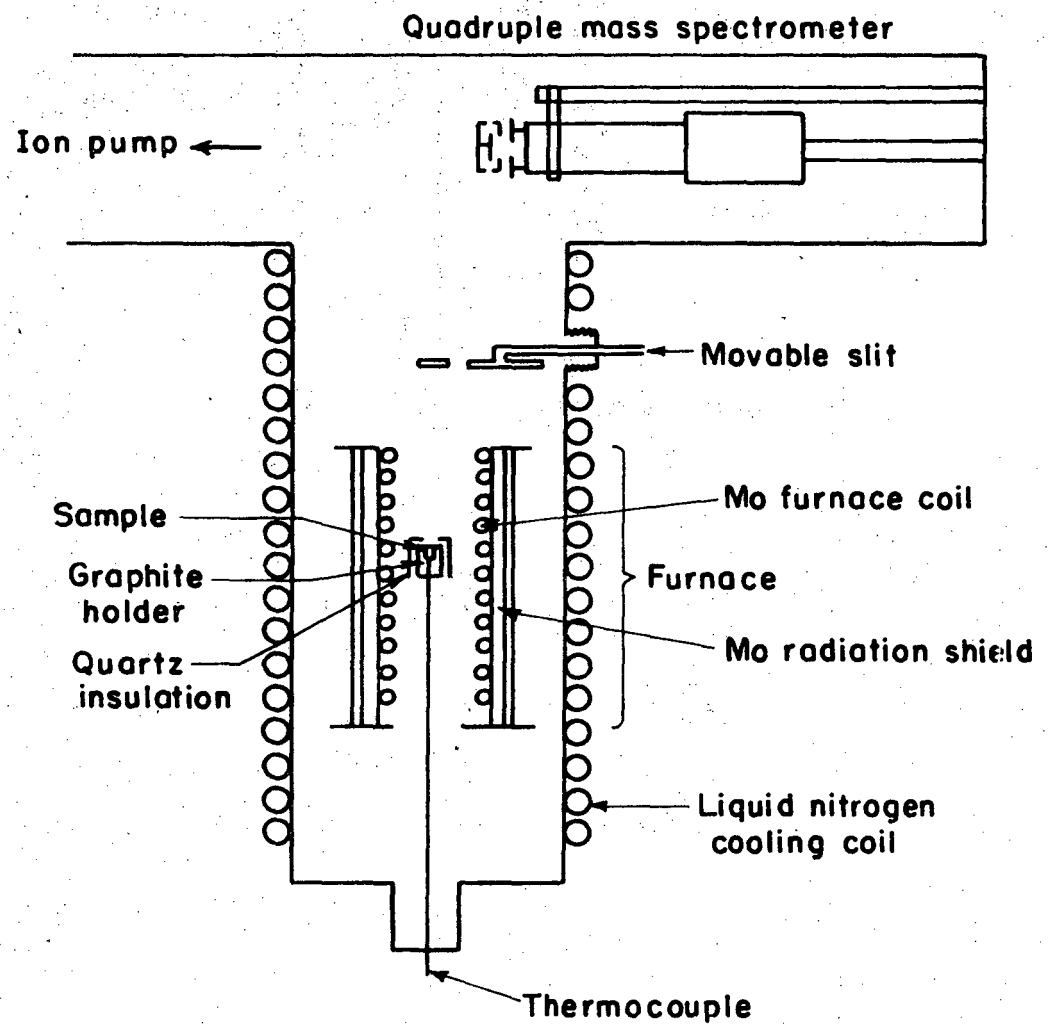

XBL 709-6617

Fig. 6.

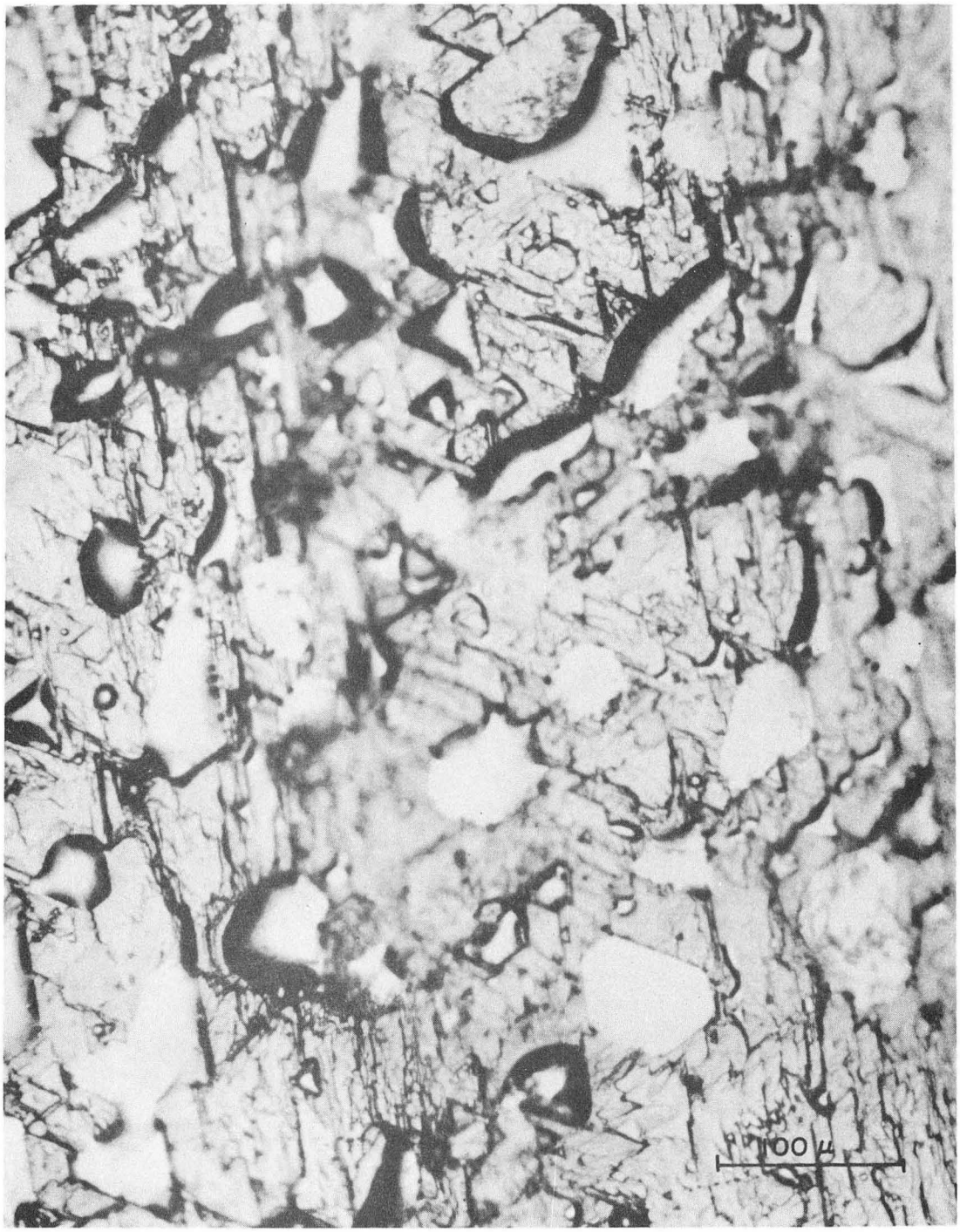

XBB708-3570

Fig. 7.

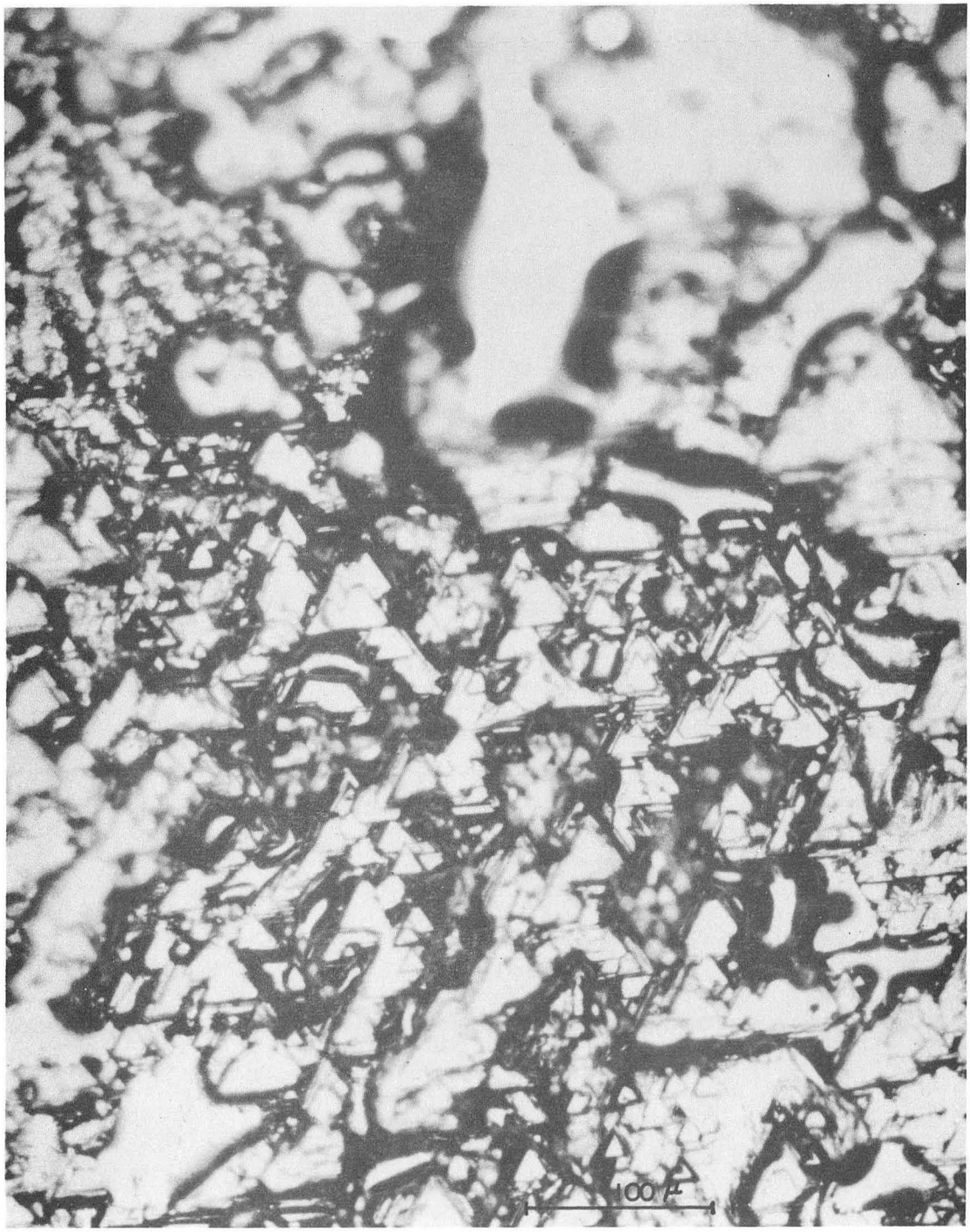

XBB708-3571

Fig. 8.

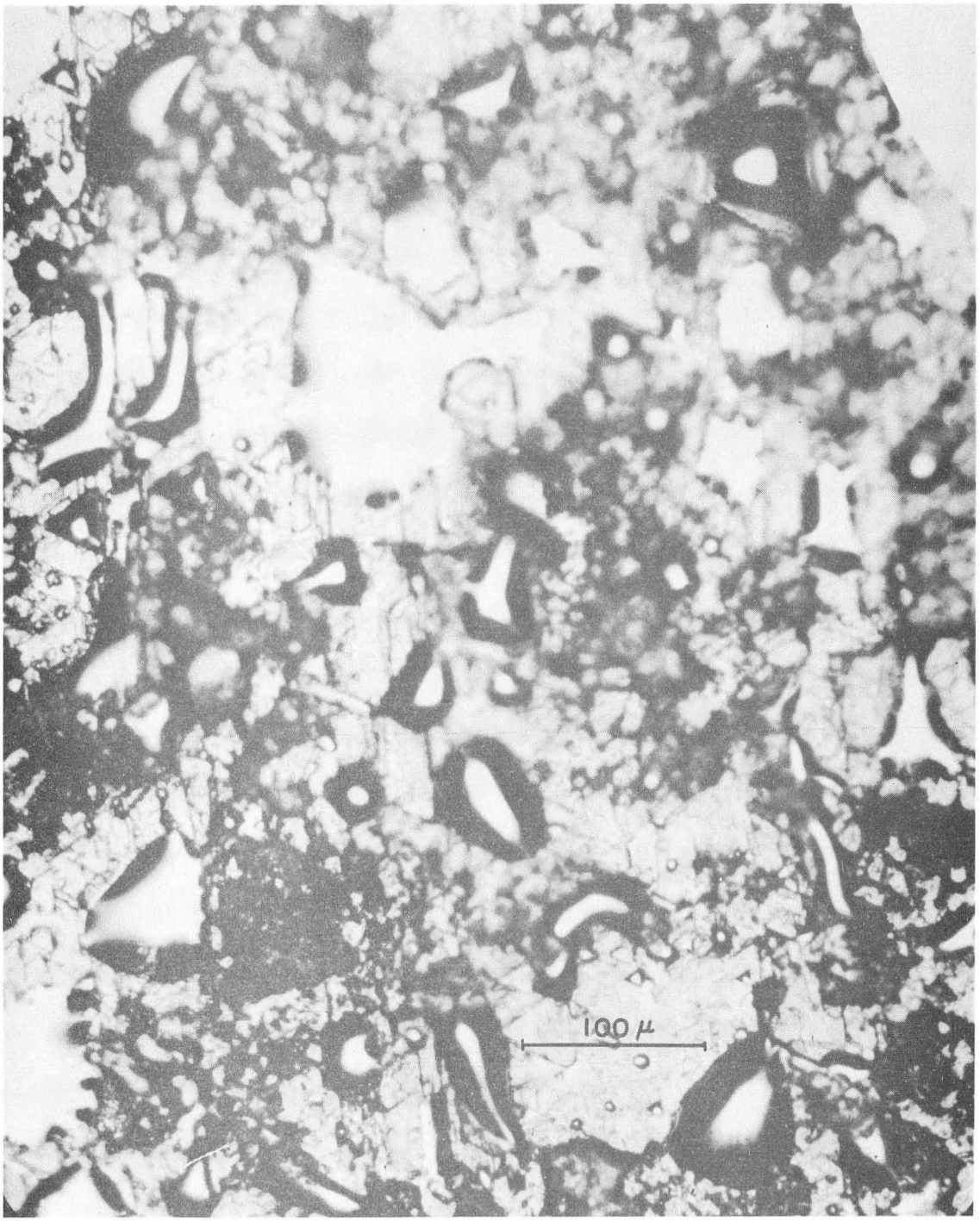

XBB708-3573

Fig. 9.

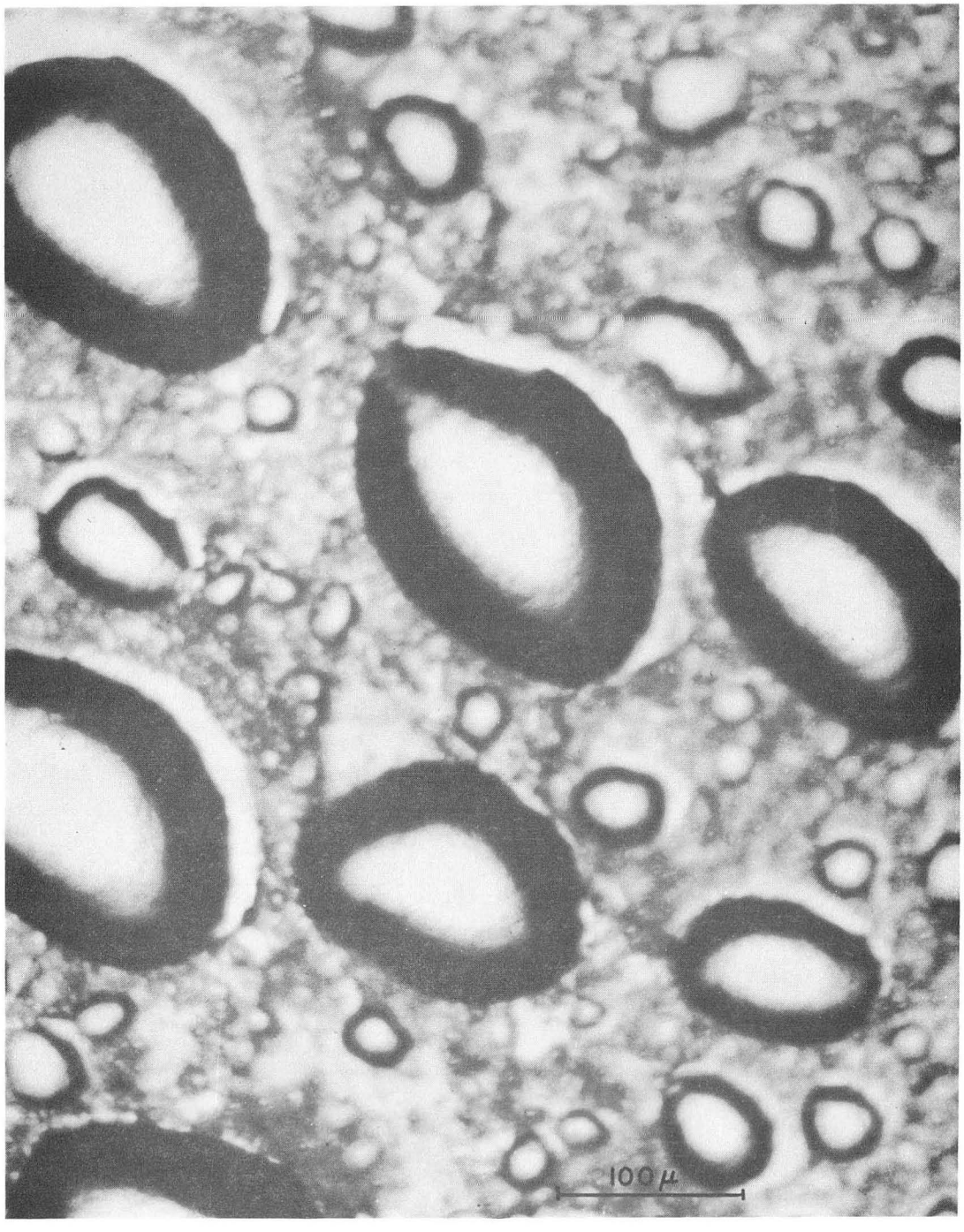

XBB708-3572

Fig. 10.

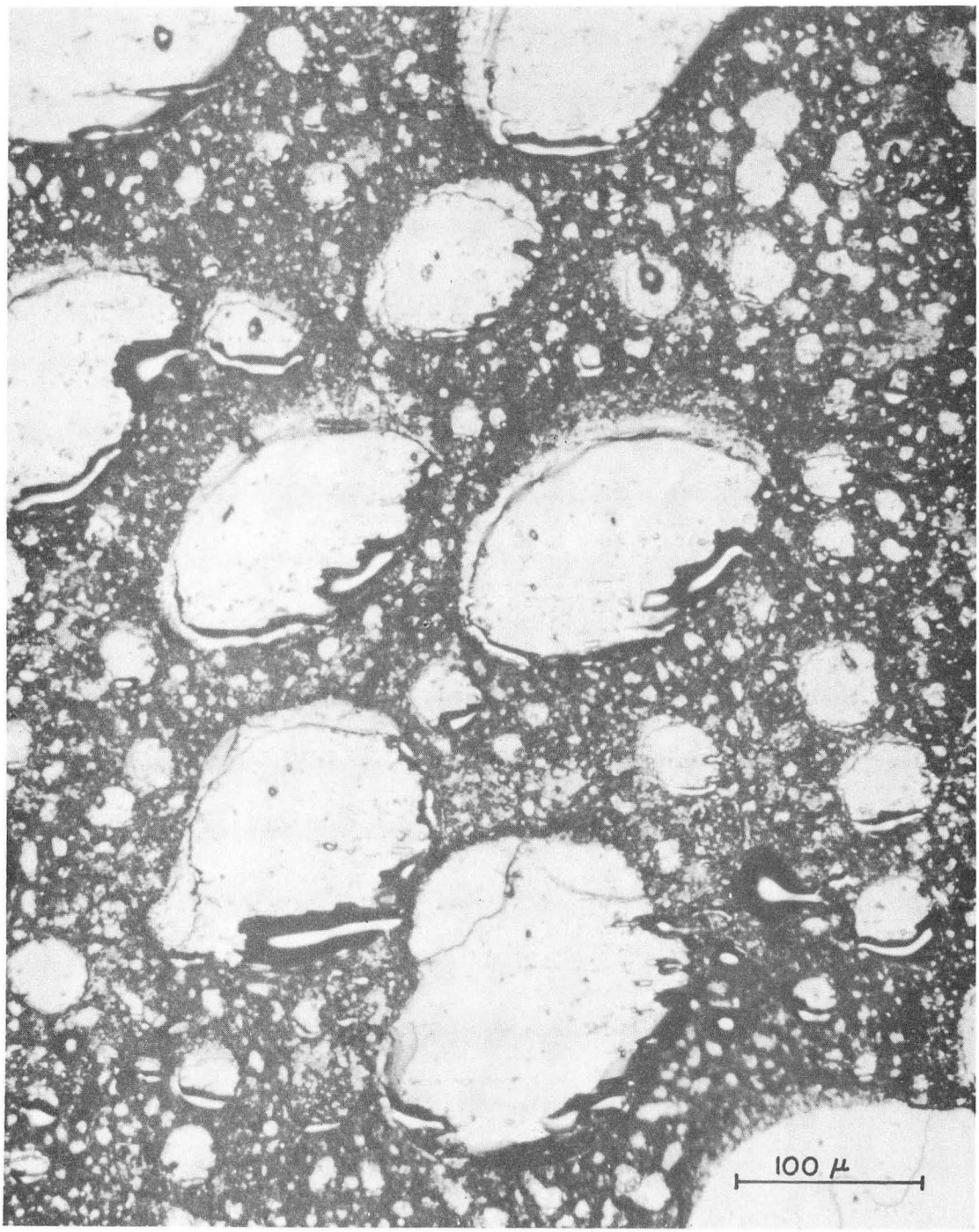

XBB708-3575

Fig. 11.

XBB708-3576

Fig. 12.

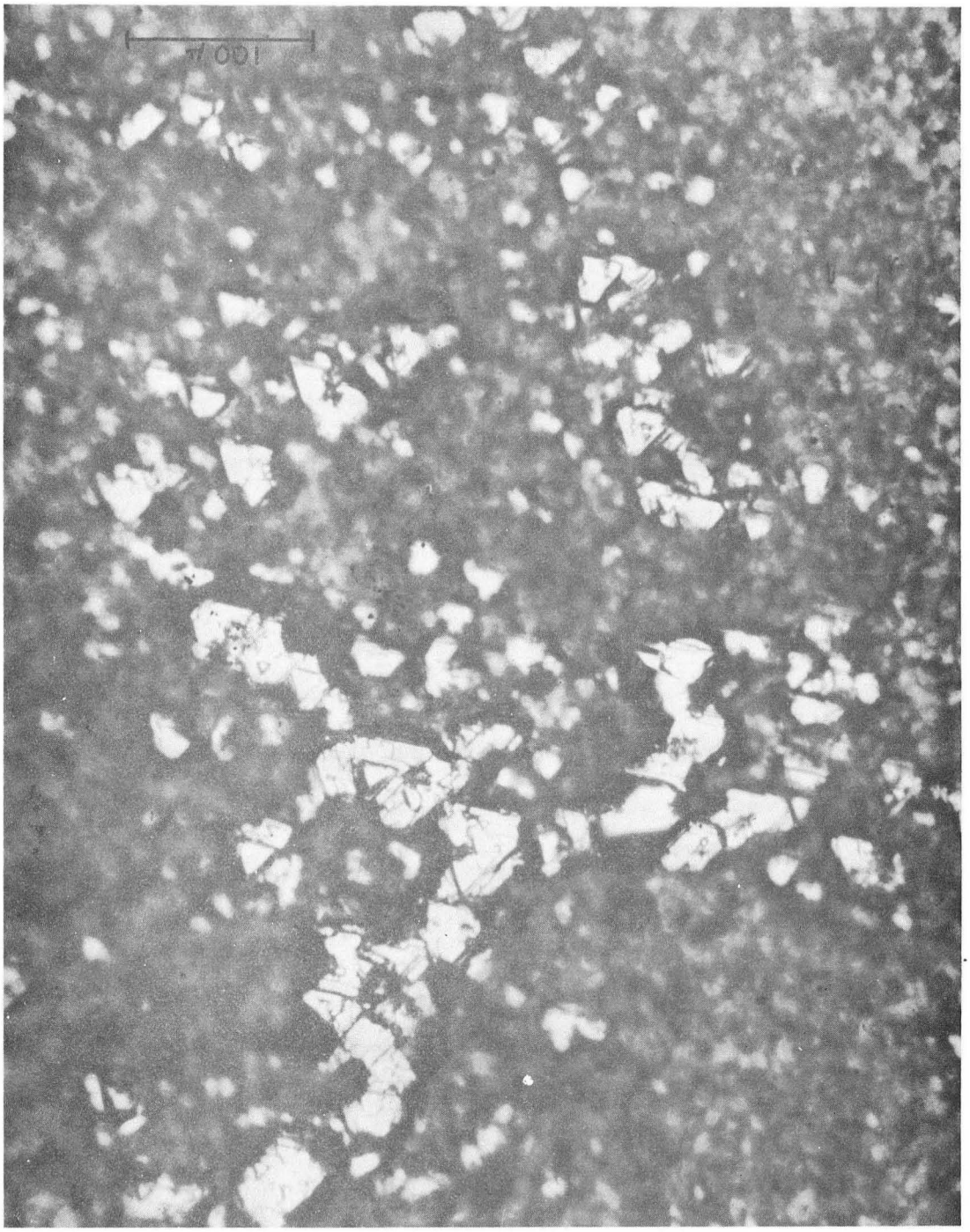

XBB708-3577

Fig. 13.

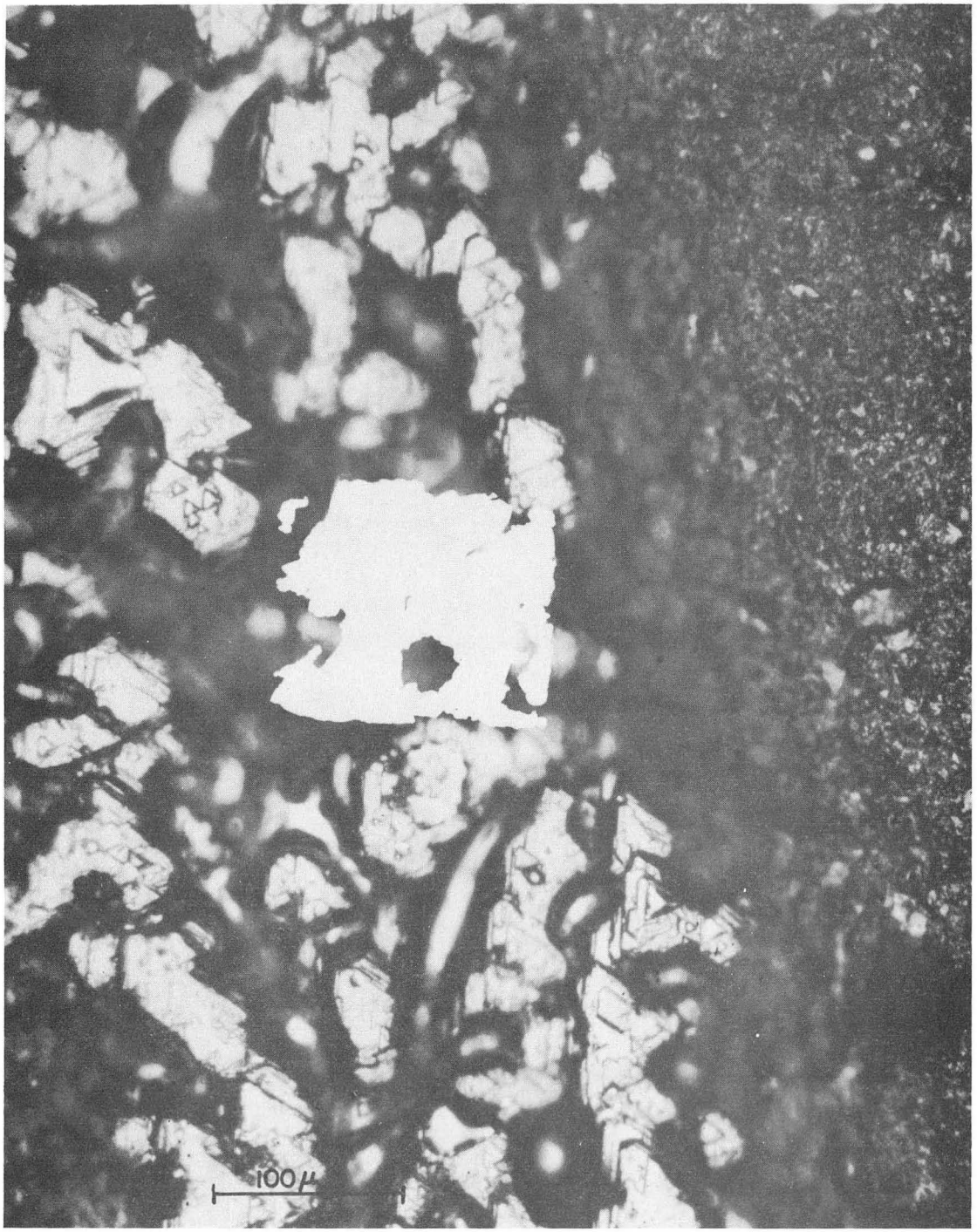

XBB708-3507

Fig. 14.

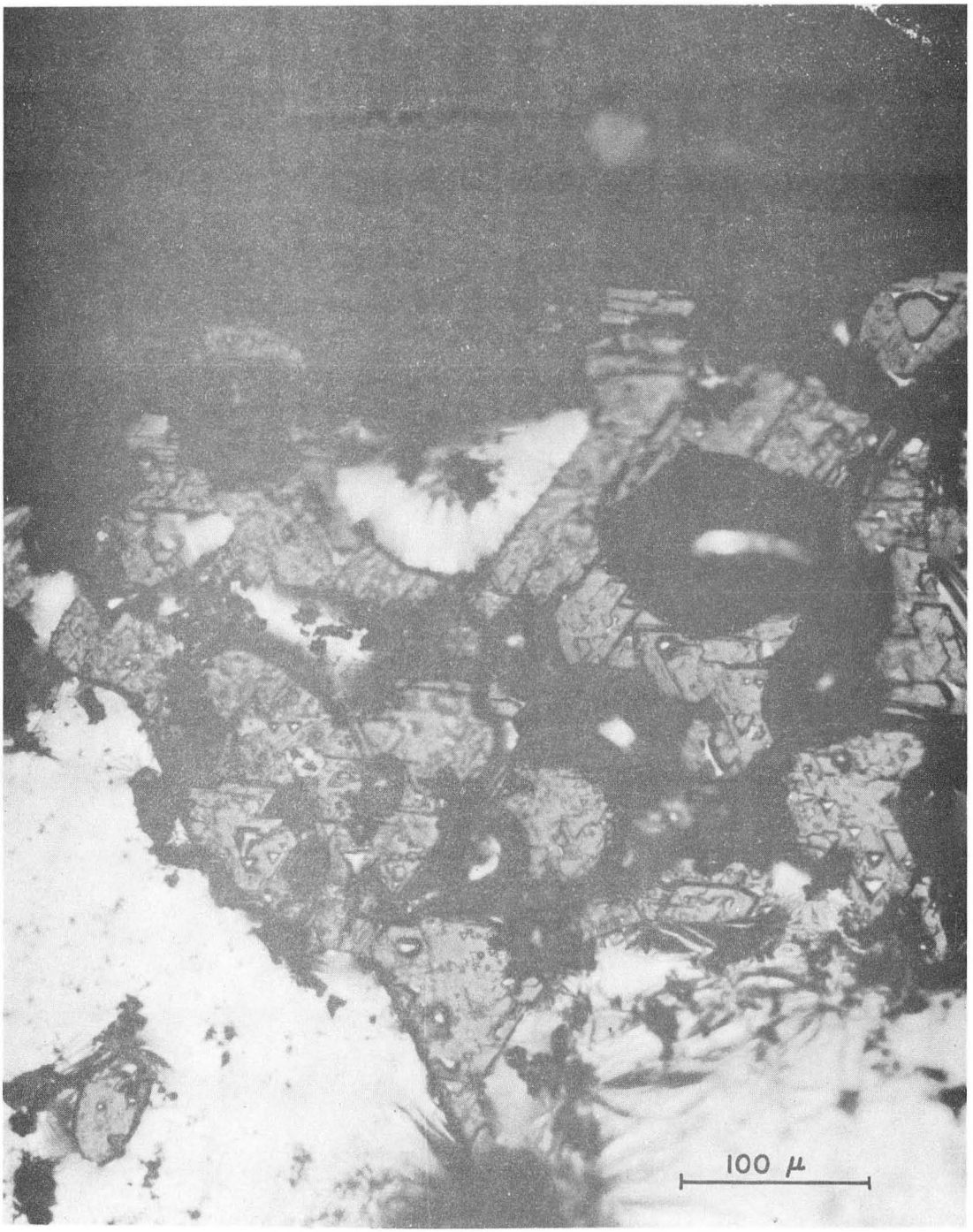

XBB708-3569

Fig. 15.

XBB708-3568

Fig. 16.

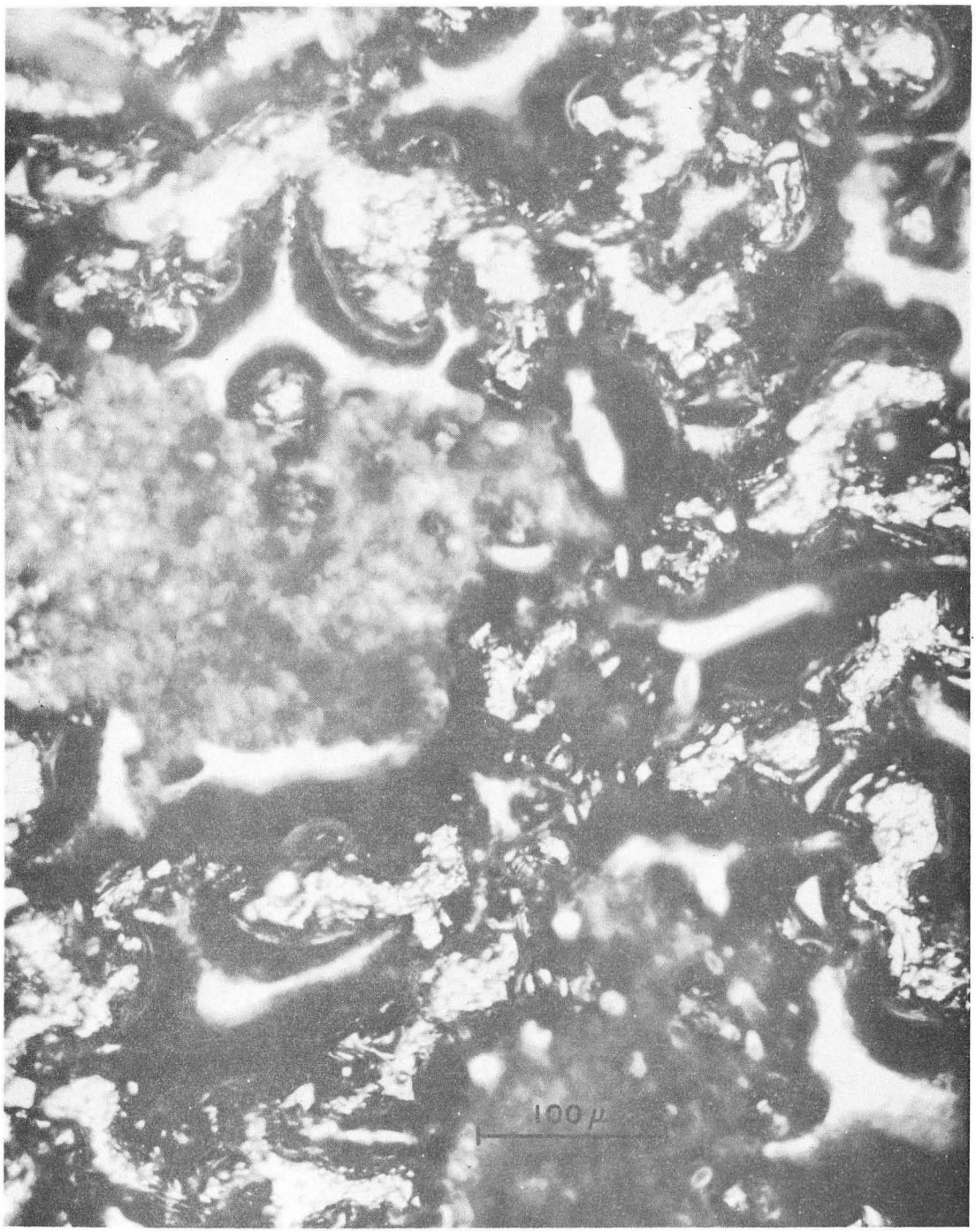

XBB708-3574

Fig. 17.

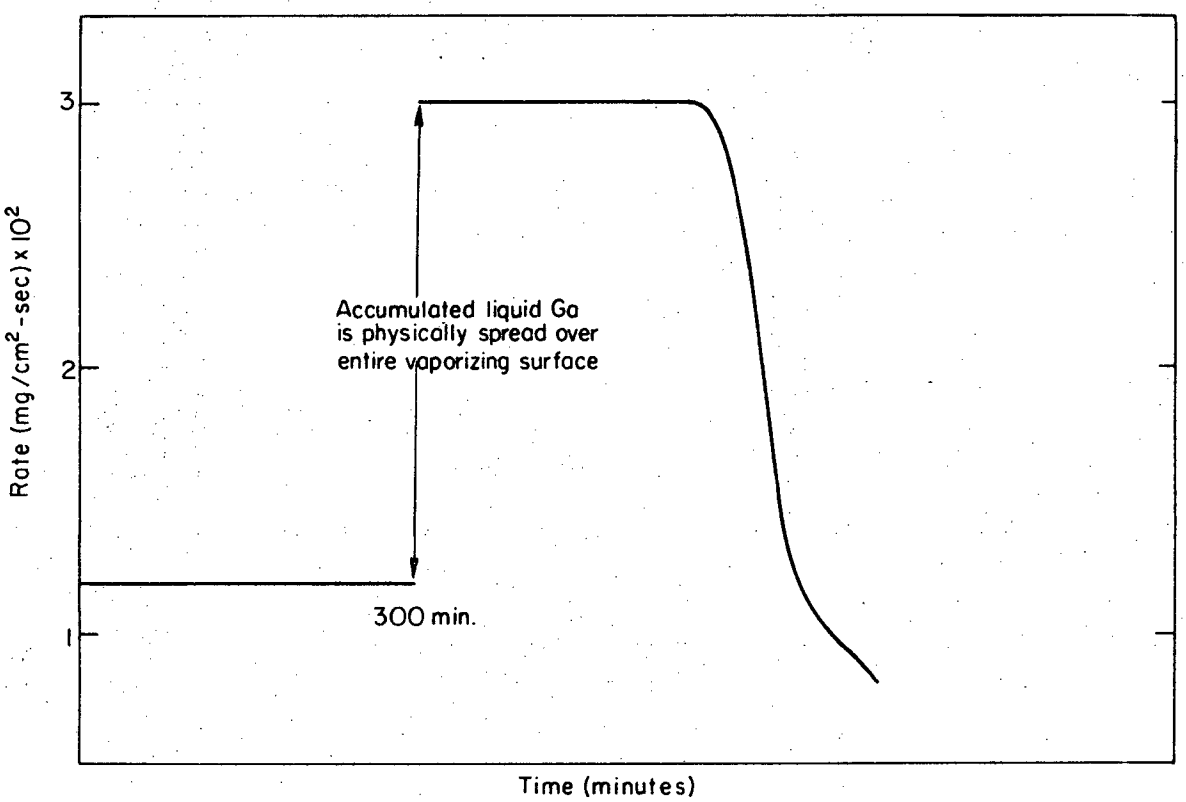

XBL 709-6541

Fig. 18.

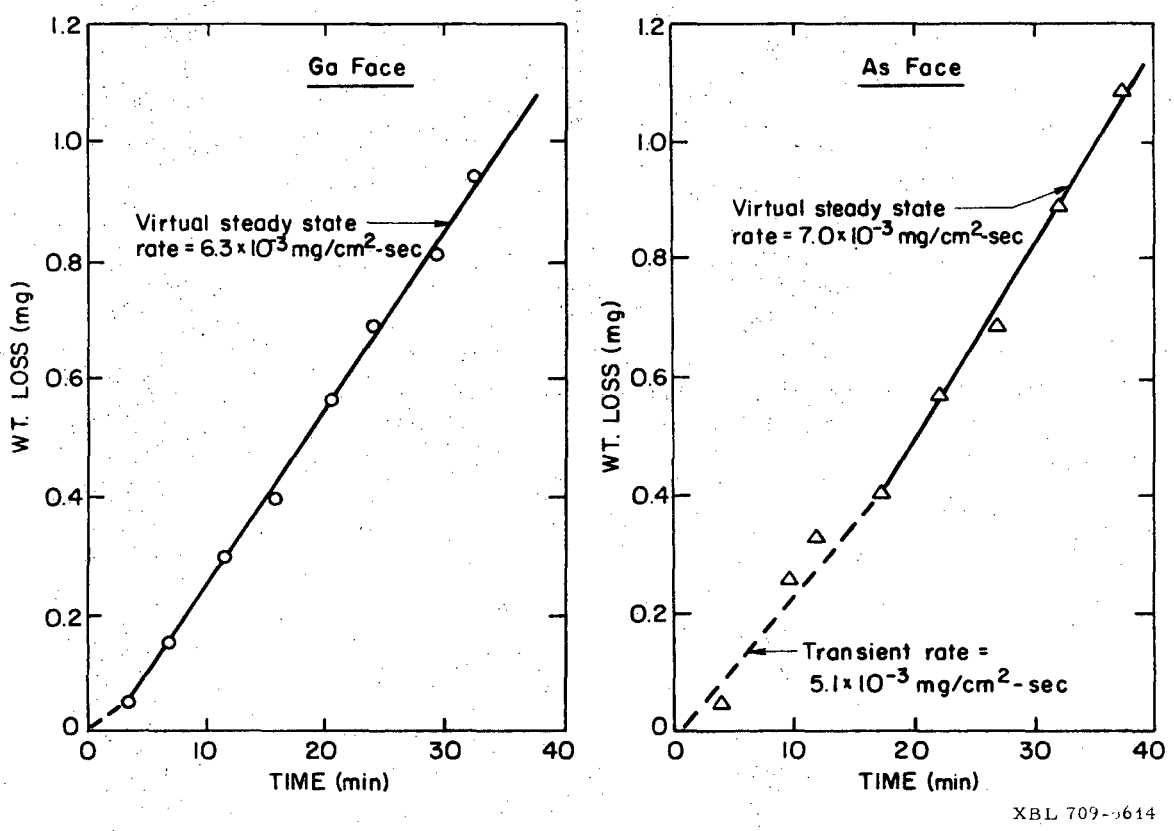
Ga Face
Virtual steady state
rate = 6.3 x 10-3 mg/cm2-sec
WT. LOSS (mg)
TIME (min)
As Face
Virtual steady state
rate = 7.0 x 10-3 mg/cm2-sec
Transient rate =
5.1 x 10-3 mg/cm2-sec
WT. LOSS (mg)
TIME (min)
XBL 709-3614

Fig. 19.

Explanation of the symbols used in the following figures:

○ vaporization rates of gallium face upon heating.

◐ vaporization rates of gallium face upon cooling.

△ vaporization rates of arsenic face upon heating

▲ vaporization rates of arsenic face upon cooling.

⊕ vaporization rates of gallium face with excess gallium placed on top of surface before evaporation (heating)

● vaporization rates of arsenic face with excess gallium placed on top of surface before evaporation (cooling).

△ vaporization rates of arsenic face with excess gallium placed on top of surface before evaporation (heating).

▲ vaporization rates of arsenic face with excess gallium placed on top of surface before evaporation (cooling).

⊘ vaporization rates of gallium face with excess tin placed on top of surface before evaporation (heating).

◕ vaporization rates of gallium face with excess tin placed on top of the surface before evaporation (cooling).

△ vaporization rates of arsenic face with excess tin placed on top of surface before evaporation

1. The first time the crystal face was being vaporized.
2. The second time the crystal face was being vaporized.

The data points are taken from one experiment whereas the slope drawn through these points is the average value of all experiments done under the identical conditions.

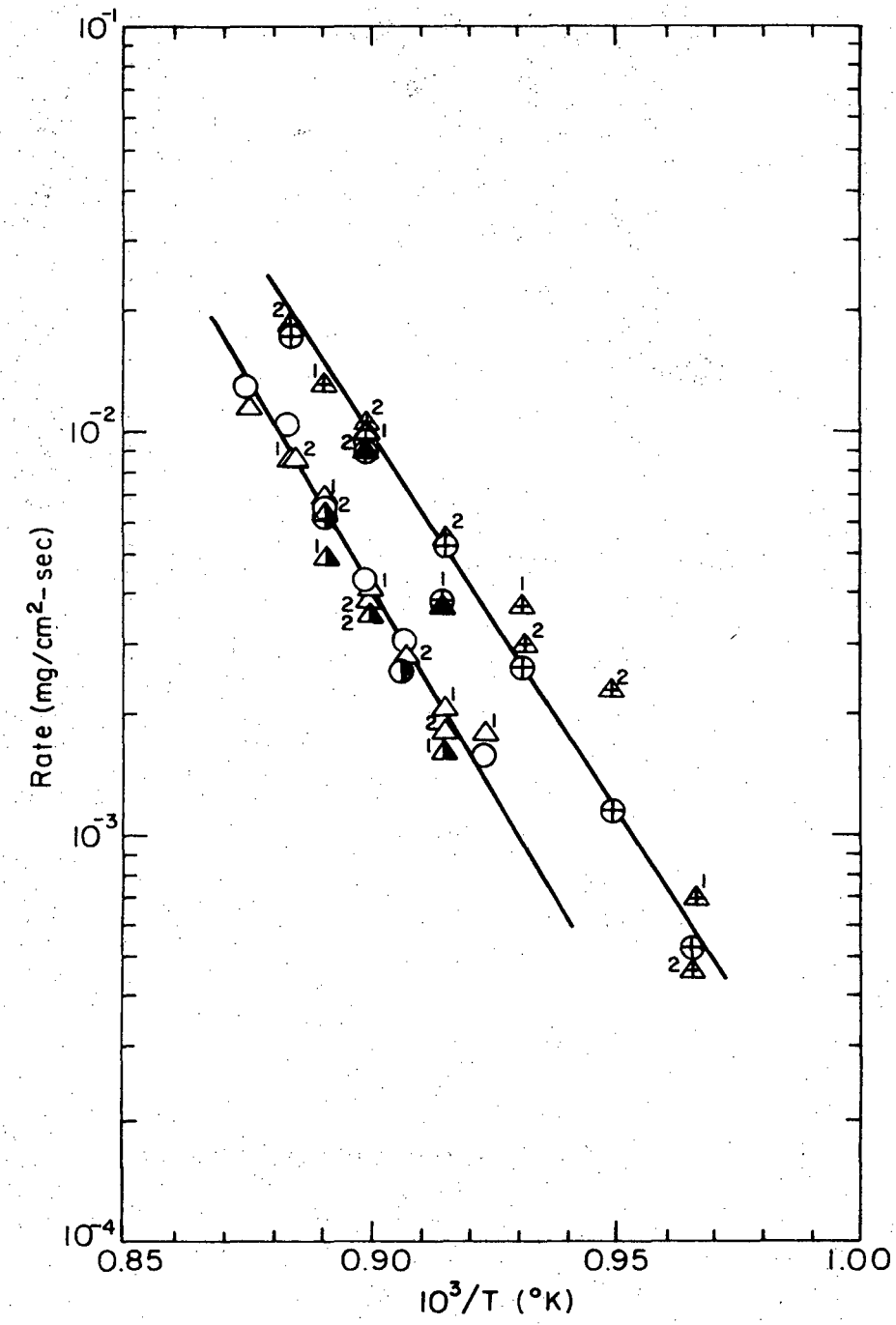

XBL 709-6542

Fig. 20.

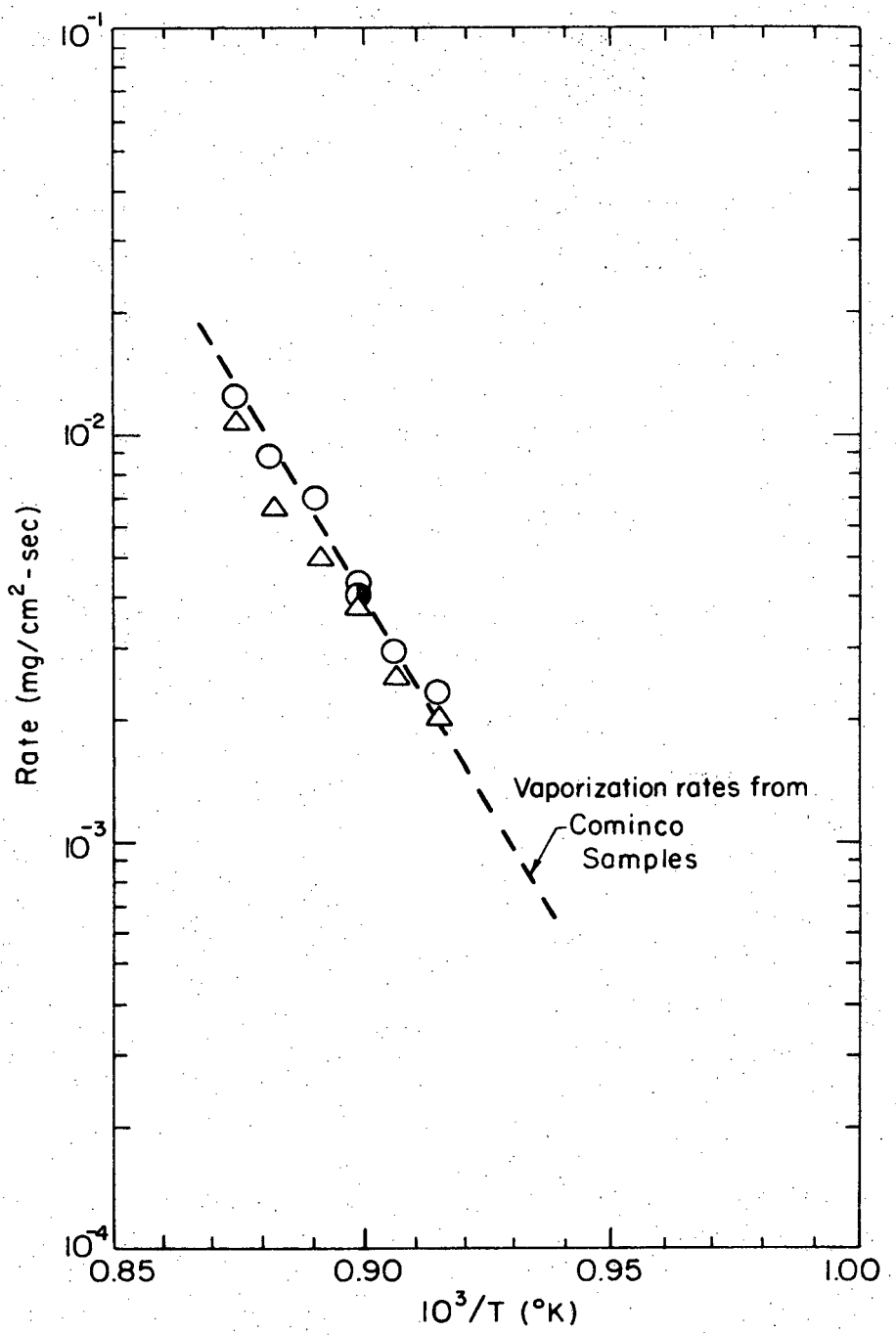

XBL 709-6540

Fig. 21.

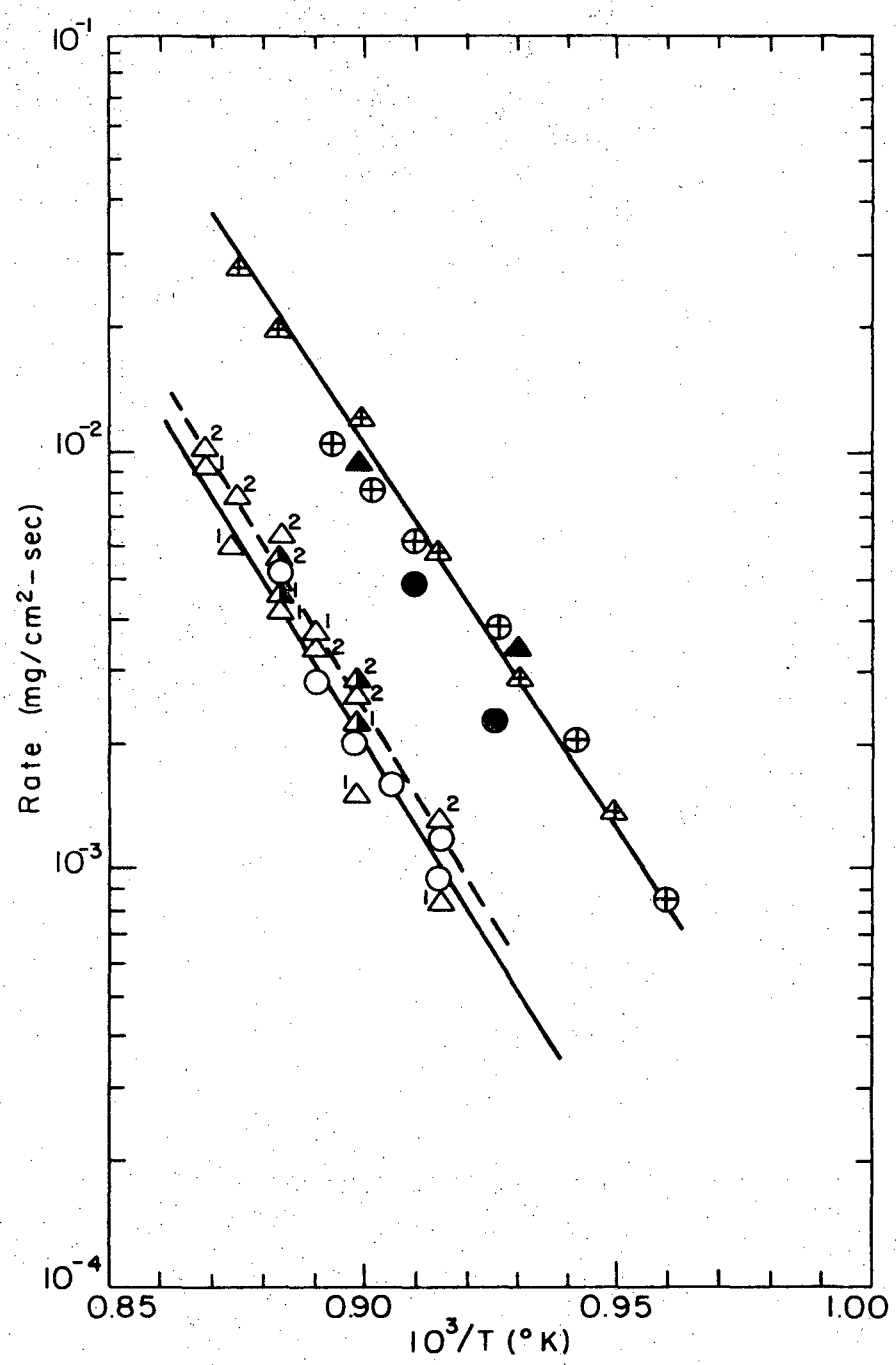

XBL 709-6543

Fig. 22.

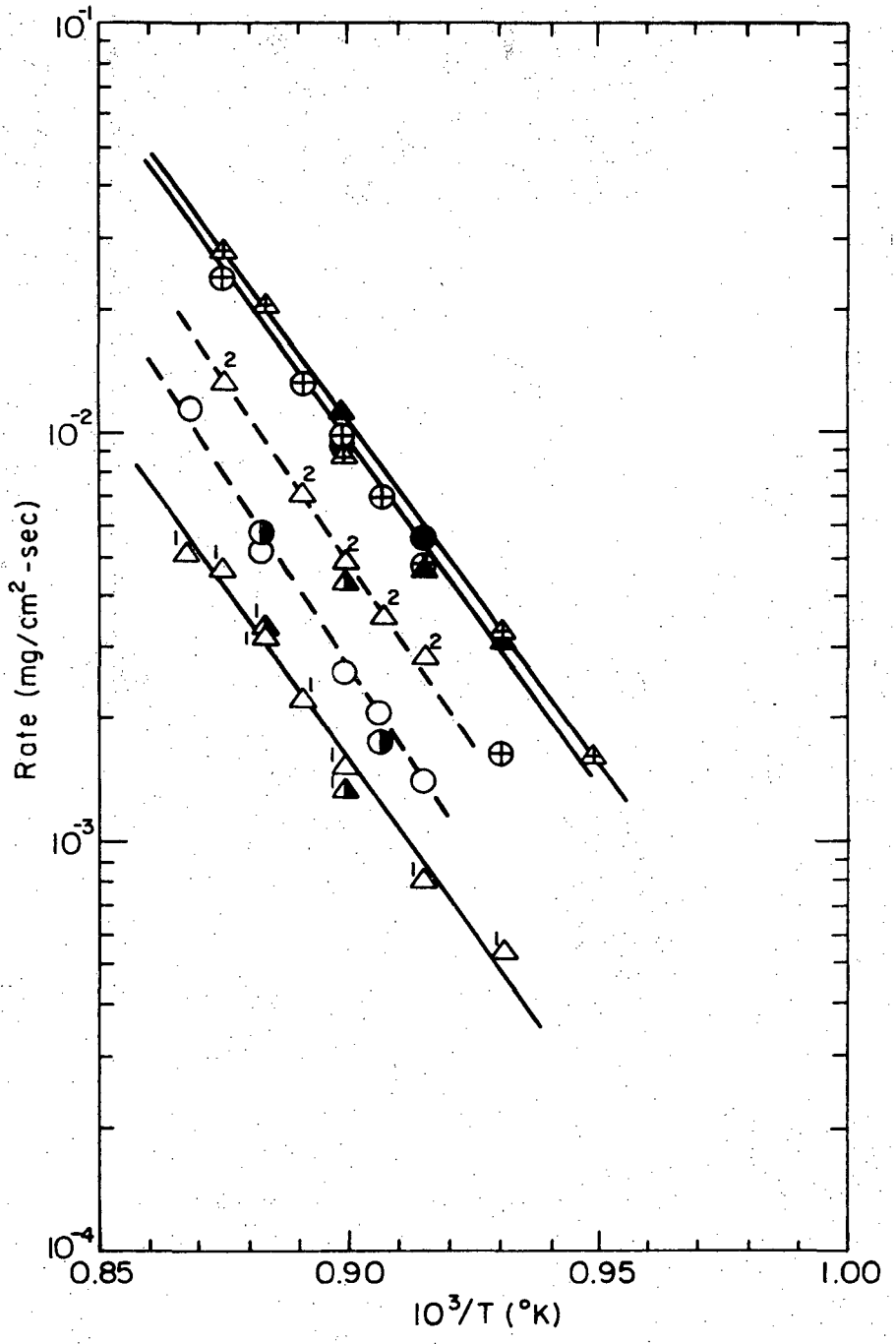

XBL 709-6544

Fig. 23a.

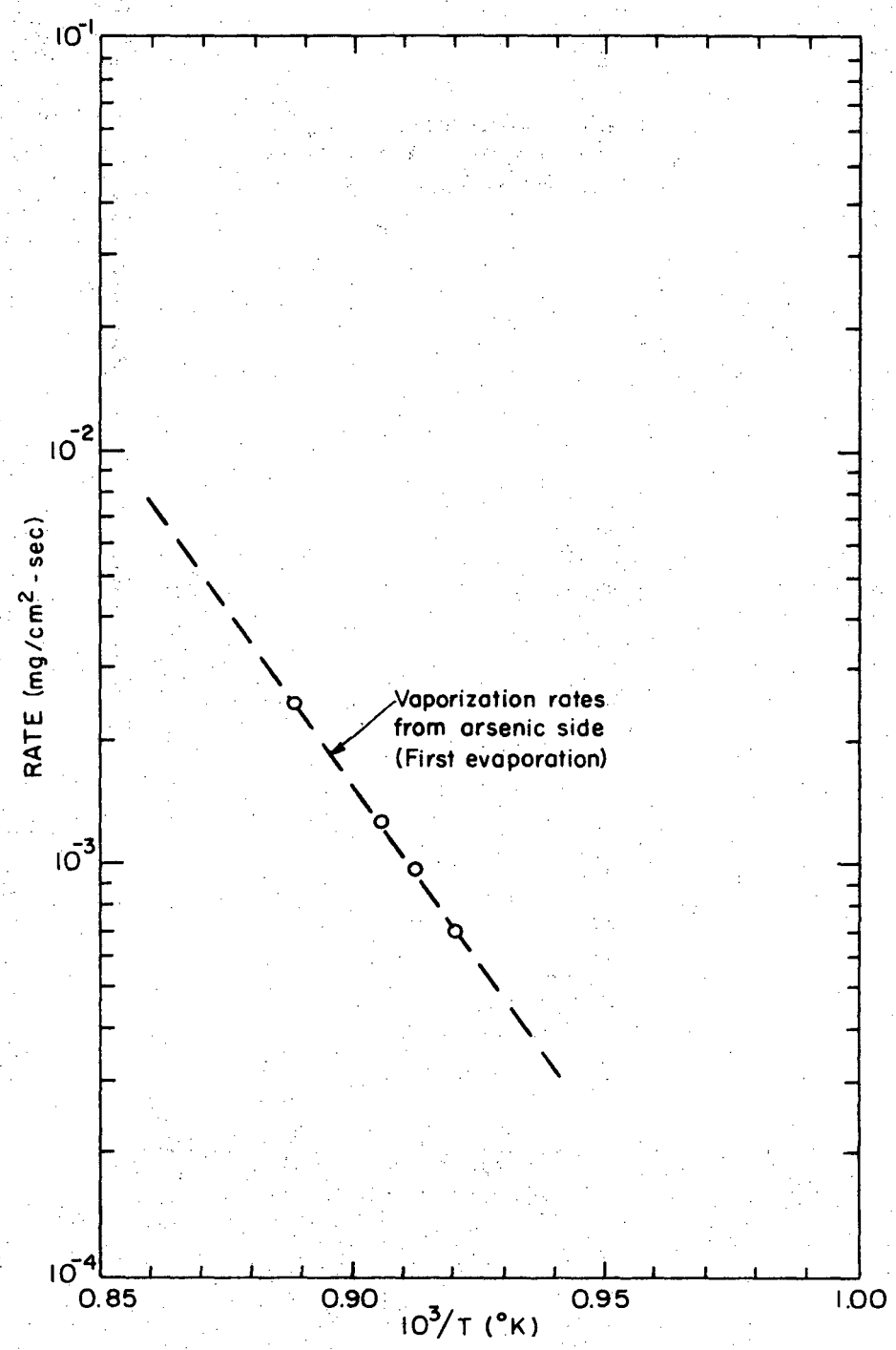

XBL 709-6622

Fig. 23b.

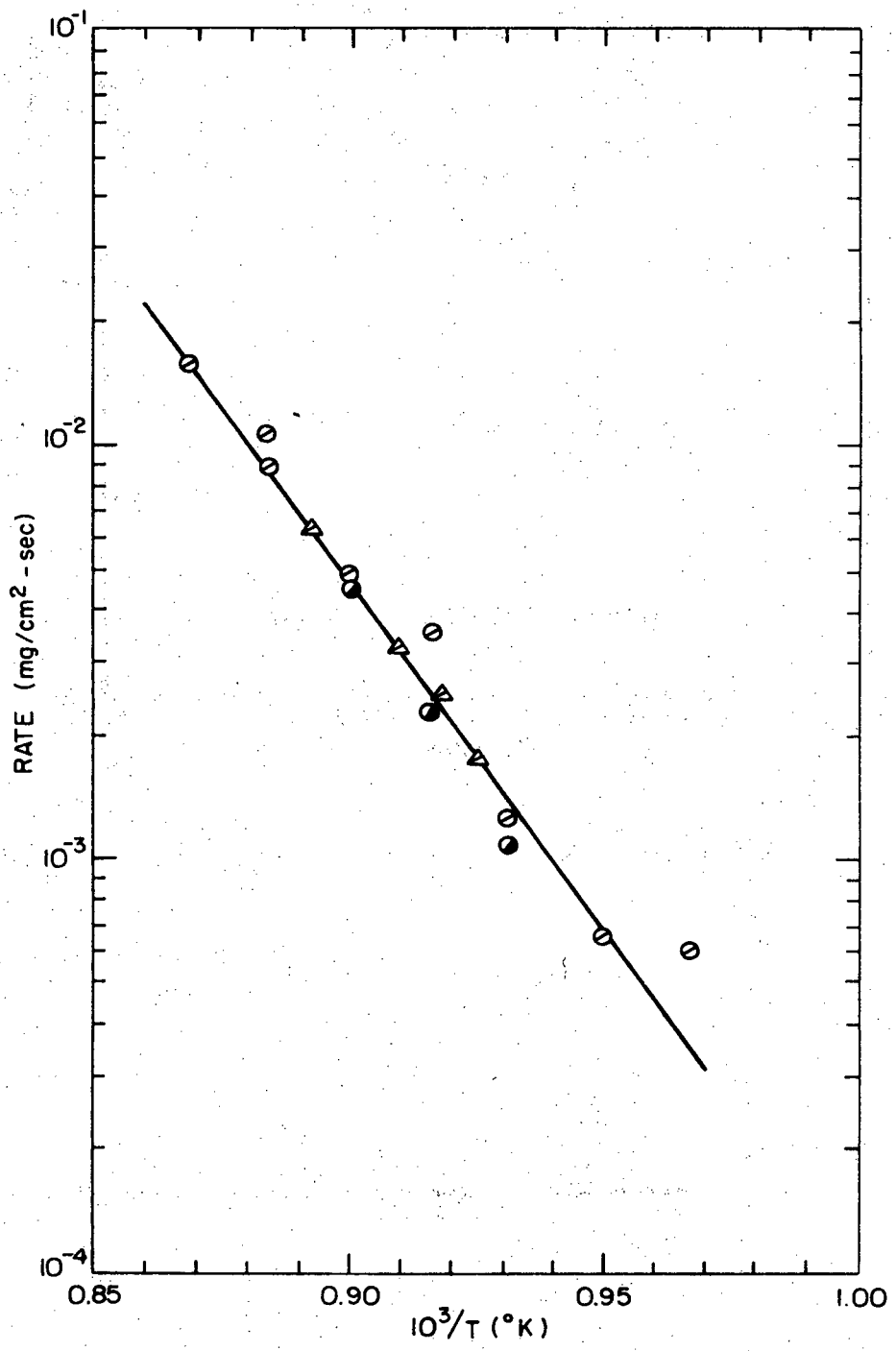

XBL 709-6623

Fig. 24.

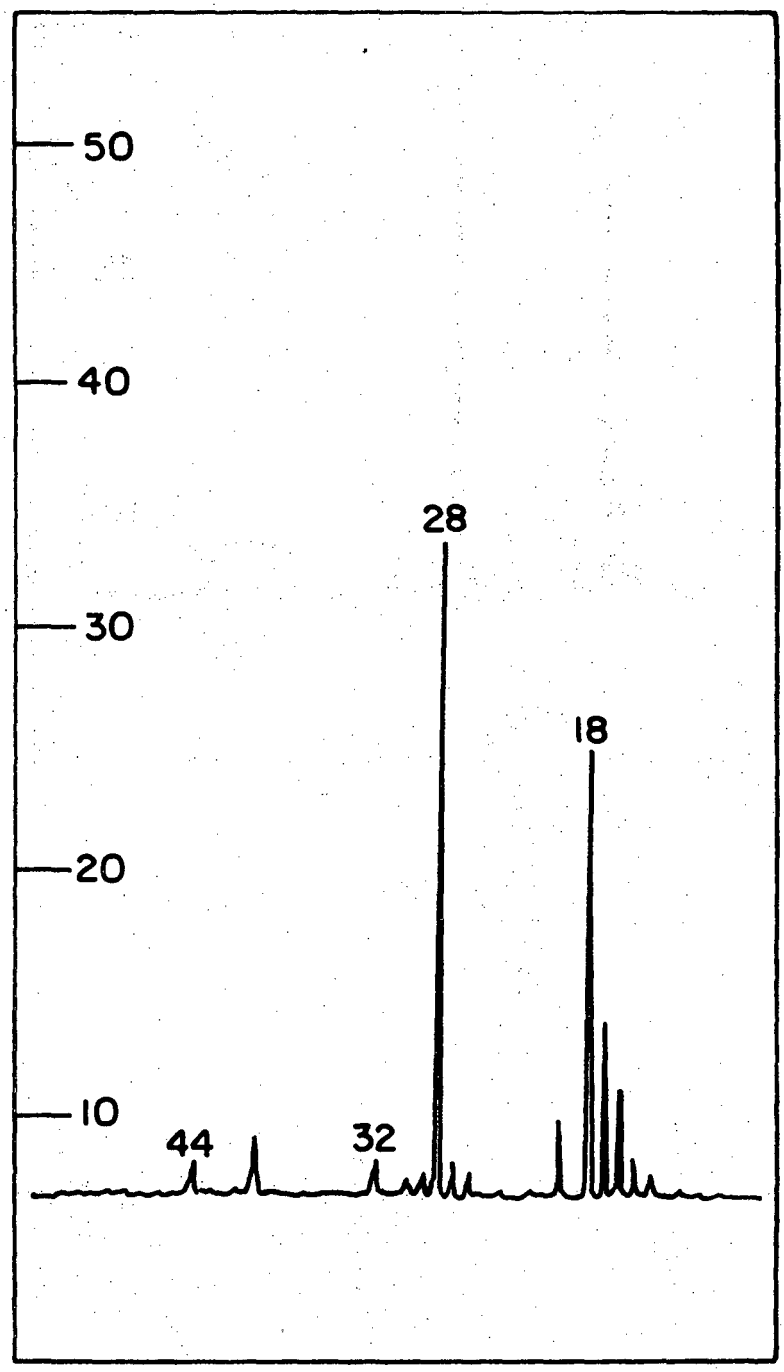

XBL 709-6553

Fig. 25.

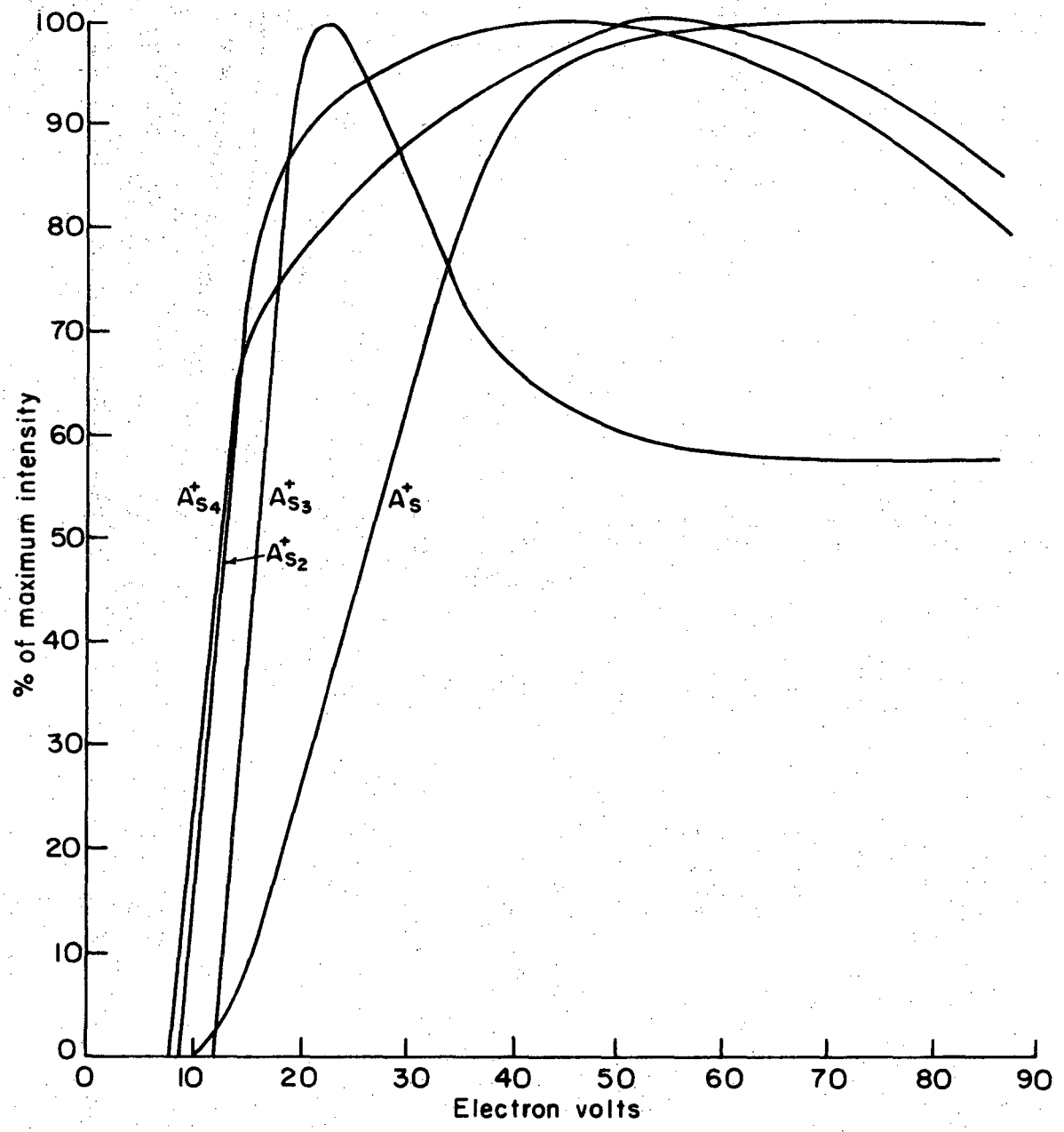

XBL 709-6552

Fig. 26.

Explanation of symbols used in the following figures.

△ Intensities of As_4 upon heating

▲ Intensities of As_4 upon cooling

⊕ Intensities of As_2 upon heating

● Intensities of As_2 upon cooling

The data points are taken from one experiment whereas the slope drawn through these points is the average value of all experiments done under the identical conditions.

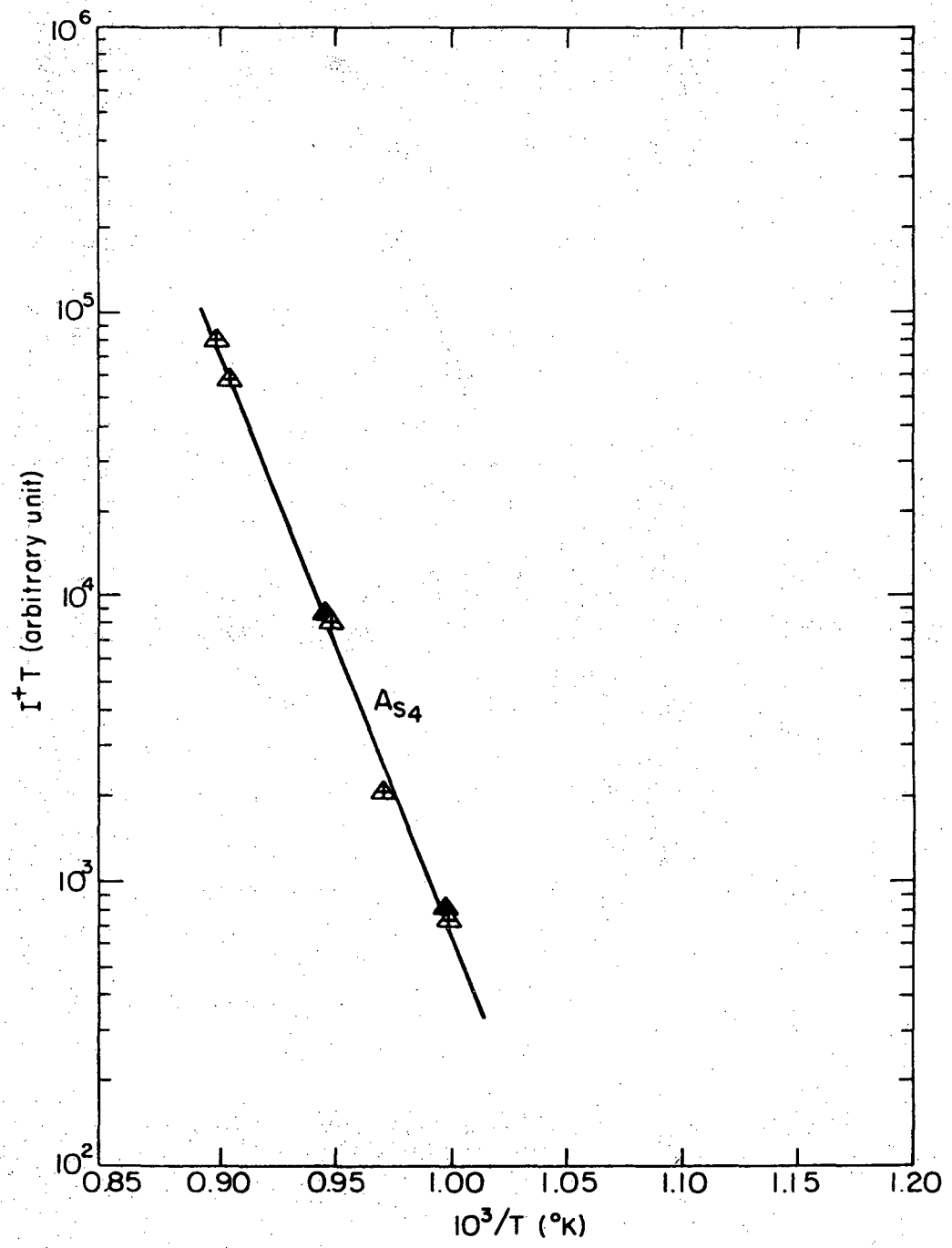

XBL 709-6549

Fig. 27.

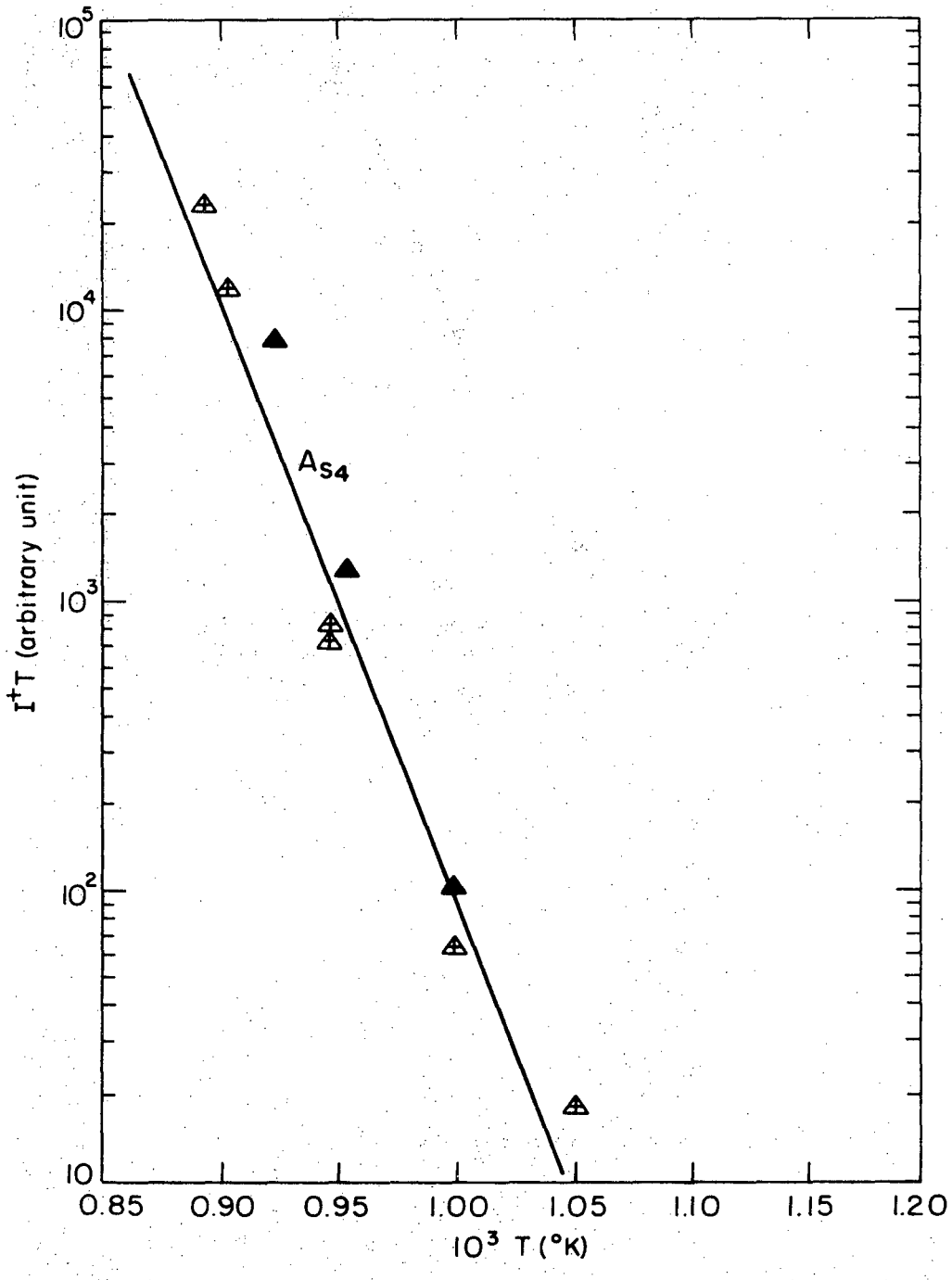

XBL 709-6550

Fig. 28.

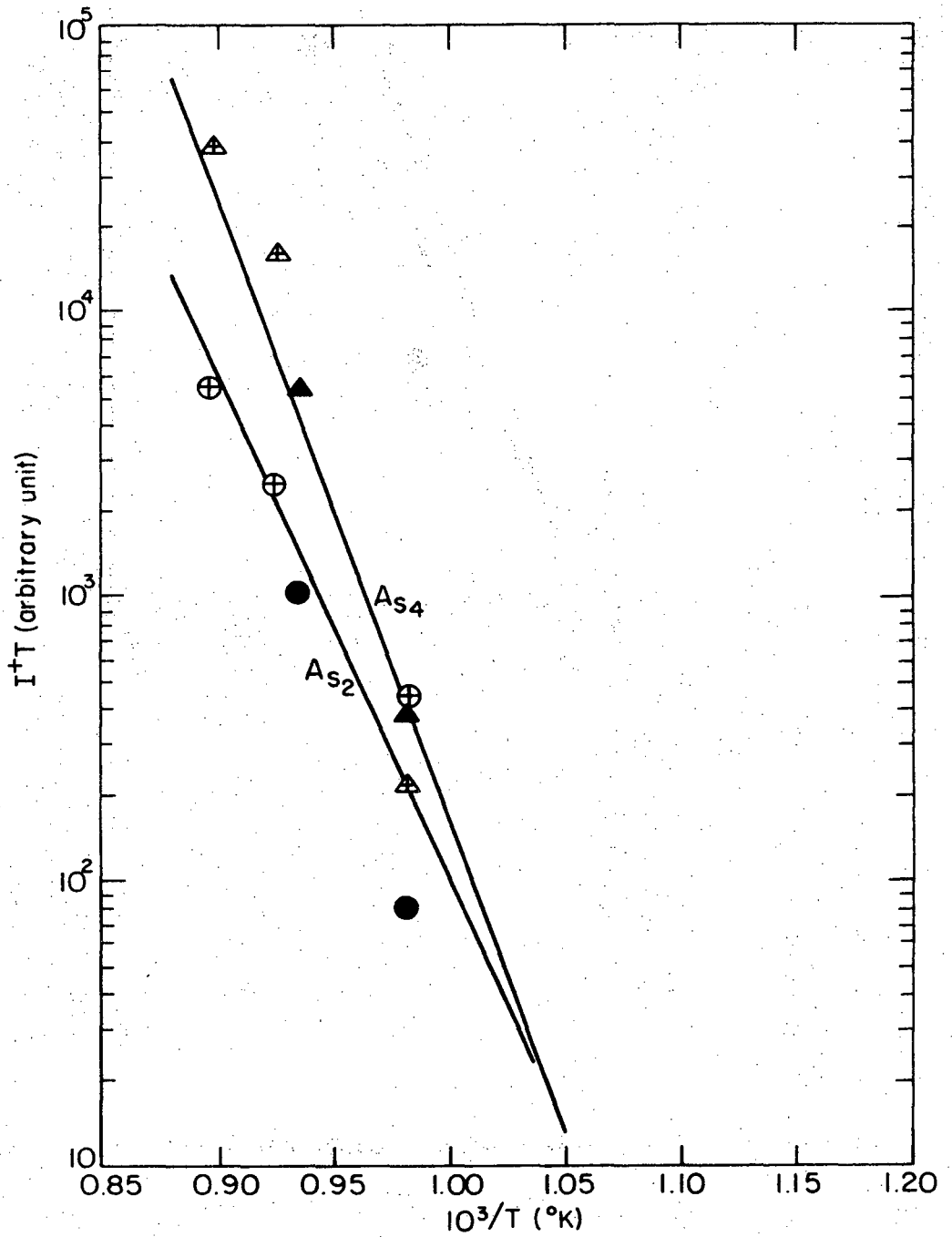

XBL 709-6545

Fig. 29.

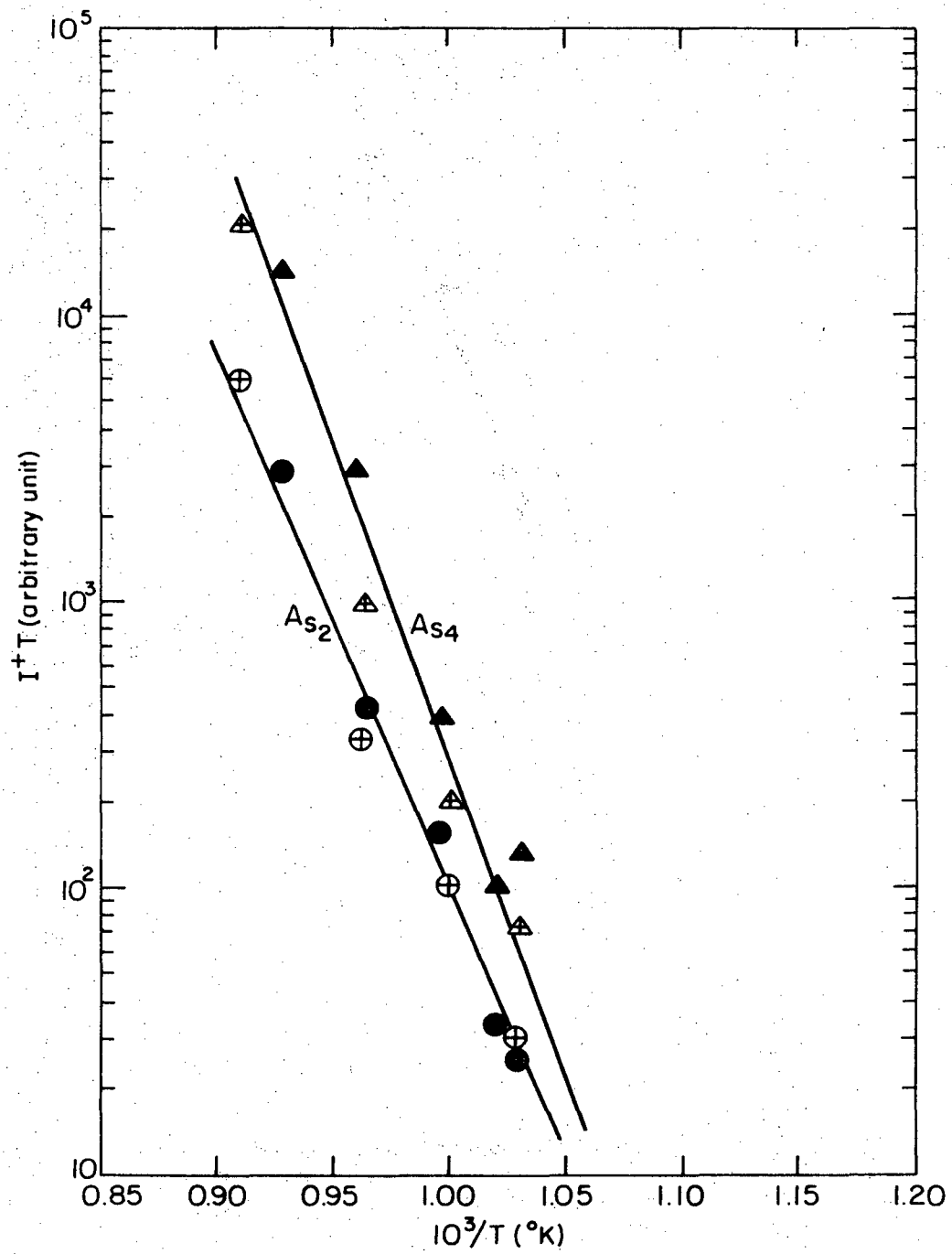

XBL 709-6546

Fig. 30.

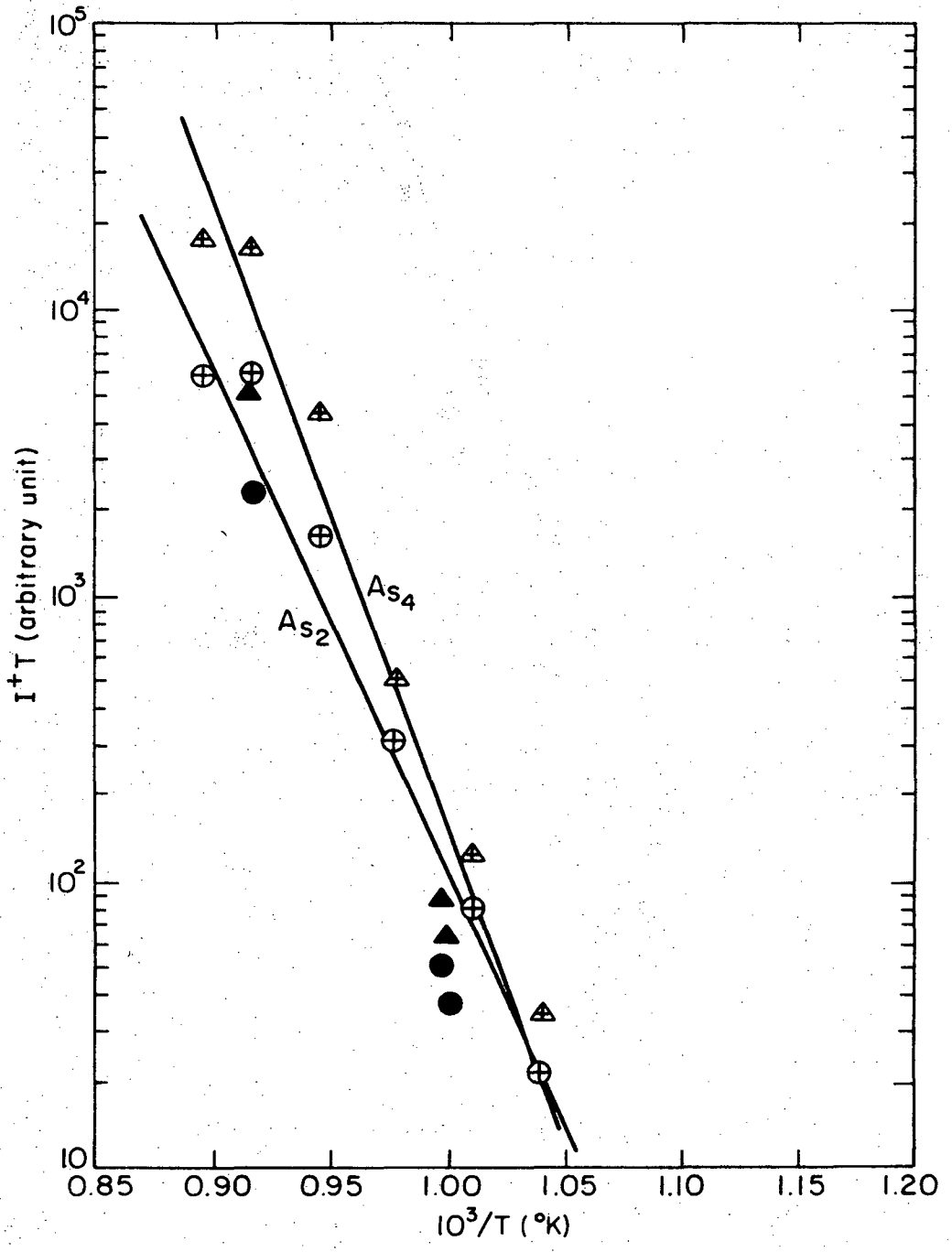

XBL 709-6547

Fig. 31.

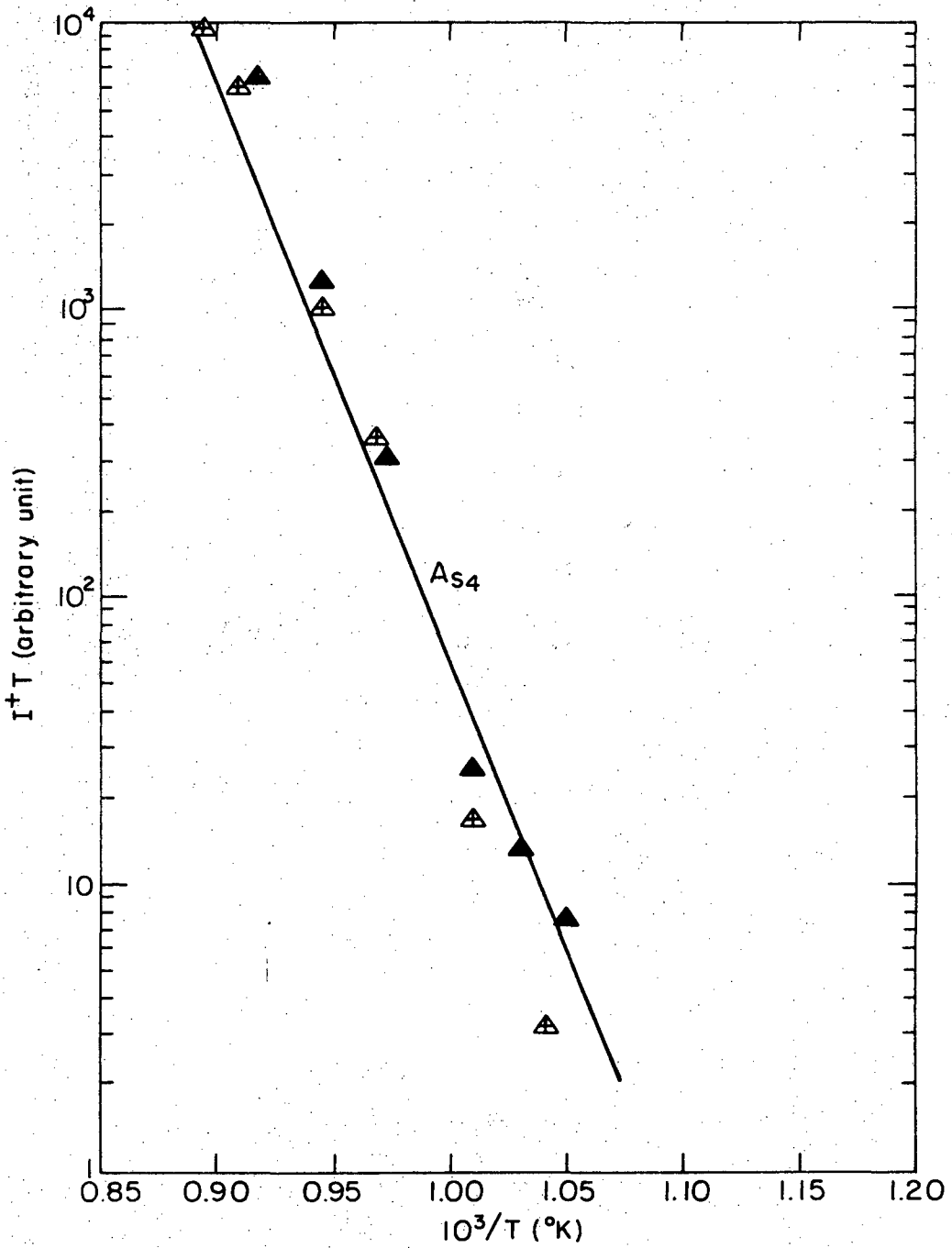

XBL 709-6551

Fig. 32.

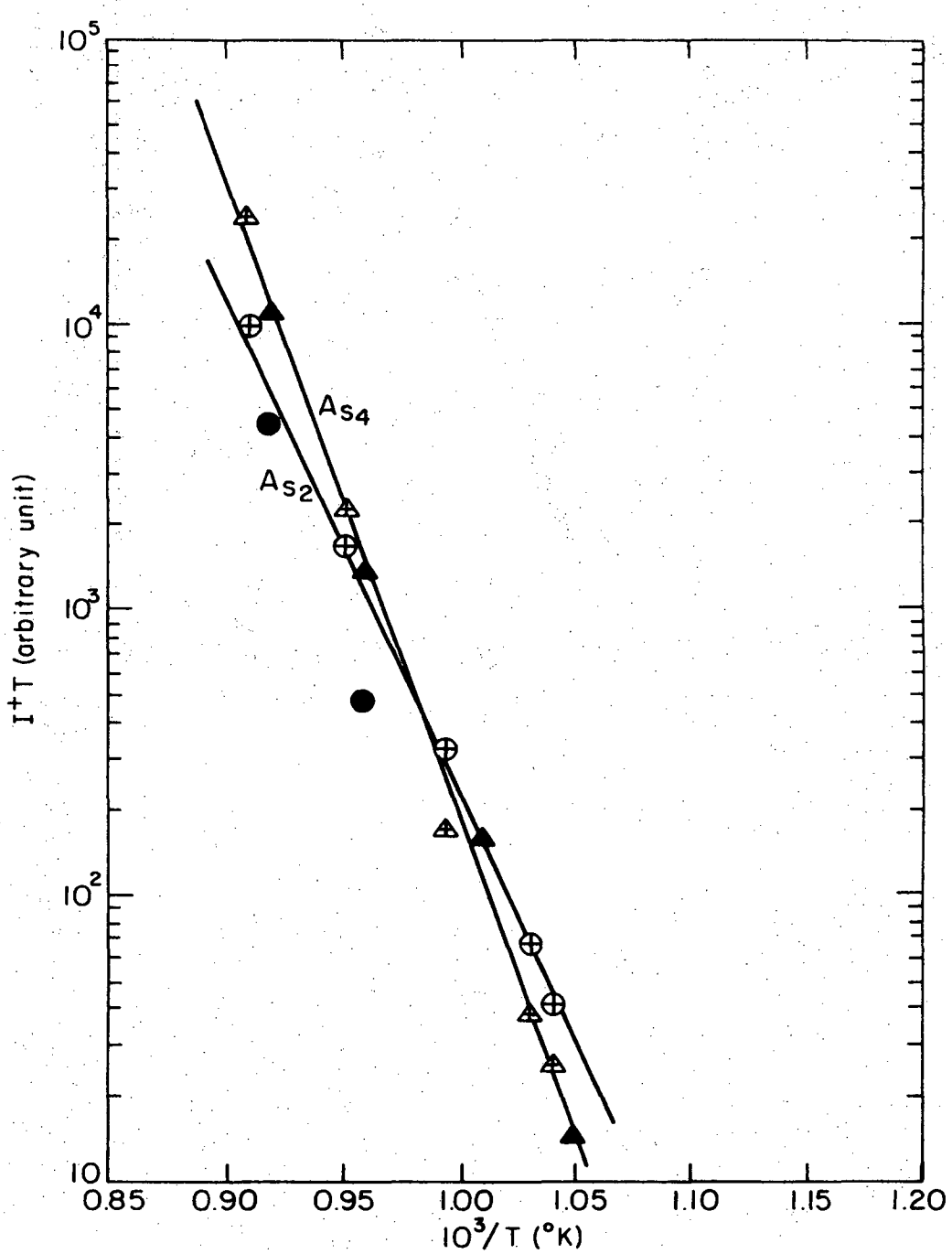

XBL 709-6548

Fig. 33.

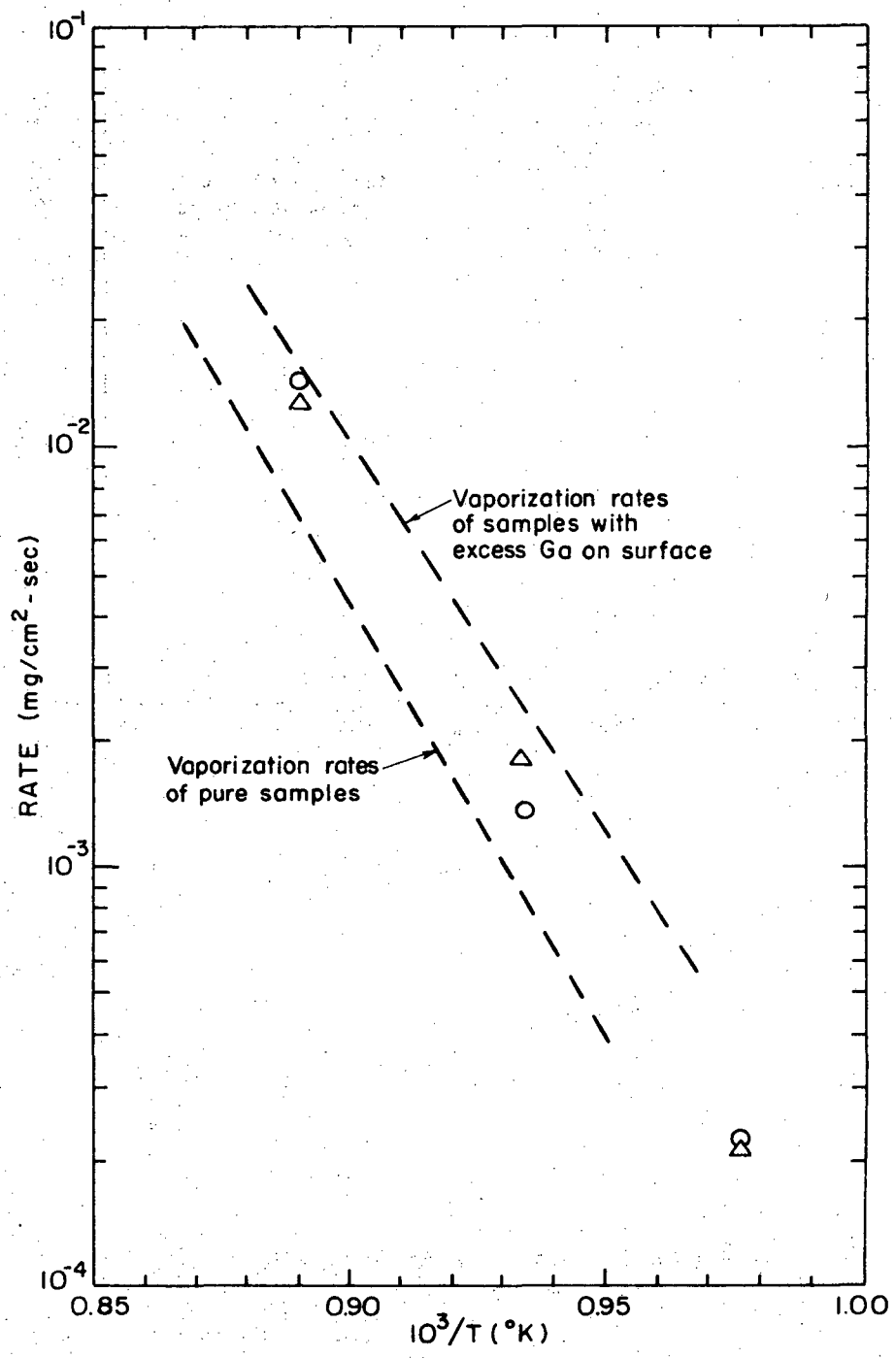

XBL 709-6619

Fig. 34.

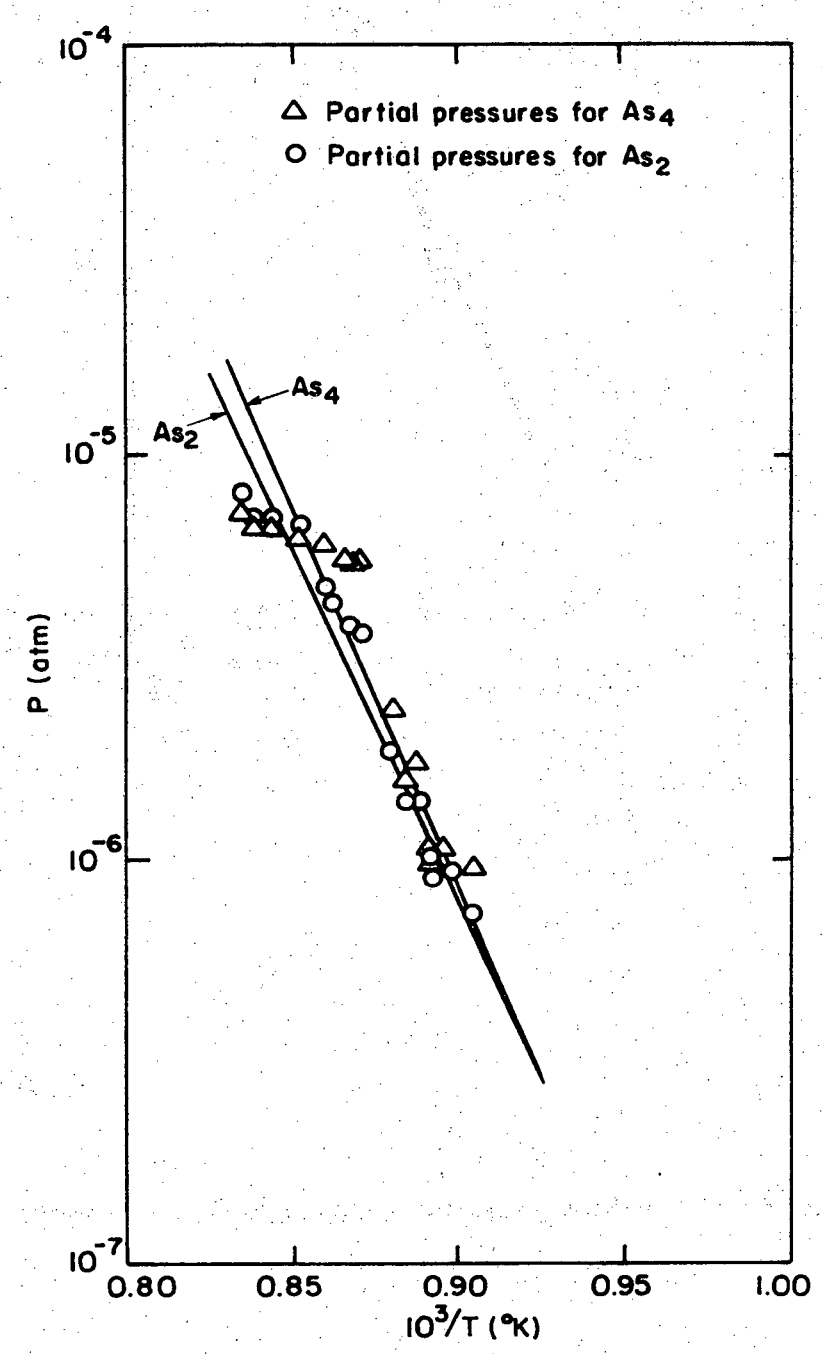

XBL 709-6620

Fig. 35.

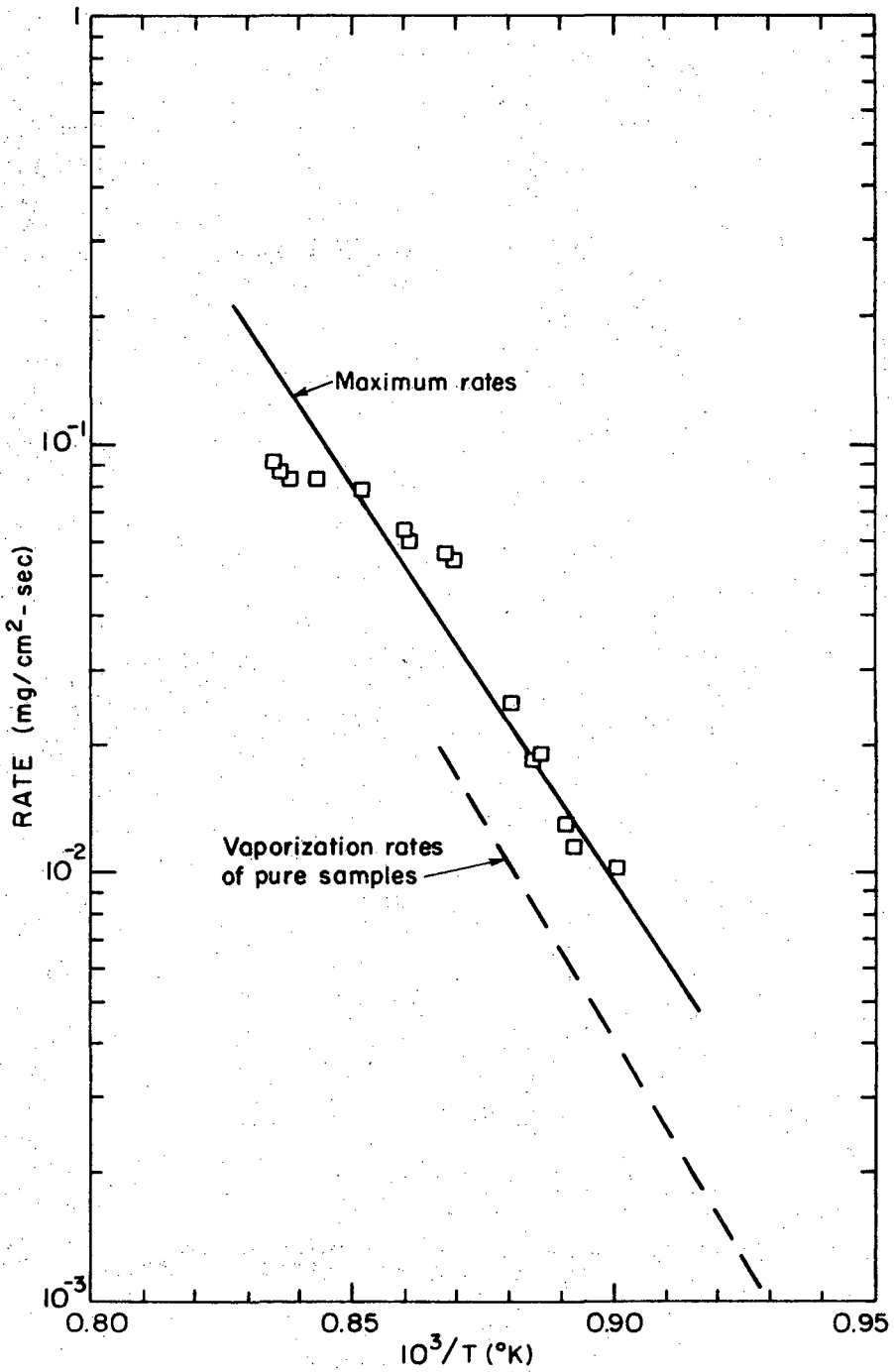

XBL 709-6621

Fig. 36.

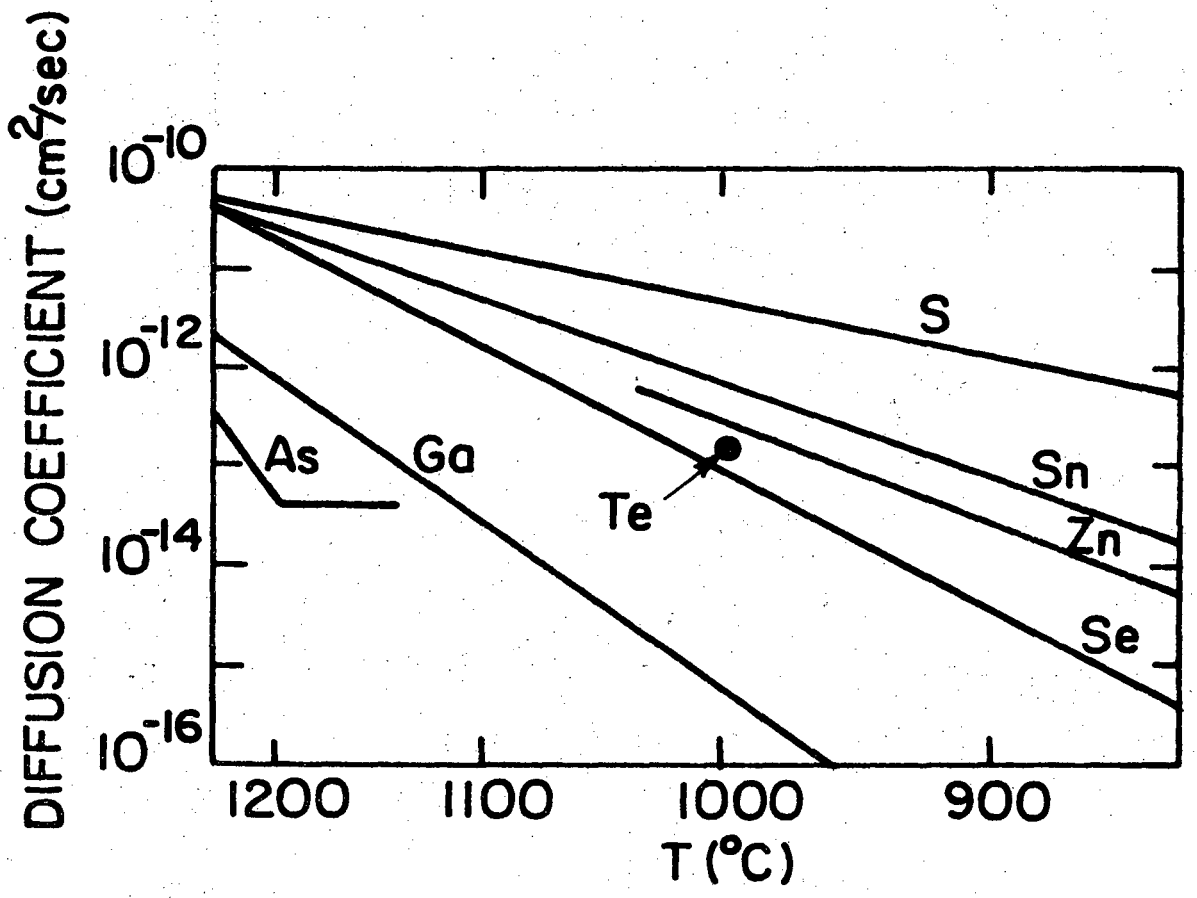

XBL 709-6624

Fig. 37.

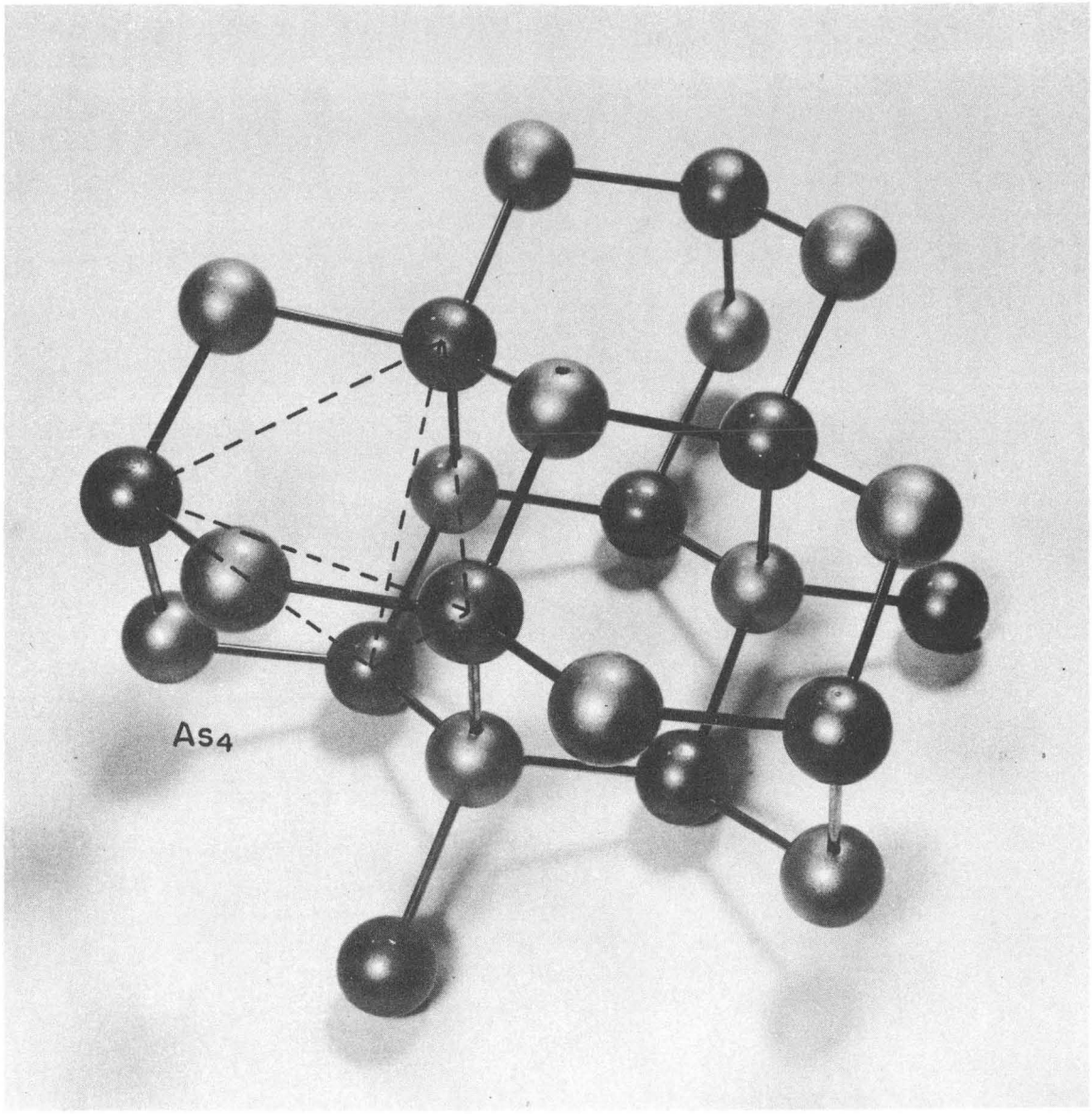

XBB708-3836

Fig. 38.

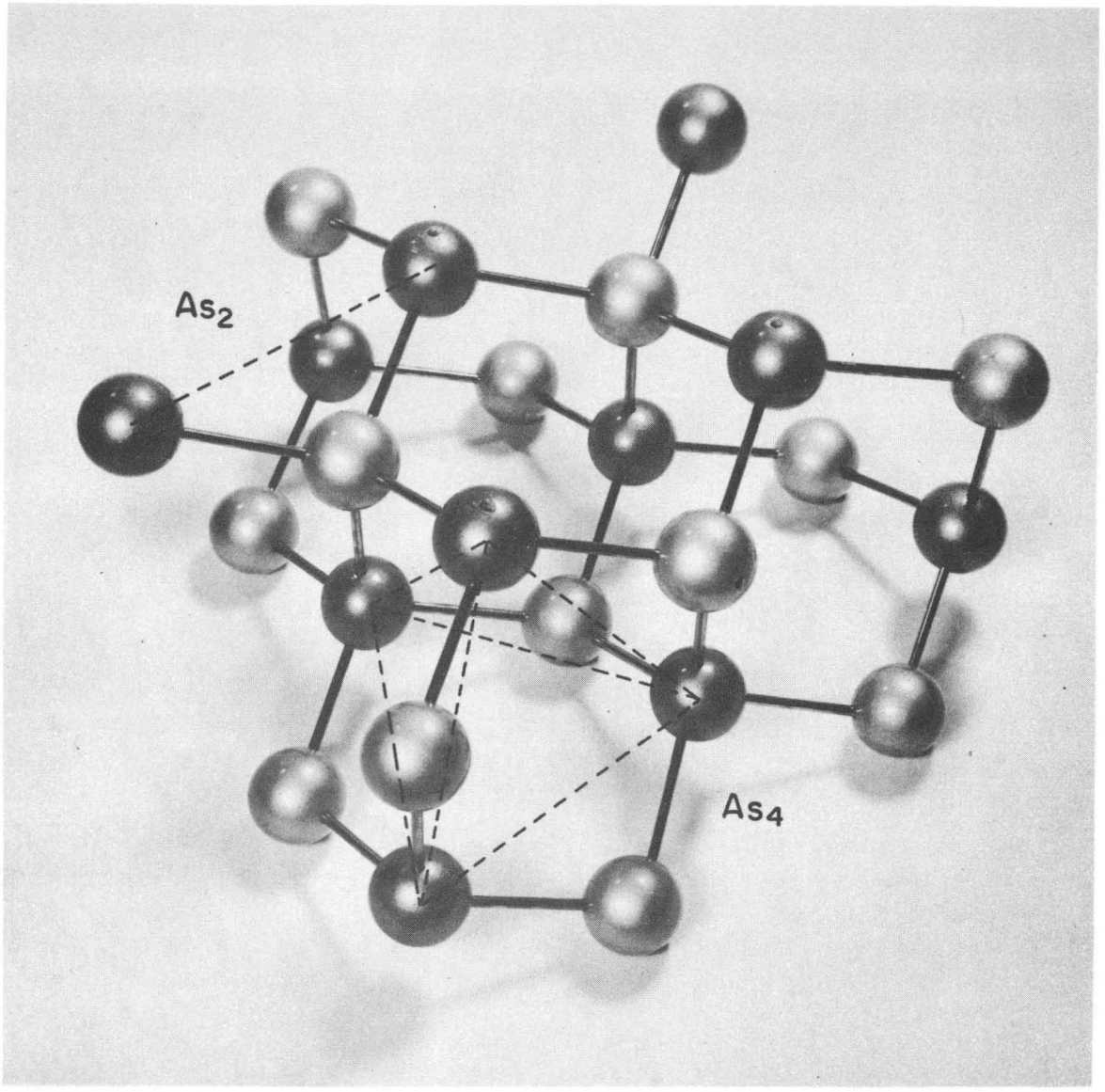

XBB708-3835

Fig. 39.

LEGAL NOTICE

This report was prepared as an account of Government sponsored work. Neither the United States, nor the Commission, nor any person acting on behalf of the Commission:

A. Makes any warranty or representation, expressed or implied, with respect to the accuracy, completeness, or usefulness of the information contained in this report, or that the use of any information, apparatus, method, or process disclosed in this report may not infringe privately owned rights; or

B. Assumes any liabilities with respect to the use of, or for damages resulting from the use of any information, apparatus, method, or process disclosed in this report.

As used in the above, "person acting on behalf of the Commission" includes any employee or contractor of the Commission, or employee of such contractor, to the extent that such employee or contractor of the Commission, or employee of such contractor prepares, disseminates, or provides access to, any information pursuant to his employment or contract with the Commission, or his employment with such contractor.

TECHNICAL INFORMATION DIVISION
LAWRENCE RADIATION LABORATORY
UNIVERSITY OF CALIFORNIA
BERKELEY, CALIFORNIA 94720